Towards Strategic and Sustainable Region-wide Road Weather Information Systems (RWIS) Network Planning and Management

by

Simita Biswas

A thesis submitted in partial fulfillment of the requirements for the degree of

Doctor of Philosophy

in

TRANSPORTATION ENGINEERING

Department of Civil and Environmental Engineering
University of Alberta

ABSTRACT

Road Weather Information Systems (RWIS) are considered one of the most critical highway intelligent transportation system (ITS) infrastructures, combining several advanced technologies to collect, process, and disseminate road weather information. The collected information is used by road maintenance authorities to make operational decisions aimed at improving safety and mobility before, during, and after inclement weather events. Acknowledging their significant operational and environmental benefits, many North American transportation agencies have invested millions of dollars in deploying RWIS stations to strengthen the monitoring coverage of winter road surface conditions. However, considering their high deployment costs and the seemingly random nature of road weather fluctuations, little is known about the optimal distribution density required to provide adequate monitoring coverage under varying circumstances. What is also resurging is the development of comprehensive RWIS siting guidelines in an effort to maximize return on investment while keeping our roads safe and mobile.

As an initial step, a series of geostatistical semivariogram models were constructed and compared using topographic position index (TPI) and weather severity index (WSI). A geostatistical approach in conjunction with large-scale optimizations were then conducted to determine the optimum number of RWIS stations across several topographic and weather zones using nationwide weather, geographical, and topographical datasets covering 20 different states in the US. The findings indicate that RWIS density strongly depends on the varying environmental characteristics of the region under investigation.

In the subsequent step, a new methodological framework was developed to determine optimal RWIS locations by taking into account spatial characteristics of multiple critical RWIS variables;

namely, air temperature, road surface temperature, and dew point temperature. A multi-variable semivariogram model was developed by integrating the impact of multiple crucial weather parameters. This integrated model, combined with the traffic parameters, was employed to refine the location optimization algorithm; which was then solved using a popular metaheuristic algorithm; namely, spatial simulated annealing. The developed location allocation model was then illustrated using a case study for the region-wide RWIS network planning and statewide gap analysis.

In addition to this, this study involved sensitivity analysis of optimal locations generated for various planning scenarios to further validate the conclusiveness of the findings and to furnish decision-makers with a range of solutions, providing flexibility in the decision-making process. The findings revealed that the weighting of weather and traffic parameters influences optimal location selection. The resulting solution sets from the sensitivity analysis offer adaptability in selecting parameter weights tailored to the requirements of decision-makers, encompassing considerations of both weather variables and safety implications associated with traffic.

In addition to location determination, this study introduced a novel bi-level sequential optimization model for comprehensive RWIS network planning, which addresses the need to pinpoint both the location and type of RWIS stations; namely, Regular RWIS and Mini-RWIS. Regular RWIS stations capture regional weather trends while Mini-RWIS stations capture local trends. Therefore, considering the type is critical for achieving cost-effectiveness and maximizing coverage. By comparing the gap in monitoring coverage, substantial enhancement in RWIS network planning is achieved by offering a method to fine-tune both station placement and type. This decision is pivotal as the choice directly impacts the network’s financial sustainability and operational efficiency.

Therefore, determining the optimal type of station in conjunction with its placement is essential for constructing an effective and economically viable RWIS network.

At the last step, the impact of optimal RWIS network on traffic safety was assessed by introducing a new parameter, named network coverage index (NCI). NCI analyzes and quantifies the advantages of an optimized RWIS network through the enhancement of transportation safety. The findings reveal a strong dependency between the NCI and the RWIS network configuration. Based on the findings obtained in this study, road agencies and RWIS planners can now be assisted with conceptualizing the capabilities of an optimized RWIS network, which will help them increase monitoring coverage, and in the process, gain a quantitative understanding on its potential impact on traffic safety.

The methodologies developed and analyzed in this thesis provide RWIS planner with the evidence-based RWIS planning and management strategies, which in turn will benefit winter travellers with improved safety, mobility, and a more environmentally sustainable RWIS network. Moreover, RWIS network planning solutions derived from this research are conveniently implemented for real-world applications.

PREFACE

The works presented in this thesis have been published or presented in peer-reviewed journals or conferences within the field of transportation engineering.

The list of published articles:

i. **Biswas S.,** M. Wu, S. J. Melles, and T. J. Kwon (2019). Use of Topography, Weather Zones, and Semivariogram Parameters to Optimize Road Weather Information System Station Density across Large Spatial Scales. Transportation Research Record: Journal of the Transportation Research Board, vol. 2673, no. 12, pp. 301-311. https://doi.org/10.1177/03611981198 46467

ii. **Biswas, S.,** and T. J. Kwon (2020). Developing Statewide Optimal RWIS Density Guidelines Using Space-Time Semivariogram Models. Journal of Sensors, vol. 2020, Article ID 1208692. https://doi.org/10.1155/2020/1208692

iii. **Biswas, S.,** and Kwon, T. J. (2022). Development of a novel road weather information system location allocation model considering multiple road weather variables over space and time. Transportation research record, 2676(8), 619-632. https://doi.org/10.1177/03611981221084678

iv. **Biswas, S.,** Sharma, D., & Kwon, T. J. (2022). Safety Impact Assessment of Optimal RWIS Networks—An Empirical Examination. Sustainability, 15(1), 327. https://doi.org/10.3390/su15010327

v. **Biswas, S.,** and Kwon, T. J. (2023). Strategic Planning for Equitable RWIS Implementation: A Comprehensive Study Incorporating a Multi-variable Semivariogram Model. Journal of Geographical Research, 6(4), 54-72.

https://doi.org/10.30564/jgr.v6i4.5973

In preparation:

i. **Biswas, S.,** and Kwon, T. J. (2024). Novel Method for Optimizing Dual-Type RWIS Networks - A Case Study of Maine, USA

Dedicated to my parents, Mukul Biswas and Aparna Biswas

My husband, Susen Das

My sister, Bani Biswas

And

My daughter, Hridima Tridha Das

ACKNOWLWDGEMENT

First and foremost, I praise God, the Almighty for providing me the strength and granting me the capability to complete my research work successfully.

I would like to express my sincere appreciation and deepest gratitude to my supervisor, Dr. Tae J. Kwon, for his continuous support, guidance and invaluable encouragement throughout my research and studies. I am grateful for the opportunity to collaborate with a fantastic supervisor who has supported me in building confidence, enhancing critical thinking skills, and gaining profound academic knowledge. Without his tremendous support and valuable advice, this dissertation would not have been possible.

I would like to take this opportunity to thank my PhD supervisory committee: Dr. Tae J. Kwon, Dr. Karim El-Basyouny, Dr. Stephen Wong for their advice and assistance during the research. I would also like to express my gratitude to the members of my final PhD examination committee including my PhD supervisory committee, Dr. Yong Li, Dr. Alex Klein-Paste, and Dr. Hassan Dehghanpour Hossein Abadi for their contributions in reviewing this research work and for providing valuable suggestions to enhance this dissertation.

I would like to thank Natural Sciences and Engineering Research Council of Canada (NSERC, https://www.nserc-crsng.gc.ca/index_eng.asp) for providing me with the prestigious Alexander Graham Bell Canada Graduate Scholarship – Doctoral (CGS D) over three years of time during PhD studies. I am also grateful for receiving Alberta Innovates (https://albertainnovates.ca/) Graduate Student Scholarship, Faculty of Graduate Studies (FGSR), University of Alberta. I would like to thank Aurora Program (www.aurora-program.org), Maine Department of Transportation (DOT) and Vanasse Hangen Brustlin (VHB) for funding my research. Acknowledgment is also given to the Iowa Environmental Mesonet, WxDE (Weather Data Environment: https://wxde.fhwa.dot.gov/) and NOAA (National Oceanic and Atmospheric Administration: https://www.noaa.gov/) for providing necessary data for this research.

I would like to express my gratitude to my friends and colleagues in our research team – Mingjian Wu, Davesh Sharma, Michael Urbiztondo, Shuoyan Xu, Tasnia Nowrin, Andy Wong, Lian Gu, Cindy Wang, Qian Xie, Nancy Huynh, Sabrena Jahan Ohi, Mudasser Seraj and Xueru Ding.

Finally, I wish to extend my heartfelt appreciation to my family, especially my dedicated husband, for being the person who understand me in every circumstance, support me even on the toughest days, tirelessly providing me with every possible opportunity I could ever dream of. The unwavering support, understanding, and encouragement from my parents and sister have been invaluable throughout this long journey. I'm also thankful for my cherished bundle of joy, my daughter, who entered my life during my PhD studies. Her unconditional love and infectious enthusiasm have been a constant source of inspiration and motivation throughout my academic journey.

TABLE OF CONTENTS

LIST OF FIGURES

LIST OF TABLES

List of Acronyms

AADT	Annual Average Daily Traffic
ASOS	Automated Surface Observing Systems
AT	Air Temperature
AVHRR	Advanced Very High Resolution Radiometer
AWOS	Airport Weather Observation Systems
BPSO	Binary Particle Swarm Optimization
CPU	Central Processing Units
DEM	Digital Elevation Model
DOT	Department of Transportation
DPT	Dew Point Temperature
ESS	Environmental Sensor Stations
FAA	Federal Aviation Administration
FHWA	Federal Highway Administration
GAM	Generalized Additive Model
GIS	Geographic Information System
ITS	Intelligent Transportation Systems
MADM	Multi-Attribute Decision Making
MCO	Multi-Criteria Optimization
METAR	Meteorological Terminal Aviation Routine Weather Report
MODM	Multi-Objective Decision Making
MODIS	Moderate-Resolution Imaging Spectroradiometer
MST	Mean Surface Temperature
NAM	North America Mesoscale Forecast System
NDVI	Normalized Difference Vegetation Index
NIP	Nonlinear Integer Programming
NOMADS	National Operational Model Archive and Distribution System
NWS	National Weather Service
OK	Ordinary Kriging

PSO	Particle Swarm Optimization
RDR	RWIS Deficient Regions
RMSE	Root Mean Square Error
RPU	Remote Processing Units
RSC	Road Surface Condition
RST	Road Surface Temperature
RWIS	Road Weather Information System
SA	Simulated Annealing
SNODAS	Snow Data Assimilation System
SSA	Spatial Simulated Annealing
SWE	Snow Water Equivalent
TPI	Topographic Position Index
VST	Variability of Surface Temperature
WRM	Winter Road Maintenance
WSI	Winter Severity Index

Chapter 1

Introduction

1.1 Background

Intelligent Transportation Systems (ITS) are an integral part of modern transportation engineering. ITS significantly improve transportation mobility and safety, particularly in how it relates to the prevention of weather-related road crashes, which is a vital and challenging issue for countries with cold regions. Over 1.5 million road crashes, 800,000 injuries, and 7,000 fatalities occur annually in the U.S. due to adverse weather (Jin et al. 2014). In its Northern neighbor—Canada, about 3,000 deaths result from weather-related accidents every year, and one in 135 people experience driving-related injuries (Andrey et al. 2001). Preventing these tragedies is a complex task that requires the collaboration of many decision-makers. While there can be several different approaches to mitigate the effect inclement weather events have on our vast road networks, one approach is to provide better road conditions through more efficient maintenance operations. However, achieving this requires maintenance personnel to thoroughly understand the current state of road weather within their network, which can be facilitated through one of the most critical highway ITS infrastructure, namely Road Weather Information Systems (RWIS).

RWIS consist of a group of road weather and surface conditions monitoring sensors installed on a roadside station. This combination of advanced sensors gathers, processes, and disseminates road weather and surface condition information used extensively by winter road maintenance authorities to make operative decisions before and during inclement weather events. It is also used by travelers via RWIS connected dynamic message signs to help them make more informed trip-related decisions during inclement weather events (Pilli-Sihvola et al. 2012). These systems not only enhance decision-making for travelers but also offer key benefits such as improved traffic safety, mobility, and winter road maintenance. Despite these benefits, there are a few limitations associated with both RWIS and the data collected by these stations. A significant constraint is the installation cost, which could be as high as US $100K per station depending on the type and number of sensors equipped (White 2006, Manfredi et al. 2008). Furthermore, while RWIS data provides valuable point-based measurements, it often falls short in capturing the spatial variability of surrounding road surface conditions. Therefore, understanding the degree of spatial continuity and variance associated with the measured road weather data is imperative to understand the effective spatial coverage range of each RWIS station. Moreover, RWIS stations can vary in their capabilities, ranging from comprehensive regular-RWIS with full sensor suites to more cost-effective mini-RWIS with limited sensors. Therefore, the decision of which RWIS type to deploy at a given location requires careful consideration of both data needs and budget constraints. Given these financial and technological limitations, transportation authorities face the challenge of optimizing RWIS deployment to maximize their return on investment. This necessitates addressing the critical issues of optimal RWIS density (i.e., how many stations are necessary), optimal RWIS location (i.e., where should they be located), and the appropriate type of station for each location.

To address these challenges, only a limited number of researchers around the world have conducted studies to quantify the spatial coverage of RWIS data and determine the optimal RWIS density and location based on available RWIS data. One of the earlier studies was conducted by Eriksson and Norrman (2001) in Sweden where RWIS site locations were recommended based on hazardous road condition. The research findings also revealed that optimal RWIS locations could be determined by using topographic parameter and land use information (Eriksson and Norrman 2001). The Federal Highway Administration (FHWA) initiated extensive efforts to provide RWIS siting guidelines based on the knowledge and experience of field operators (Manfredi et al. 2008). A more recent study by Kwon and Fu (2017) examined how topographical features affect the deployment of RWIS stations. Their findings indicated that more RWIS stations are needed in mountainous areas than in flatland areas and that a region with a longer spatial autocorrelation range would require fewer stations than a region with a shorter range. Although these earlier studies provided some preliminary guidance on RWIS distribution, the dependency on regional topographic and weather variations, and were limited in scope to specific case studies, thus lacking generalizability. This can make implementation and planning by regions or agencies difficult if they have limited or no RWIS stations. Furthermore, since road weather variables are known to vary over space and time, spatiotemporal analyses must be performed to better understand the effective coverage of road weather variables.

Besides installation guidelines, several studies were conducted in the past to identify optimal RWIS locations. One of the earlier studies by Kwon et al. (2013) used a GIS-based method to evaluate RWIS locations in Minnesota, US by quantifying the benefits of road safety and maintenance services. Another attempt was taken by Jin et al. (2014), where a formal location optimization method was proposed that maximized spatial coverage of existing RWIS sensors using a safety concern index. A cost-benefit-based approach was used later by Zhao et al. (2016) to determine the optimal locations of RWIS by maximizing spatial coverage by considering the standard deviation of weather severity. In a more recent study, Kwon et al. (2016) implemented a geostatistical analysis technique to determine the RWIS locations by examining the underlying spatial structure of road surface temperatures.

Spatial analysis within GIS platform was also incorporated in several different fields of study. Valjarević et al. (2021) examined the Morava city conurbation in Serbia, utilizing Kriging-based spatial analysis with a particular focus on the interaction between rural and urban areas, traffic connectivity, geographical positioning, and sustainability and profitability (Valjarević et al. 2021). Moreover, Timalsina and Subedi explored the growing significance of open spaces in urban development planning in Nepal. This paper examines the evolution of open space integration in recent urban planning practices in Nepal, highlighting the growing emphasis on sectoral integration with open space development, particularly within Periodic Planning, Integrated Urban Development Planning (IUDP), and Smart City Planning, aiming to create resilient and sustainable cities (Timalsina and Subedi 2022).

Although the previously mentioned studies have made valuable contributions to the development of RWIS location models, they focused solely on investigating the spatial characteristics of a single variable, specifically road surface temperature (RST). While RST is undoubtedly an essential measurement, a methodological framework that incorporates multiple weather variables is critical for effective spatial analyses and subsequent location optimization. Additionally, existing research has not yet provided a definitive answer regarding the appropriate installation choice between a Regular RWIS (R-RWIS) station or a Mini-RWIS (M-RWIS) station. Therefore, it is crucial to determine not just the optimal location but also the specific type of RWIS station for each site within a network.

1.2 Characterization of Road Weather Variables

The spatial variation of road weather parameters such as road surface temperature (RST), air temperature (AT) and dew point temperature (DPT) depends on meteorological, geographical, traffic, and road construction factors. Among them, geographical and road construction factors are constant, while meteorological factors and traffic conditions also tend to vary on a daily basis.

Geographical factors that can impact road weather variables consists of topography, longitude, latitude, altitude, sky-view factors (SVF), land use, etc. Among them, SVF is the most influential factor for RST variation. SVF is a dimensionless parameter with a value between zero and one. For a flatland and open area, the SVF is one, and if obstructions are present, then the SVF will vary between zero and one. Other variables, including topography, altitude, and land use, also significantly impact road weather variables. Topography is considered a major influencing factor as slight variations in topography cause large changes in AT and RST. On the other hand, meteorological factors include AT, DPT, precipitation, wind speed, cloud cover, etc. The most imperative parameter among these variables is AT, which significantly influences the RST. Another major factor is cloud cover, which varies with location and time, making it difficult to include in the numerical modeling of RST. Outside of AT and cloud cover, DPT is a crucial parameter that controls the formation of hoar-frost on the road surface and can be used for ice detection, but it does not significantly affect RST (Boselly et al. 1993, White et al. 2006). From the abovementioned discussion, it is clear that AT and DPT are analogous to RST in terms of forecasting road weather conditions. Therefore, it is essential and equally important to consider these critical variables and analyze their underlying spatial characteristics prior to RWIS network planning, which has not been done as existing research tends to focus solely on RST.

Semivariogram analysis is an advanced geostatistical method that is used to evaluate spatial and temporal dependency of parameters that tend to fluctuate over space and time (i.e., road weather variables). This method works by combining spatial and time series analysis to preserve the interactive effect of temporal variation on the spatial domain and vice-versa, allowing for the visualization of the spatiotemporal variability in the variable of interest and the determination of autocorrelation range over space and time. For this reason, spatiotemporal analysis has been established as more accurate than spatial analysis alone (Graler et al. 2016). Several researchers used the above-mentioned technique to model air pollutants by measuring the space-time variability of certain particles' concentrations (Graler et al. 2016, Li et al. 2017, Ahmed et al. 2018, and Network 2016). Hu et al. (2017) applied spatiotemporal regression kriging to predict precipitation using Moderate-resolution Imaging Spectroradiometer (MODIS) and Normalized Difference Vegetation Index (NDVI) data. In the field of transportation, spatiotemporal data has been used for the evaluation of spatiotemporal outlier and the identification of erroneous sites (Galarus and Angryk 2018) and traffic accident prediction using deep learning approach (Yuan et al. 2018). One notable study related to the topic of interest is the investigation of spatiotemporal variability of road weather and surface conditions using RWIS data from Alberta, Canada (Wang et al. 2019). The output of this study provided both spatial and temporal features of road surface temperature but further investigation is warranted to generate a spatiotemporal model that is representative of multiple RWIS variables. Moreover, the dependency of the spatiotemporal feature of RWIS measurements on topographic and weather severity has yet to be scrutinized and spatiotemporal analysis has never been considered in prior efforts pertaining to optimal RWIS network planning.

As discussed, the existing literature predominantly focuses on single-variable analyses, particularly of RST, and often neglects the spatiotemporal dynamics of road weather phenomena. This leaves a significant gap in our understanding of how to effectively incorporate the multifaceted nature of road weather including the interplay of multiple variables, their spatial and temporal variations into RWIS network planning.

1.3 Problem Statement and Research Motivation

Considering the numerous benefits of RWIS information and their limitations, i.e., high installation cost and maintenance cost and minimal spatial coverage, RWIS stations must be strategically placed to maximize network monitoring coverage. Although previous research has attempted to provide some guidelines for RWIS installations, significant gaps remain in knowledge and methodology for large-scale RWIS network planning and strategic implementation.

Initially, RWIS installation guidelines were based on heuristic and qualitative approaches, which were time-consuming and subjective to the knowledge and experience of maintenance personnel. Over time, it was established that topographic conditions significantly influence regional RWIS density planning; however, the specifics of this dependency were never quantitatively measured. Additionally, there is a lack of deployment guidelines for regions with limited or no RWIS stations. Given that topography and weather severity are dominant factors for winter road maintenance operation (Mewes 2011), understanding the dependency of RWIS measurements on these factors is essential. The two measures of particular interest are the Topographic Position Index (TPI) and Winter Severity Index (WSI). TPI defines the relative topographical variation of an area of interest and its surrounding area while WSI is an aggregate indicator of weather severity encompassing factors such as yearly snowfall accumulation and duration, blowing snow duration, and freezing rain duration (Weiss 2001; Jenness 2006; Mewes 2011). Both measures, being commonly available and influential in determining the number of RWIS stations required, could be used to develop new RWIS siting guidelines, especially for regions with limited or no RWIS data.

In terms of RWIS location-allocation, previous optimization models focused solely on the spatial characteristics of a single RWIS variable, Road Surface Temperature (RST). While RST is important, RWIS provide many other road weather variables that also need to be considered. Hence, there is a resurgent need to develop a novel approach for RWIS network planning that incorporates the spatial characteristics of multiple weather variables. This thesis pioneers the creation of an innovative multi-variable semivariogram model tailored to crucial weather variables such as air temperature (AT), road surface temperature (RST), and dew point temperature (DPT). Additionally, the developed methodology considers areas susceptible to traffic accidents, enhancing safety and ensuring an equitable distribution across various maintenance zones. Furthermore, the developed network optimization methodology is applied to ascertain the optimal number of RWIS stations necessary for adequate monitoring coverage of any given area.

This study also addresses a critical network planning question: 'What type of RWIS stations (regular or mini) are required at each location?' Given the higher installation costs of regular RWIS, decision-makers often opt for mini RWIS for cost-effective network densification. However, determining the appropriate locations for installing regular and mini RWIS can be challenging due to the difficulty in quantitatively assessing their inherent differences and formally integrating them into the location allocation framework. Our innovative bi-level sequential optimization model is designed to answer this question, thereby facilitating effective and efficient RWIS network planning.

Moreover, no prior efforts have been made to examine and quantify the benefits of an optimally situated RWIS network which can be defined as an RWIS configuration with the optimal number of stations systematically placed at the optimal locations to provide maximized monitoring coverage. To address this gap, evaluating the performance of optimal RWIS locations on the transportation system is essential. This assessment will provide insights into the associated benefits and quantify the monetary advantages of an optimized RWIS network. Consequently, it will offer the first empirical evidence-based validation of RWIS benefits in the literature.

1.4 Objectives

Building on the aforementioned challenges and gaps in the existing literature, the primary objective of this thesis is to develop a comprehensive and generalizable methodological framework for the strategic planning and management of RWIS networks. This framework will utilize large-scale datasets from diverse North American regions, considering the spatiotemporal characteristics of road weather and surface conditions, to inform decision-making regarding optimal RWIS deployment, particularly in areas currently lacking such infrastructure.

To achieve this primary objective, this research encompasses the following sub-objectives:

1. ***Development of an RWIS Density Guideline:***
   This study will develop comprehensive RWIS siting guidelines by evaluating the relationship between optimal RWIS density and readily available data, such as topographic position index (TPI) and weather severity index (WSI). In this research optimal RWIS density will be determined by investigating spatiotemporal autocorrelation of RWIS measurements, aiming to incorporate both spatial and temporal domain to better understand the effective coverage of road weather variables. Research findings will aid transportation agencies in planning RWIS deployment, particularly for region that do not have existing RWIS.

2. ***Development of a Comprehensive RWIS Deployment Strategy:***
   This research will advance RWIS station placement optimization by incorporating the spatial attributes of multiple critical weather variables: air temperature (AT), road surface temperature (RST) and dew point temperature (DPT). The resulting multi-criteria location optimization model will be used to:

   Implement the developed model for the planning of a regional RWIS network: An RWIS network planning tool will be developed to prioritize potential RWIS sites and conduct a statewide gap analysis to validate those sites and identify new optimal locations.

   Perform sensitivity analyses to offer flexibility to decision-makers: Sensitivity analyses will be conducted to explore how varying weather and traffic factors influence optimal location selection, allowing decision-makers to tailor parameter weights to their specific needs.

3. ***Formulation of a Bi-Level Sequential Optimization Model:***
   This thesis will introduce a novel bi-level sequential optimization model to determine both the optimal location and type of RWIS stations (i.e., R-RWIS and M-RWIS). This approach aims to promote a cost-effective network planning strategy that balances comprehensive data collection with budgetary constraints.

4. ***Evaluation of the performance of the optimized RWIS network:***
   This thesis will assess the impact of optimized RWIS network on transportation systems. Using monitoring coverage as a performance indicator, the benefits of optimal location solutions will be quantified, potentially translating these into monetary benefits.

The outcome of this thesis will serve as a guideline for long-term RWIS network planning and management strategies that involve different topographic and weather severity zones. This comprehensive deployment strategy will provide a large number of RWIS communities and jurisdictions with a valuable decision support tool for sustainable RWIS network planning and management by keeping our roadways safe and environmentally friendly.

1.5 Organization of the Thesis

The remainder of this thesis is organized as follows:

- **Chapter 2:** Provides a literature review covering relevant topics, including an component of RWIS and the synthesis of current deployment practices.
- **Chapter 3:** Discusses the proposed methodology employed to achieve the research objectives.
- **Chapter 4 and 5:** Present the results on RWIS density optimization and RWIS location allocation, respectively.
- **Chapter 6:** Details the impact assessment of optimal RWIS Network.
- **Chapter 7:** Summarizes the key findings of this thesis and offers recommendations for future research.

Chapter 2

Literature Review

2.1 Introduction

The prevention of weather-related road crashes continues to be a vital and challenging issue, particularly for countries in cold regions. As an important part of modern transportation engineering, ITS play an essential role in everyday life by improving transportation safety and mobility. A road weather information system (RWIS)—a critical piece of ITS infrastructure—is a combination of advanced technologies that collect, process, and distribute road weather and condition information. Road maintenance agencies use RWIS information to make operative decisions during the winter season to ensure traffic safety and mobility of the travelling public. For this reason, many North American transportation agencies have invested millions of dollars in deploying and/or expanding their RWIS network to improve road surface conditions monitoring coverage. However, because of the significant cost associated with RWIS station installation, jurisdictions limit the number of new installations due to budgetary constraints. Therefore, it is essential to develop an optimal RWIS network planning and siting guideline that maximizes the effectiveness of RWIS station deployments.

2.2 Road Weather Information Systems

For countries with regions where winter conditions can significantly affect the mobility and safety of their transportation networks, information regarding the road surface and weather conditions is collected, processed, and distributed by RWIS stations generally installed alongside roads and highways. The major elements of RWIS are ESS (Environmental Sensor Stations), RPU (Remote Processing Units), CPU (Central Processing Units), and communication hardware. ESS consists of atmospheric, pavement, and water-level monitoring sensors, whereas the atmospheric sensors are mounted on the tower, and pavement sensors are embedded in and beneath the pavement surface. Water level sensors are generally installed in flood-prone regions to monitor site-specific characteristics.

From these sensors, the types of data collected by RWIS stations include air, surface, and sub-surface temperatures; precipitation rate, type, and intensity; atmospheric pressure; wind speeds and direction; and road surface condition. Collected data are initially processed in RPU, which can be made available to the road users via a dynamic message sign (DMS) to alert them of hazardous road conditions. RWIS information is then transmitted to the CPU server along with forecasts from other weather information providers (e.g., National Weather Service (NWS), vendors, and others) and disseminated to the user interface. The NWS provides weather, hydrologic, and climate information for the United States and their dataset includes air temperature, dew point temperature, wind speed and direction, visibility, sky conditions, relative humidity, pressure, and pressure tendency on an hourly basis.

The uniqueness of RWIS in comparison to other conventional weather stations is that RWIS data provides road weather and condition information. This additional information provided by RWIS is essential for winter road maintenance personnel to forecast pavement slipperiness and the probability and timing of icing events (Agah and Pape 2002, Manfredi et al. 2008, Ye et al. 2009). RWIS setups generally come in two types: (a) stationary and (b) mobile RWIS. Stationary RWIS are installed along a roadway, collecting point-measured data of a fixed location, thereby providing high temporal but low spatial coverage. On the other hand, mobile RWIS are installed on patrol vehicles that collect data while traveling along the road network. The data from these mobile units provide high spatial coverage but low temporal coverage. The major components of a stationary RWIS station are presented in **Figure 2-1**.

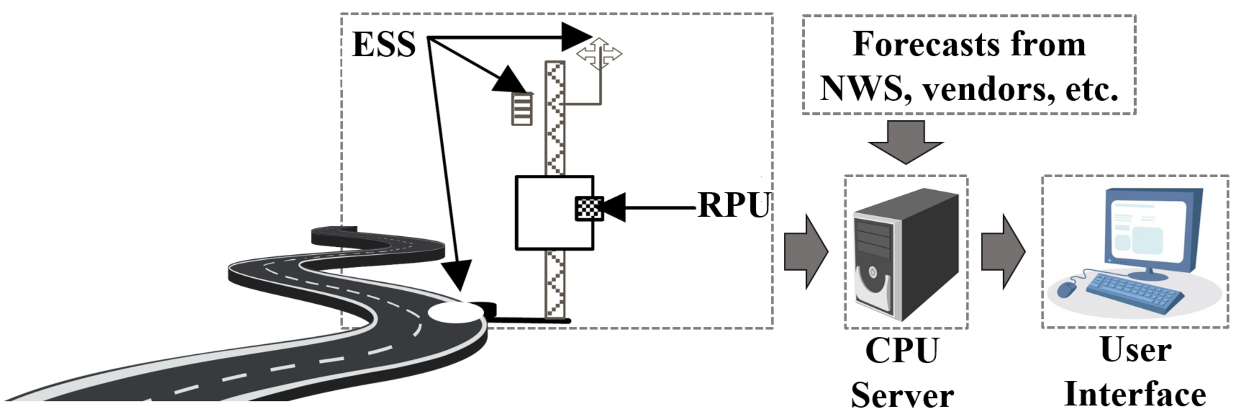

Figure 2- 1: Major Components of an RWIS Station

There are two types of stationary RWIS stations: regular RWIS and mini-RWIS. Regular RWIS consists of full sensor configuration, providing comprehensive data for extensive regional road condition monitoring. In contrast, mini-RWIS stations have a limited sensor configuration, offering basic, localized road condition monitoring and serving as gap-filling stations. The installation cost of mini-RWIS ranges from $10,000 to $45,000, which is significantly lower than that of regular RWIS. Data collected by mini-RWIS includes air temperature, road surface temperature, humidity, wind speed and direction, and hourly still camera images.

Information disseminated by an RWIS station is collectively used by road operations personnel to make effective and timely winter road maintenance decisions and help travelers make more informed decisions about scheduling their trips. In addition, RWIS information is also used for initializing road weather and surface conditions forecasts to improve the quality of winter road maintenance services. With forecasted road weather information (e.g., subsurface and surface temperatures), proactive maintenance strategies such as anti-icing operations become possible, further improving the quality of road surface conditions (Sato et al. 2004). The accuracy of the forecasts depends on various factors, such as climate characteristics, geographical and topographical settings, etc. (Ahrens 2009). The key benefits of an RWIS are improved traffic safety, mobility, and winter road maintenance as described below.

It has been established in previous literature that the performance of highway networks is greatly affected by adverse weather and road surface conditions. Inadequate and inefficient winter road maintenance (WRM) causes a significant increase in traffic collisions and winter traffic congestion. As a result, North American transportation authorities spend more than 3 billion annually on WRM like plowing and salting to ensure traffic safety and mobility (Ye et al. 2009, Strong et al. 2010). Since the use of salt causes environmental concern, it is crucial to minimize its usage, which also reduces the WRM cost.

RWIS has become an essential tool in the WRM decision-making process by providing agencies with localized road weather and surface condition information. The critical information provided by RWIS enables transportation agencies to execute proper maintenance activities regarding when and where to deploy snowplows and deposit road salts, i.e., restoring safety and mobility while using minimum resources. Improved winter maintenance operation (i.e., anti-icing, pre-wetting, and sanding) has been shown to improve road surface condition, resulting in lower rates of weather-related collisions (Fu et al. 2005, Usman et al. 2012). Furthermore, real-time road weather and condition information provided by RWIS is used to predict near-future road surface conditions. Such information is used to predict the occurrence of a snowstorm and help maintenance agencies decide on the usage of anti-icing chemicals. These chemicals prevent the bonding of snow and ice with the pavement, which results in a less slippery road surface, thereby improving traffic safety and mobility. Due to proactive maintenance measures, comparatively fewer anti-icing chemicals are required, which reduces maintenance costs and environmental impact. Previous studies proved that, by taking advantage of their RWIS information, proactive use of anti-icing chemicals can significantly reduce maintenance cost (Epps and Ardila-Coulson 1997, C-SHRP 2000). Additionally, RWIS provide travelers with better information to help them make more informed travel decisions and contribute to safer travel behavior and less weather-related crashes and injuries (Boon and Cluett, 2002).

Despite these benefits, there are a few limitations associated with both RWIS and the data collected by these stations. The biggest limitation is the installation cost, which could be as high as US $100,000 per station depending on the type and number of sensors. In addition, RWIS data provides point-based measures, which are often limited in capturing the spatial heterogeneity of the surrounding road surface conditions. For these reasons, it is important to measure the spatial and temporal continuity range of the measured data and its associated variance in order to understand the monitoring coverage range of the RWIS stations.

2.3 Current Best Practices of RWIS Network Planning

RWIS site selection is an important and challenging issue because of the numerous benefits associated with RWIS information. To address these challenges, a limited number of studies were conducted in the past that can assist road authorities in making an informed decision on RWIS station installation.

An extensive effort was first initiated in 2005 by the US FHWA to provide a standard for RWIS network planning based on the analysis of published information and interviews with state's Department of Transportation (DOT) RWIS managers. According to this study, several steps needed to be followed to determine the locations of RWIS stations. Firstly, regional representativeness needs to be examined alongside weather zone maps to determine which regions exhibit similar weather characteristics. Having similar weather characteristics minimizes the possibility of adverse local weather effects and influences from other non-weather factors (i.e., heat, moisture, and wind barriers). Next, the unique characteristics of each region were identified by consulting with local maintenance personnel, who then provided a list of candidate siting locations. The selected RWIS locations should satisfy the road weather information requirements. Some example locations are: (a) regions with slippery conditions or a location where significant blowing, drifting, or heavy snow accumulation occurs; (b) low lying road segments where surface flooding occurs; (c) visibility distance where the local environmental conditions contribute to low visibility (e.g., a large local moisture source); and (d) areas with high wind speeds, such as those that occur in hurricanes and terrain-induced crosswinds along a confined valley or ridge top. Additional local siting considerations included power, communication, aesthetics, safety, and security. This study recommended 30 to 50 km (20 to 30 miles) spacing for RWIS station installation based on the knowledge and experience of field operators (Manfredi et al. 2008).

Given that the recommended guidelines are based on expert, yet personal, opinion, several researchers attempted to implement a more objective way to quantify the spatial coverage of RWIS data and identify an optimal set of locations and densities for RWIS stations. Several studies were conducted to identify the location and number of RWIS stations required for specific regions. A comprehensive study was conducted by Zwahlen et al. (2003) that provided a state-wise RWIS network expansion plan for Ohio, US, by considering the distance between existing RWIS stations, declared snow days, and amount of annual snowfall recorded by the region under investigation. This study recommended installing fourteen additional RWIS stations by identifying the 'unserved area' with a focus on ensuring state-wise monitoring and prediction.

A study was also conducted in Sweden to determine the hazardous conditions on a roadway by multiple regression analysis of RWIS data. In this study, road climate was described using slipperiness classification, where ten types of slipperiness were identified to classify road climate, and the RWIS site locations were recommended based on the slipperiness. The outcome of this study showed that the spatial patterns for different types of slipperiness are heavily related to local parameters. In addition, the results also indicated that optimal RWIS locations could be determined by using topographic and land use information (Eriksson and Norrman 2001). Although this study provides a strong reference for RWIS location optimization, the authors made a heuristic assumption that the benefits of RWIS are proportional to road weather conditions.

Similarly, Alberta's Ministry of Transportation conducted an RWIS expansion study to determine both station location and density. RWIS deficient regions (RDR) were identified and analyzed in this study by considering various factors, including traffic loads, collision rates, climatic zones, availability of meteorological information, and discussions with regional road maintenance personnel and key stakeholders. After determining the candidate sites for RWIS installation, the provincial budget guidelines were used to verify how a given set of stations could be deployed. In this study, the station density was determined solely on the available budgets, which is heuristic and not applicable for regions where the governing body wants to determine the actual RWIS density required to ensure improved road safety during the winter season (Mackinnon and Lo 2009). Thus, more reliable and logical RWIS planning guidelines are needed to determine the optimal RWIS density rather than making decisions based on available financial resources.

In a GIS-based study conducted by Kwon and Fu (2013) in Ontario, Canada, a location ranking criterion was introduced to obtain the potential benefits of real-time road weather information, i.e., weather severity, traffic exposure and collision rate. A framework for RWIS network location evaluation was presented in this study, where the variability of surface temperature (VST), mean surface temperature (MST), and snow water equivalent (SWE) were considered alongside topographic location attributes. The study's findings revealed the feasibility of developing a systematic process for locating RWIS stations using an integrated location criterion to capture multiple factors being considered in practice. Alternatively, based on weather-related crash data, Jin et al. (2014) proposed a spatial optimization method of RWIS location identification using the maximization algorithm of spatial coverage, which was converted into a safety concern index. The proposed methodology was illustrated using crash and GIS data from the Austin District in Texas. RWIS location model was formed using a discrete network representation of the roads. Each link in the network was divided into equal length segments before a formulation of the optimization problem for choosing the location (segment in the network) of new stations was proposed. The model only had one objective function: minimizing the sum of safety concern index defined for each segment as the product of the crash rate and a reduction factor. Their solution method was based on a greedy heuristic, but no optimality gap was offered.

Zhao et al. (2015) proposed a method for RWIS location optimization using a mathematical programming approach. In this research, the potential RWIS locations were identified based on their distance to existing RWIS locations. The effects of regional weather conditions and traffic volume were captured using the concept of influencing area. They extended their effort by developing a two-stage sequential model, which considers the variation of regional weather severity and cost-benefit factor (Zhao et al. 2016). Although the developed model partially accounted for spatial variability, the effect of spatial patterns associated with a particular region was not fully utilized. Moreover, the underlying temporal variation of the variable of interest was not accounted for during the determination of monitoring coverage.

In another study conducted by Kwon et al. (2017), the RWIS network location optimization was done by employing an innovative geostatistical analysis technique, kriging. Optimization was formulated as NIP problem to maximize the monitoring capability while minimizing the spatially averaged kriging variance of hazardous road surface conditions. RWIS data used in this study were taken from the state of Minnesota, US. Using this data, the effectiveness of the current RWIS location setting was evaluated, along with recommendations for future network expansion. Although the method developed therein contributed to delineating RWIS locations, it only dealt with the spatial domain, and did not take into account the inherent temporal variations of road weather parameters, thereby making their location solutions less conclusive.

A more recent study by Fetzer et al. (2018) proposed a methodology for multi-objective RWIS location optimization for the state of New York by considering vehicular accident data, vehicle miles traveled (VMT), area coverage, access to power and maintenance, and existing ESS. A multi-objective optimization algorithm was formulated using three defined objectives: to maximize (a) the VMT within the station range, (b) geographic area covered by the station ranges, and (c) traffic safety or reduction of crash rate. This study used a modified e-constraint method to solve the optimization algorithm and generate a Pareto optimal solution that will allow the decision maker to choose a single most preferred solution based on their need. Although this study provides an advanced technique to optimize RWIS locations using multiple objective functions, the authors made a heuristic assumption for the effective radius, a critical parameter for optimization. Moreover, this study did not consider the spatial characteristics of the weather variables, and a minimum separation distance of 10 miles was used for new stations without providing any proper justification. Hence, it is important to study these critical parameters while quantifying the monitoring coverage of RWIS measurements.

In contrast, there exist very limited studies conducted in the past dedicated to quantifying the optimal RWIS density. Since density is closely related to many external factors, few studies attempted to understand the factors that influence road weather and surface conditions during inclement weather events. White et al. (2006), one of the studies that investigated this relationship, found that meteorological, geographical, road construction, and traffic parameters contribute to the spatial variation in the RST. Amongst these factors, topography was noted as the primary factor that influences RST variation over a region (Gustavsson 1990; Boselly et al. 1993; Manfredi et al. 2005; Chapman and Thornes 2005; White et al. 2006).

For this reason, Kwon and Fu (2017) further extended their previous work by proposing that the optimal RWIS spacing of a region may depend on the spatiotemporal variability of road weather conditions and their respective topographic settings. The authors conducted case studies using data from three US states (Iowa, Utah and Minnesota) and one Canadian province (Ontario). While their results indicated that the number of RWIS stations required would depend on the topographical characteristics, the analysis was based on a single road weather variable (i.e., RST) and provided no systematic method that can be applied to other regions with limited or no RWIS information.

2.4 Summary

The appropriate deployment of RWIS is a major concern, as it can greatly contribute to the improvement of traffic safety, mobility, and proper road maintenance during inclement weather events. Former practices of RWIS network planning are solely based upon the knowledge and experiences of field operators. Additionally, very little research has been conducted to identify RWIS density and locations systematically. It is also clear from the stated literature that the determination of optimal RWIS location requires a full understanding of the spatial variation of road weather conditions. Although existing studies provide some RWIS planning guidelines, the most critical unresolved question is what the optimal density and location of an RWIS network should be to provide adequate monitoring coverage of a given region. Our research attempts to answer this question, along with identifying the type of RWIS stations needed at each optimal location by developing an innovative and transferrable methodological framework to optimize regional RWIS network, incorporating the use of multiple RWIS variables for improved spatiotemporal inference. In addition, this study will also evaluate the performance of an optimally located RWIS network into the transportation system.

Chapter 3

Proposed Methodology

3.1 Introduction

Preventing weather-related crashes is a significant part of maintaining the safety and mobility of the traveling public during the winter months. Transportation authorities rely on real-time and near-future road weather and surface conditions (RSC) information to mitigate the detrimental effects of winter road conditions. Road weather information is disseminated by RWIS to make more timely and accurate winter road maintenance-related decisions. However, the high installation and maintenance costs of these systems have motivated governments to develop a framework for determining a region-specific optimal RWIS network based on readily available regional data. By doing so, the resultant guidelines would be able to provide RWIS network planning recommendations for regions with limited or no RWIS stations. As discussed before, topographic variation of a region significantly affects the road surface condition and is considered a crucial influencing factor of RWIS density. In contrast, weather severity is an essential parameter for winter road maintenance operations. Hence, the topographic and weather characteristics of the study area need to be analyzed to create several topographically unique regions within the study area with varying levels of winter severity.

Therefore, in the first step of this study, one of the most comprehensive spatiotemporal sampling techniques based in Geostatistics is employed in conjunction with geographically distributed data. This technique maximizes the probability of capturing the spatial and temporal variations of the RWIS variables and minimizes the potential bias associated with input data. More specifically, spatiotemporal analysis is performed by constructing empirical variograms from RWIS measurements, which optimizes parameter estimations for unsampled locations and captures the possible autocorrelation associated with the RWIS variables. During this process, the effective spatial and temporal range of continuity is determined under different topographic and weather settings, and the dependency of weather data on the topographic variation and weather severity of the region is also evaluated. The optimal density of RWIS stations is then determined for different topographic and weather severity zones and a zone-based optimal RWIS density chart is developed.

In the next step, multi-variable RWIS location optimization is performed using three key RWIS weather parameters: namely, Air Temperature (AT), Road Surface Temperature (RST), and Dew Point Temperature (DPT). RST is an important RWIS measurement that represents real-time road weather information, while AT and DPT are considered the two most critical parameters in forecasting road weather conditions. Hence, it is essential to integrate the multiple RWIS variables into the geostatistical analysis and develop a multi-variable semivariogram model. A model-based approach via kriging is subsequently utilized in this stage to obtain unbiased estimates with the lowest variance (i.e., uncertainty) to determine the optimal RWIS locations. This step also involves generating a bi-level sequential optimization model to determine the type of RWIS stations needed for each optimal location.

At the last step, the goodness of the optimal location solutions is determined to quantitatively assess the monetary benefit of location solutions on the transportation system. Research procedures for this study are summarized in **Figure 3-1**.

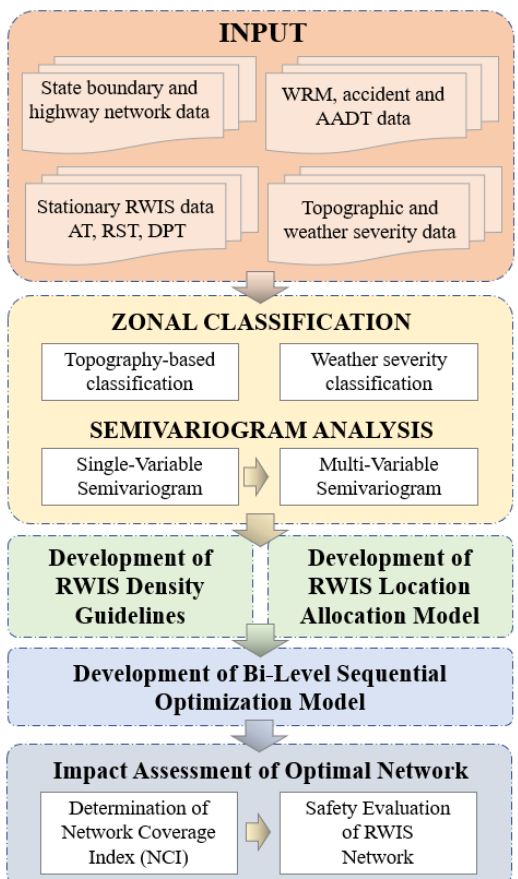

Figure 3- 1: An Overview of the Proposed Methodology

3.2 Characterizations of Topography and Weather

To evaluate the relationship among RWIS measurements, topographic variability, and weather characteristics of the regions under investigation, the study area is initially classified into topography and weather-based classes. Topographic analysis is performed using the topographic position index (TPI) parameter; while the Weather Severity Index (WSI) parameter is used for weather-based classifications using an ESRI shapefile generated for the United States by Meridian Environmental Technology (Mewes 2011). The following sections discuss TPI and WSI based zonal classification in detail.

Topographic Position Index (TPI)

The topography based zonal classification is conducted using TPI, which defines a relative topographical variation of an area of interest and its neighboring area. TPI values compare the elevation of every point in a DEM to the mean elevation of a specified region around that cell. Higher TPI values indicate hilly and mountainous areas, whereas lower TPI values represent flatlands (Weiss 2001, Jenness 2006). The TPI calculation algorithm was provided by Jenness Enterprises, which is the most promising and widely used algorithm for landform classification (Jenness 2006, Seif 2014a, Mokarram et al. 2015). The equation for TPI at a given location, i, is calculated as follows:

$$TPI_i = M_0 - \sum_{n-1} {}^{M_n}/_{n} \tag{3-1}$$

Where, M_0 = the elevation of the model point, i; M_n= the elevation of neighboring points; n = the total number of surrounding points employed in the evaluation. A neighborhood is defined as a circle or square surrounding the model point. In this study, TPI values for each point are calculated by considering a circle neighborhood of 50 km diameter around the point. TPI values are sensitive to the neighborhood size, and circle diameter is selected based on the application. For example, a finer diameter is appropriate for analyzing small landforms such as individual ridges or valley lines, whereas a larger neighborhood diameter is appropriate for major topographic landforms (Weiss 2001).

Positive TPI values indicate that a point is higher than the average elevation of the neighborhood while negative TPI values represent locations that are lower than the average elevation, and TPI values close to zero indicate regions where the elevation is similar to the average elevation of the surroundings (Seif 2014b). Relatively speaking, lower average TPI values indicate flatland, and higher ranges represent hilly and mountainous regions. An illustrated example of TPI values is presented below (**Figure 3-2**).

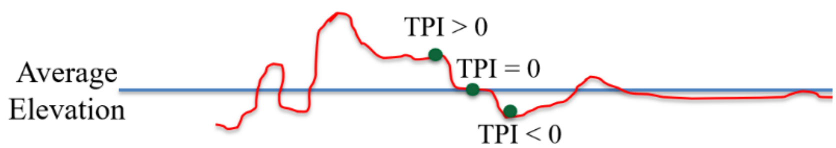

Figure 3- 2: Positive and Negative TPI Values for a Typical Land Surface.

Several previous studies have classified regions using topographic parameters (TPI). Grain Mountain in Iran was classified into nine different topographic categories depending on TPI using Digital Elevation Model (DEM) with 90 m resolution. Recorded TPI values were -128 to 161 (Seif 2014). Another study was conducted in the salt dome of Korsia of Darab plain, Iran, evaluating the landform classification algorithm of Jenness. The study area was 1083 square km, and a DEM with 30 m resolution was used for elevation. In terms of the results, land area was classified into ten different classes according to TPI values. This study confirmed the algorithm of Jenness as the most appropriate method of landform classification (Mokarram et al. 2015).

In this thesis, an elevation map of the study area is generated in ArcGIS using DEM data. A TPI value is calculated for every 30 m grid point (at the resolution of the DEM) using the Topography Tool that follows Jenness's algorithm. Later, the area will be classified into three zones based on TPI values.

Winter Severity Index (WSI)

Several previous studies developed standards to calculate WSI, which is generally used as a decision support tool to determine where road maintenance activities are needed. A common practice of winter severity investigation is to generate a daily-basis WSI number using specific weather parameters, subsequently summarizing the daily values into weekly, monthly, and seasonal WSI (Matthews et al. 2017a, 2017b). Winter severity is tracked in many different states using several meteorological parameters. However, most of the methods are developed from a winter maintenance perspective, are region-specific, and were not designed for country-wide use. Recognizing this limitation, a large-scale weather severity mapping method was developed by

Meridian Environmental Technology in 2012 to compare winter severity for all U.S. states. Parameters used were yearly average accumulation and duration of snowfall, average annual duration of freezing rain, and blowing snow. Parameters representing weather severity were selected through an iterative process based on previous experiences of Meridian and the solicitor's interest. Data acquisition details for WSI measurement are listed below:

- Snowfall accumulation data from National Weather Service's United States Climate Normals from 1971 to 2000 and snow precipitation data from Snow Data Assimilation System (SNODAS) for the winter seasons of 2004 to 2011.
- Snowfall duration data from Meteorological Terminal Aviation Routine Weather Report (METAR) observation of weather stations from Federal Aviation Administration (FAA) and National Weather Service (NWS) for the winter seasons of 2000 to 2010, and analysis of precipitation type from the North American Mesoscale Forecast System (NAM) through National Operational Model Archive & Distribution System (NOMADS) for the winter season of 2004 to 2011.
- Average annual duration of freezing rain data from METAR observation from 2000 to 2010 winter seasons and analysis of precipitation type from NAM model from 2004 to 2011 winter seasons.
- Hours of blowing or drifting snow were estimated from wind speed data using NAM model through NOMADS and one-km AVHRR based landcover data from the University of Maryland for the winter seasons of 2004 to 2011.

The formula used for WSI calculation provides equal weights for all listed factors. Since the unit of snowfall accumulation was in inches, and the annual duration of snowfall, blowing snow, and freezing rain were calculated in hours, the typical 'inches to hours = 10:1' weighting ratio was applied. For extra caution, a double weighting factor was provided for the duration of freezing rain. There was no specific explanation of the index values other than a relative comparison of winter severity from a winter maintenance viewpoint (Mewes 2011). The resulting WSI formula is shown below:

Winter Severity = 0.50 × (annual average snowfall in inches) + 0.05 × (annual snowfall duration in hours) + 0.05 × (annual duration of blowing snow in hours) + 0.10 × (annual duration of freezing rain in hours)

The ESRI shapefile generated for the United States by the project under Meridian Environmental Technology is used in this research to classify the study area according to WSI.

3.3 Effective Coverage of RWIS Measurements

In this stage, the effective coverage of RWIS variables for different TPI and WSI classes is generated using geostatistical semivariogram modeling. A semivariogram measures the dissimilarity between two measurements as a function of separation distance. A larger autocorrelation range indicates greater spatiotemporal continuity of RWIS measurements and vice versa. Spatial semivariogram analysis considers only the spatial domain of the variable of interest; it does not account for temporal variations. Since the weather variables (AT, RST and DPT are considered in this analysis) vary over space and time, it is necessary to investigate both the spatial and temporal variability of these variables. Hence, spatiotemporal semivariogram analysis is incorporated in this study to determine the effective coverage of RWIS measurements. It will also indicate how representative road surface weather variables are over space and time. The output of semivariogram analysis will be used as an input for RWIS density and location optimization. The details of such analyses are described below:

3.3.1 Spatial Semivariogram Analysis

A semivariogram is a plot of mean semivariance (y-axis) versus separation distance between point pairs (x-axis). Semivariance is a statistic that measures the similarity between two measurements as a function of separation distance (Olea 2012). Semivariance can be calculated by taking the average of the squared differences between measurements in a spatial domain separated by a specific lag distance. The most common formula for semivariance estimation is shown below:

$$\gamma(h) = \frac{1}{2n(h)} \sum_{i=1}^{n(h)} [z(x_i + h) - z(x_i)]^2 \tag{3-2}$$

Here, $\gamma(h)$is the semivariance; $z(x_i + h)$ and $z(x_i)$ are two measurements taken at location x_i and $(x_i + h)$, which are separated by a lag distance h. The following figure shows a typical semivariogram plot.

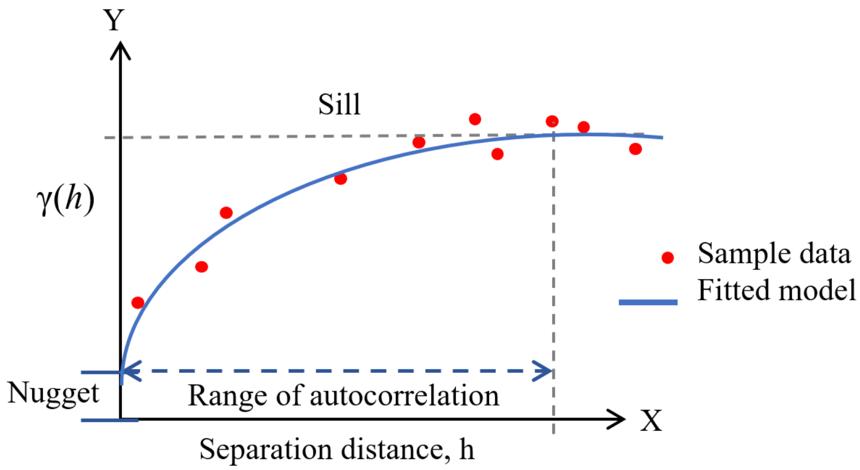

Figure 3- 3: A Typical Semivariogram with Parameters

Three basic parameters are used to define a semivariogram model: range, nugget, and sill. The value at the origin (zero separation distance) should theoretically be zero. But due to measurement and sampling errors, the value of the semivariogram at the origin could differ significantly from zero, in other words, the nugget effect. The semivariance value at which the semivariogram levels off is known as the sill parameter. Generally, a partial sill is the difference between the actual sill value and the nugget effect and is often encountered during a semivariogram analysis. The distance at which the semivariogram reaches the sill value is known as the spatial range of autocorrelation. Autocorrelation is considered as zero beyond this spatial range. Three commonly used semivariogram model forms are considered in this analysis (Bohling 2005, Olea 2006, and Solana-Gutiérrez and Merino-de-Miguel 2011). The models and their associated equations are as follows:

Spherical model:
$$g(h)=\begin{cases} c\cdot\left(1.5\left(\frac{h}{a}\right)-0.5\left(\frac{h}{a}\right)^3\right) & \text{if } h\le a \\ c & \text{otherwise} \end{cases}$$

Gaussian model:
$$g(h)=c\cdot\left(1-\exp\left(\frac{-3h^2}{a^2}\right)\right)$$

Exponential model:
$$g(h)=c\cdot\left(1-\exp\left(\frac{-3h}{a}\right)\right)$$

Here, h = lag distance, a = spatial range of continuity and c = sill.

Best-fitted semivariogram models are selected based on cross-validation results (mean standardized error, correlation between the predictors and observed values, and root-mean-square-error).

3.3.2 Spatiotemporal Semivariogram Analysis

Spatiotemporal analysis is generally conducted for variables that vary over space and time such as those road weather variables (e.g., RST, AT, DPT) considered in this study.

Spatiotemporal semivariogram modelling is conducted by integrating both spatial and temporal effects of regionalized random variables (e.g., road weather). Generally, a set of variables in a spatiotemporal field can be defined as, $z = \{z(s,t) | s \epsilon S, t \epsilon T\}$, where S = spatial domain and T = temporal domain. Thus, random field can be specified as Z is $z_i = Z(s,t), i = 1,2,3, \ldots\ldots n \times T$. Here, n = number of stations, and T = number of time points. The random fields $Z(s,t)$ can be modeled as $Z(s,t) = \mu(s,t) + \varepsilon(s,t)$, where $\mu(s,t)$ = the deterministic part and $\varepsilon(s,t)$ = the stochastic part. The deterministic part refers to the spatiotemporal trend, while the stochastic part is the zero-mean second-order stationary spatiotemporal random field (Network 2016). Spatiotemporal semivariogram modelling is conducted using the stochastic part. Spatial and temporal variances are estimated as half of the mean squared difference between data pairs separated by a user defined spatial (h_s) and temporal lag (h_t). The general equation of semivariance is presented in Equation 3-3.

$$\gamma(h_s, h_t) = \frac{1}{2n(h_s,h_t)} \sum_{k=1}^{n(h_s,h_t)} [z(s_k, t_k) - z(s_k + h_s, t_k + h_t)]^2, \qquad (3\text{-}3)$$

Here, $\gamma(h_s, h_t)$ = estimated semivariance value, $n(h_s, h_t)$ = total number of pairs in analysis domain, $z(s_k, t_k)$ = measurement at spatial location s_k and temporal location t_k (Gething et al. 2007; Shekhar and Zhou 2008). A three-dimensional spatiotemporal semivariogram is presented in **Figure 3-4.**

After constructing the empirical variogram, a mathematical model is used to smooth the graph by resolving the irregular pattern. There are several covariance models used for spatiotemporal semivariogram modelling (Shekhar et al. 2008, Pebesma and Graeler 2012, Pebesma and Gräler 2018, and Pebesma et al. 2019). The most popular and widely used covariance models are: (a) separable covariance model, (b) product-sum covariance model, (c) metric covariance model, (d) sum-metric covariance model, and (e) simple sum-metric covariance model, and their details are as follows.

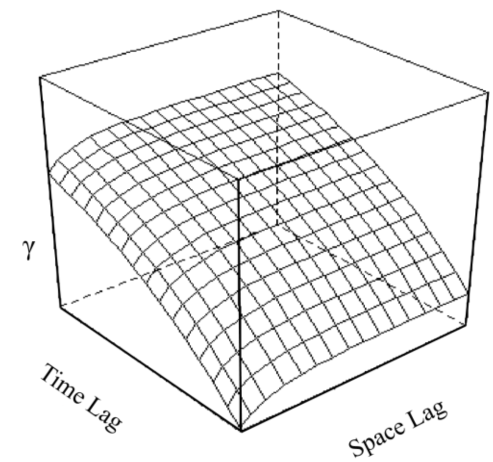

Figure 3- 4: A Typical Spatiotemporal Semivariogram

Separable Covariance Model

The separable covariance model assumes that the spatiotemporal covariance function can be represented as the product of a spatial and temporal term. The covariance function can be written as $C_{sep}(h,u) = C_s(h)C_t(u)$. Thus, the equation of variogram is $\gamma_{sep}(h,u) = sill.(\gamma_s(h) + \gamma_t(u) - \gamma_s(h)\gamma_t(u)$. Spatial & temporal sill is ignored in this model and kept constant at 1. A joint sill (= 1) is used, which combines both spatial and temporal effects.

Product-sum Covariance Model

This model introduces a new parameter k as a weighting factor of the product ($k > 0$). The equation for the covariance function is $C_{ps}(h,u) = k.C_s(h)C_t(u) + C_s(h) + C_t(u)$, and its equation for the variogram can be written as: $\gamma_{ps}(h,u) = (k.sill_t + 1)\gamma_s(h) + (k.sill_s + 1)\gamma_t(u) - k\gamma_s(h)\gamma_t(u)$. The expression of the joint sill is $sill_{st} = k.sill_s.sill_t + sill_s + sill_t$. Here, the spatial and temporal nugget is ignored and kept constant at 0; joint nugget is used to account for both spatial and temporal effects.

Metric Covariance Model

For this model, identical spatial and temporal covariance functions are assumed, except for its spatiotemporal anisotropy. Spatial, temporal, and spatiotemporal distances are treated equally in a joint covariance model by matching space and time by spatiotemporal anisotropy parameter, k (stAni). The equation for the covariance function is $C_m(h,u) = C_{joint}\left(\sqrt{h^2 + (k.u)^2}\right)$. The equation for the metric variogram can be written as: $\gamma_m(h,u) = \gamma_{joint}\left(\sqrt{h^2 + (k.u)^2}\right)$. Temporal distances are internally re-scaled to an equivalent spatial distance to determine the equivalent factor in terms of the dependence of 1m separation in a second or a minute. The expression of spatiotemporal anisotropy is $k(StAni) = \frac{\text{Spatial unit}}{\text{Temporal unit}} = \frac{\text{m}}{\text{Sec/min}}$.

Sum-metric Covariance Model

This model is a combination of spatial, temporal, and metric models. The equation for a covariance function is $C_{sm}(h,u) = C_s(h) + C_t(u) + C_{joint}\left(\sqrt{h^2 + (k.u)^2}\right)$. The equation for a sum-metric variogram can be written as $\gamma_{sm}(h,u) = \gamma_s(h) + \gamma_t(u) + \gamma_{joint}\left(\sqrt{h^2 + (k.u)^2}\right)$. Spatial, temporal, and joint nugget are estimated separately in this model.

Simple Sum-metric Covariance Model

This simplified version of the Sum-metric model restricts the spatial, temporal, and joint variograms to nugget free models. A single spatiotemporal nugget is introduced in this model. The equation for a variogram is $\gamma_{ssm}(h,u) = nug.1_{h>0,u>0} + \gamma_s(h) + \gamma_t(u) + \gamma_{joint}\left(\sqrt{h^2 + (k.u)^2}\right)$. Here spatial, temporal, and joint nuggets are set to 0; Only joint nugget are fitted.

Several previous studies attested the superior performance of the sum-metric model in fitting the spatiotemporal variogram using environmental parameters (i.e., smallest mean squared errors). Therefore, the sum-metric model is selected and used in this analysis (Ahmed et al. 2018, and Hu et al. 2017). A spatiotemporal anisotropy parameter (stAni) is used to create the joint semivariogram by combining the spatial and temporal semivariance. The number of space units equivalent to one time unit is defined as stAni. RMSE (root-mean-square-error) is used in this study to measure the goodness-of-fit of the resultant model. RWIS density and location optimization involve using the joint semivariogram parameters, which will be discussed in sections 3.4 and 3.5, respectively.

3.4 Density Optimization via Particle Swarm Optimization

Density optimization in this study is conducted in order to compare the number of RWIS stations needed per unit area in different TPI and WSI-based classes. Semivariogram parameters generated from different classes are used in the optimization process to represent the spatial characteristics of the zones. A randomly selected square region (an area of 10,000 square km) within the study area is used as the experimental boundary, wherein the solution is limited for density optimization of all classes. RWIS density curves for different TPI and WSI zones are generated based on a predefined number of RWIS stations. The marginal increment of benefit associated with each additional RWIS station is calculated to determine the optimal RWIS density.

The core of the density optimization done here is conducted using the Particle Swarm Optimization (PSO) technique. PSO is an evolutionary computation technique and population-based global optimization method developed by Kennedy and Eberhart in 1995 (Shi 2001). PSO is widely used and popular in solving heuristic problems because it can be easily implemented and is computationally inexpensive. In this optimization process, a number of n-dimensional candidate points (particle) are placed in the search space of a function, and each particle evaluates the objective function at its current location. A particle can be considered a potential solution presented by velocity and position (Wang 2012). The movement of each particle is determined based on its best fit location with one or more swarm, and the algorithm searches for optima by updating the generations (Kennedy and Eberhart 1995; Poli et al. 2007). The i^{th} particle in the search space can be represented as $x_i = (x_{i1}, x_{i2}, \dots, x_{in})$. Each particle in the swarm flies to the previous best position and global best position, named 'pbest' and 'gbest', respectively. The best previous position of the i^{th} particle can be presented as $p_i = (p_{i1}, p_{i2}, \dots, p_{in})$. The index of the best particle in the swarm is represented by the subscript g. The velocity of particle movement is represented by $v_i = (v_{i1}, v_{i2}, \dots, v_{in})$. The particle is attracted by pbest and gbest during the search process according to Equations 3-4 and 3-5.

$$v_{id} = \omega v_{id} + c_1 \zeta (p_{id} - x_{id}) + c_2 \eta (p_{gd} - x_{id}), \tag{3-4}$$

$$x_{id} = x_{id} + v_{id}, \tag{3-5}$$

Where, d = dimension, representing the total number of candidate RWIS sites, where $1 \le d \le n$; c_1 and c_2 are positive constant; ζ and η are random adjustment factors with a range of 0 to 1, and

ω is the inertia weight. The performance of each particle is measured using a predefined fitness function. However, as the original PSO is not suitable in this case, a Binary Particle Swarm Optimization (BPSO) is considered in this study to solve integer-programming problems (Kennedy and Eberhart 1997). The primary difference between these methods lies in how particles' position is updated. The sigmoid function is utilized in BPSO where every dimension in the position becomes a number between 0 and 1. The position of the particle is updated using Equation 3-6.

$$x_{id} = \frac{1}{1+e^{-v_{id}}}, \tag{3-6}$$

In the modified BPSO, a threshold probability, r is set to control whether the x_{id} becomes 1 or not, where 1 represents the selection of the element. During optimization, the total number of RWIS stations (m) is set as a constant and the algorithm is set to select the best-fit 'm' number of locations in the search space. The original BPSO shows premature convergence because of a quick loss of diversity. To treat this problem, more randomness is added into the internal mechanism of the modified BPSO to expand the search space, allowing the particle to escape from any possible local minima. Another addition is that if more than one location has the same probability for an RWIS station, a mechanism is set in the modified BPSO to select one of them as the solution randomly. Lastly, in addition to the maximum velocity set to control the speed of convergence, the inertia weight (ω), and self-learning factor (c_1) are set to decrease from 0.9 to 0.4 and 2 to 0, respectively, in the search process. On the other hand, the society-learning factor (c_2) is set to increase from 0 to 2. The parameters are chosen to ensure that the particles can fly slowly while eliminating their ability for self-learning and enhancing social-learning. The steps associated with the modified BPSO algorithm are listed below (Poli et al. 2007, Wang 2012, Gu et al. 2019).

Step 1. 'm' particles are initialized with dimensions of velocity.

Step 2. Velocities are converted to positions (probabilities) using the Sigmoid function (Equation 3-6).

Step 3. Two top probabilities are selected in each particle's position, and they are set to the selected candidate points for locating RWIS stations. Kriging variance is then calculated for all the unknown points as the fitness value.

Step 4. Memorize the current individual best positions and the global best positions.

Step 5. Update ω, c_1 and c_2 using Equation 3-7, 3-8 and 3-9.

$$\omega_{new} = \omega_{old} - \frac{\omega_{max} - \omega_{min}}{number\ of\ iterations}, \tag{3-7}$$

$$c_{1new} = c_{1old} - \frac{c_{1max} - c_{1min}}{number\ of\ iterations}, \tag{3-8}$$

$$c_{2new} = c_{2old} - \frac{c_{2max} - c_{2min}}{number\ of\ iterations}, \tag{3-9}$$

Step 6. Update each particle's velocity using Equation 3-10.

$$v_{id} = \omega v_{id} + c_1 * \zeta_{id} * \Delta x_{pid} + c_2 * \eta_{id} * \Delta x_{gid}, \tag{3-10}$$

If the $v_{id} > v_{max}$, then $v_{id} = v_{max}$.

Step 7. Update particles' positions using Equation 3-6.

Step 8. Update the individual best position and global best position by comparing fitness values. If the updated fitness value is smaller than before, accept the new solution. If not, repeat the process from Step 2.

3.5 Location Allocation via Spatial Simulated Annealing

In the third step, an innovative optimization framework is developed to optimize the spatial design of a regional RWIS network by incorporating RWIS information for spatiotemporal inference. The problem is formulated on the premise that data from individual RWIS in a region should be collectively used to maximize their overall monitoring quality that is represented by kriging variance.

In this study, a more refined location optimization model is proposed by integrating joint semivariogram parameters generated for different weather variables to represent their distinctive spatiotemporal characteristics. The objective function is formulated to minimize the sum of mean ordinary kriging (OK) estimation variance (in other words, maximizing spatiotemporal coverage) across the road network. The equations of the objective function and its related computation process are shown below.

$$G = \begin{bmatrix} \gamma(x_1, x_1)\ \gamma(x_2, x_1) \dots \gamma(x_k, x_1)\ 1 \\ \gamma(x_1, x_2)\ \gamma(x_2, x_2) \dots \gamma(x_k, x_2)\ 1 \\ \vdots \\ \gamma(x_1, x_k)\ \gamma(x_2, x_k) \dots \gamma(x_k, x_k)\ 1 \\ 1 \quad\quad 1 \quad\quad \dots \quad\quad 1 \quad 0 \end{bmatrix} \tag{3-11}$$

Where, x_i (i = 1, 2, …, k) is the sampling site of a sample subset of size k, and in this case, k is equal to the number of RWIS stations. $\gamma\left(x_i, x_j\right)$ is the semivariance between sampling site i and j.

$$\mathrm{g} = [\gamma(x_0, x_1)\ \gamma(x_0, x_2) \dots \gamma(x_0, x_k)\ 1]' \tag{3-12}$$

Where, x_0 is the estimation location and x_i (i = 1, 2, …, k) is the sampling site of a sample subset of size k. Then, the minimum mean square error for the estimation location x_0 is:

$$\sigma_{OKI}^2(x_0) = g'G^{-1}g \tag{3-13}$$

Based on the above three equations, the objective function of this work can be formulated as:

$$f(w) = \frac{\sum_{i=1}^{n-k} \sigma_{OKI}^2(x_0)}{n} \tag{3-14}$$

Subject to:

$n = \text{Total number of candidate RWIS station locations in the study area}$

The RWIS location modelling being tackled here requires mathematical and computational methods to find optimal solutions for an objective function, which is usually performed under some form of constraint. For a larger-sized optimization problem, a heuristic algorithm is an effective method for finding solutions (Revelle et al. 2008). The optimization method implemented in this study is Spatial Simulated Annealing (SSA), which is the spatial counterpart to simulated annealing (SA) (Kirkpatrick et al. 1983). SSA is a popular heuristic algorithm used to solve spatial optimization problems and has gained recognition for generating more reliable location solutions (van Groenigen and Stein 1998, van Groenigen et al. 1999, Heuvelink et al. 2006, Brus and Heuvelink 2007). SSA works by slightly perturbing previous sampling designs using random search techniques. As the optimization process continues, it is necessary to avoid local minima, and thus SSA not only accepts improving solutions, but also worsening solutions based on a certain probability. The probability of accepting worsening solutions is typically set initially at 0.2, and this probability decreases exponentially to zero as the number of iterations increases. The workflow of SSA for a certain number of RWIS stations is displayed in **Figure 3-5**.

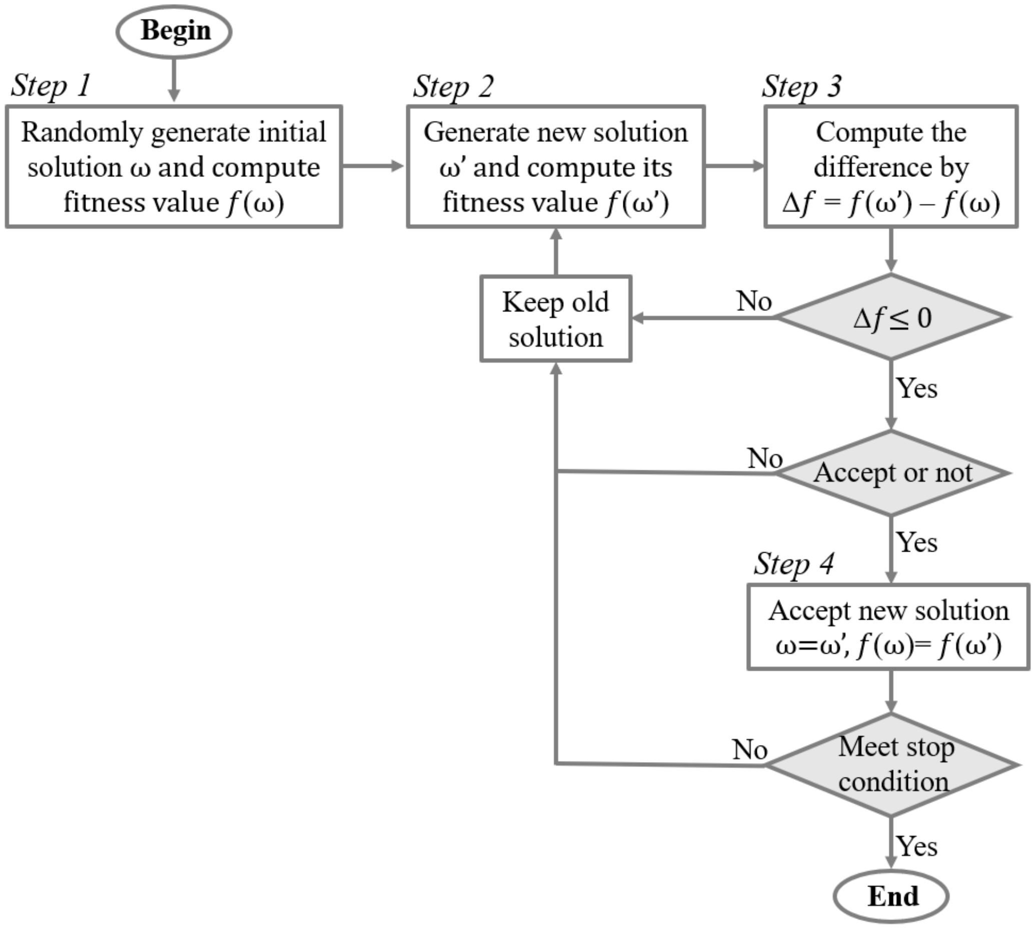

Figure 3- 5: Workflow of Spatial Simulated Annealing

The optimization process is iterative, where stations are added incrementally, and locations are selected based on heuristic attempts to minimize the objective function. When adding new stations, the placement area is limited to a square region within the study area. This will be done to reduce computational complexity and algorithm run-time. The number of RWIS stations to be located in this square region is arbitrarily limited to 10, which is equal to the existing number of RWIS stations in the square region. Regarding the optimization process, two top criteria will be implemented. If the number of iterations exceeds 100000, the optimization process will stop. And if no improvements are made in the objective function after 200 iterations, the algorithm is set to automatically stop (Graler et al. 2016).

In addition to considering various weather variables, the modified network optimization model also incorporates the distribution of traffic demand by taking into account collision and AADT data. The accident rate is calculated using Equation 3-15 as follows (Golembiewski and Chandler 2011).

$$\text{Crash rate, CR} = (\text{number of accident} * 1000000) \;/\; (\text{AADT} * 365) \tag{3-15}$$

In this context, the term "number of accidents" represents the total count of accidents observed during the study period. In this study, collisions occurring during the winter months (November to March) were considered. In addition, several factors were considered to identify the collisions caused by adverse weather conditions. Detailed description is provided in section 5.4.2. AADT, on the other hand, represents the average daily traffic volume for a specific road or road section. It serves as a measure of the number of vehicles passing through that area on a daily basis. Consequently, the resulting value of CR obtained from Equation 3-15 provides an estimate of the frequency of accidents. It indicates the number of accidents that occur per million entering vehicles.

3.6 Bi-Level Sequential Optimization Model

To determine not only the location, but also the type of RWIS stations (R-RWIS and M-RWIS), a bi-level sequential optimization model is developed. This model generates the optimal locations along with the type of RWIS stations needed for those locations. Initially, single-variable semivariogram model and multi-variable semivariogram models are employed to construct RWIS density curves through the implementation of SSA. Specifically, the single-variable semivariogram model delineates local weather characteristics and is employed in depicting M-RWIS, whereas the multi-variable semivariogram model captures regional road weather characteristics and is applied in illustrating R-RWIS. The density curves are then compared to determine the gap in monitoring coverage associated with two types of RWIS stations.

Figure 3-6 is a representation of density curve comparison for R-RWIS and M-RWIS. Here, the x-axis represents the number of RWIS stations, and the y-axis represents the criterion value. The criterion value is the objective function value generated from density optimization algorithm. The red dotted line shows the density curve for R-RWIS and blue dotted line shows the density curve for M-RWIS. Generally, with an increase in station number, criterion value decreases, meaning an increase of monitoring coverage. An R-RWIS network is supposed to provide greater monitoring coverage than a network with M-RWIS, which is represented by the gap between density curves. This phenomenon suggests that even with an infinite number of M-RWIS integrated into the network, achieving monitoring coverage equal to that of the R-RWIS network remains unachievable. Furthermore, this gap also indicates that there is a certain number of R-RWIS in a network that can be replaced by an equivalent number of M-RWIS. This number of R-RWIS can be defined as ‘Replaceable R-RWIS’ as shown in the figure below. The residual segment of R-RWIS is deemed non-replaceable, signifying that the network must maintain this minimum number of R-RWIS for optimal performance.

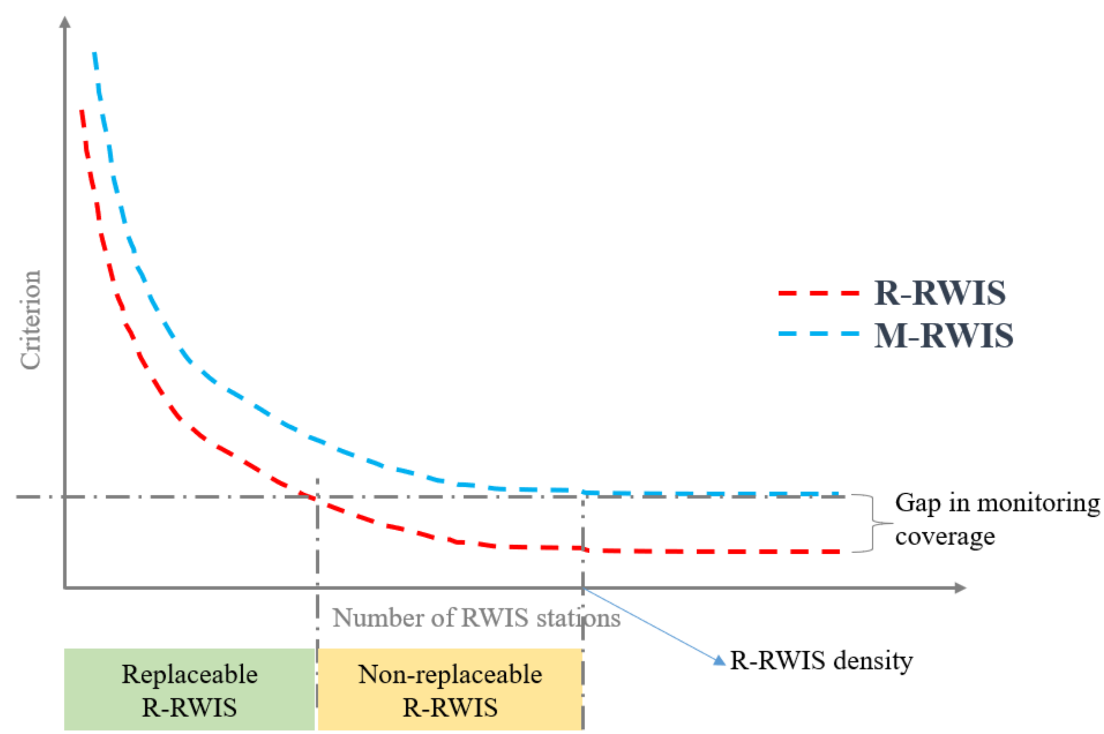

Figure 3- 6: Concept of determining replaceable and non-replaceable R-RWIS

Following the identification of both the replaceable and non-replaceable quantities of R-RWIS, the subsequent phase involves generating comparable combinations. These combinations, defined as configurations of R-RWIS and M-RWIS that offer uniform monitoring coverage across the network, are derived through the process outlined in **Figure 3-7**. With the known density of R-RWIS, a segment is designated as non-replaceable, while another portion is replaceable by an equivalent number of M-RWIS. Building upon this premise, the focus shifts to the replaceable segment, where any number within this range can be substituted. To generate these combinations, two distinct algorithms operate iteratively—one for determining the number of R-RWIS and another for establishing the equivalent number of M-RWIS through criterion checks to ensure similarity in monitoring coverage. The output of this procedure yields a collection of comparable RWIS combinations. In the final step, a cost function is applied to identify the most cost-effective combination.

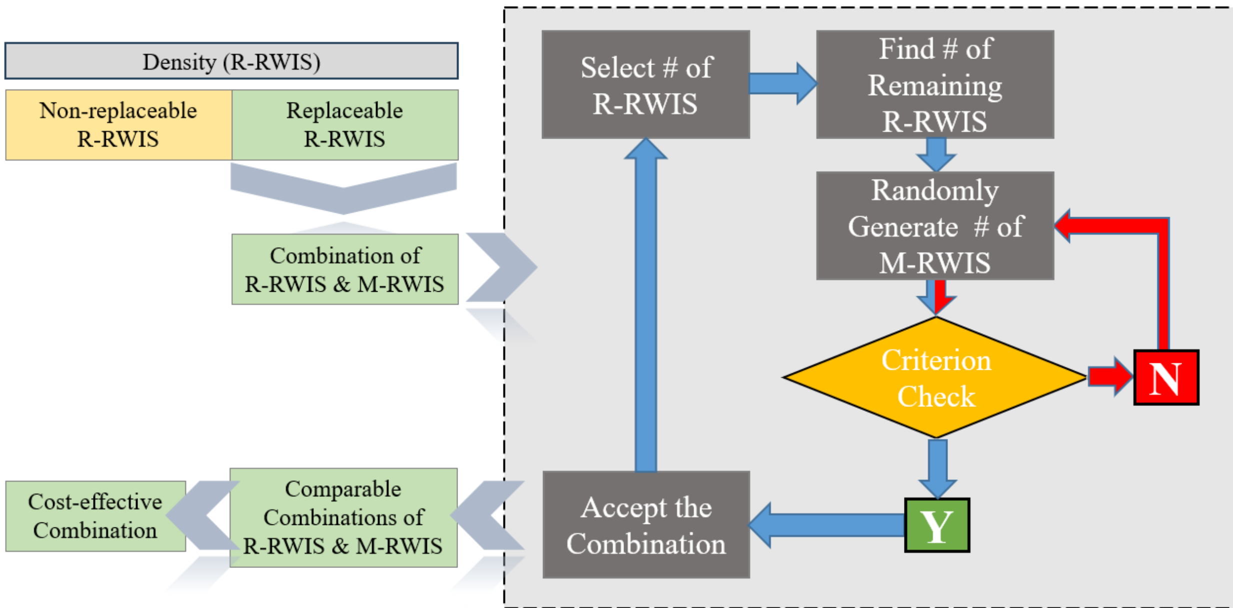

Figure 3- 7: Concept of generating comparable combinations of R-RWIS and M-RWIS

After generating optimal RWIS network, its impact on transportation system can be evaluated using impact assessment as discussed in the following section.

3.7 Assessment of RWIS Network Coverage and Safety Evaluation

Quantifying the safety effectiveness of RWIS presents significant challenges due to the inherent complexities and the multifaceted nature of how RWIS information is utilized by winter road maintenance personnel. Specifically, the intricate interplay between the collected data and its application in real-time decision-making processes complicates this task. The limited evaluation efforts in this area highlight a critical gap in understanding the benefits of RWIS. To bridge this gap, the Network Coverage Index (NCI) is introduced as a surrogate measure to evaluate the monitoring capabilities of RWIS configurations. NCI facilitates the safety evaluation of the RWIS network by quantifying its spatial coverage and thereby linking it to potential safety outcomes. The subsequent sections provide a detailed explanation of this approach.

3.7.1 Determination of Network Coverage Index (NCI)

As described, the NCI is used in this thesis to rate the monitoring capabilities of a defined RWIS configuration for a specific region. It is a surrogate measure that ranges between 0 and 1, where 0 represents no monitoring coverage, and 1 represents complete network coverage.

Determining NCI requires the use of kriging, which is a widely used geostatistical technique that provides the best linear unbiased estimate (BLUE) for variables that vary over space (Yeh et al. 2006). The weighted average of the observed data was used in kriging to predict values at unsampled locations, where the weights were determined based on the separation distance between the sampled points and unsampled locations. Kriging provides estimates at unknown locations along with estimation errors by quantifying the spatial variability over the area of interest (Goovaerts 1997). Ordinary Kriging (OK) is a form of kriging that assumes the mean to be unknown but constant over each local neighborhood (Goovaerts 1997, Ahmed et al. 2008). OK estimation variance for an estimation location, x_0 can be defined by the following equation:

$$\sigma_{OK}^2(x_0) = g' G^{-1} g \tag{3-16}$$

Where, G is the semivariance matrix between the observations and g is the semivariance matrix between observations and unsampled points. The equations of G and g are given below:

$$G = \begin{bmatrix} \gamma(x_1, x_1) & \gamma(x_2, x_1) & \dots & \gamma(x_k, x_1) & 1 \\ \gamma(x_1, x_2) & \gamma(x_2, x_2) & \dots & \gamma(x_k, x_2) & 1 \\ & & \vdots & & \\ \gamma(x_1, x_k) & \gamma(x_2, x_k) & \dots & \gamma(x_k, x_k) & 1 \\ 1 & 1 & \dots & 1 & 0 \end{bmatrix} \quad \text{and} \quad g = [\gamma(x_0, x_1)\ \gamma(x_0, x_2) \dots \gamma(x_0, x_k)\ 1]'$$

Here, x_i (i = 1, 2, …, k) is the sampling site of a sample subset of size k, where k = number of RWIS stations. $\gamma(x_i, x_j)$ is the semivariance between sampling site i and j.

Semivariance values are calculated by constructing empirical semivariograms from RWIS measurements. A semivariance is a statistic that measures the similarity between two measurements as a function of separation distance (Olea 2012). Semivariance can be calculated by taking the average squared differences between two measurements in a spatial domain separated by a specific lag distance. The general equation of semivariance estimation is presented in Equation 3-17.

$$\gamma(h) = \frac{1}{2n(h)} \sum_{i=1}^{n(h)} [z(x_i + h) - z(x_i)]^2 \tag{3-17}$$

Here, $\gamma(h)$ is the estimated semivariance; $z(x_i + h)$ and $z(x_i)$ are two measurements taken at location x_i and $(x_i + h)$ separated by a lag distance h.

Since RWIS measurements (i.e., road weather variables) vary over both space and time, spatiotemporal semivariogram models are employed in this study. Spatiotemporal modeling optimizes parameter estimations for unsampled locations and captures the possible spatial and temporal autocorrelation associated with the RWIS variables. A set of variables, z in a spatiotemporal field can be defined as a combination of spatial domain (S) and temporal domain (T): $z = \{z(s,t) | s \epsilon S, t \epsilon T\}$. The general equation of a random field Z can be defined as: $z_i = Z(s,t),\ i = 1,2,3, \ldots\ldots n\ \times T$. Here, n = number of sampled locations and T = number of points in time. The most common formula for spatiotemporal semivariance estimation is shown in Equation 3-18.

$$\gamma(h_s, h_t) = \frac{1}{2n(h_s,h_t)} \sum_{k=1}^{n(h_s,h_t)} [z(s_k, t_k) - z(s_k + h_s, t_k + h_t)]^2 \tag{3-18}$$

Here, $\gamma(h_s, h_t)$ is the estimated semivariance, $n(h_s, h_t)$ is the total number of pairs in the random field, $z(s_k, t_k)$ is the observation at location s_k and temporal point t_k, $z(s_k + h_s, t_k + h_t)$ is another observation at location $(s_k + h_s)$ and temporal point $(t_k + h_t)$. The observations pairs are separated by a user-defined spatial lag (h_s) and temporal lag (h_t) (Biswas and Kwon 2020, Gething et al. 2007, Shekhar et al. 2008, Network 2016) [18, 27-29]. Spatial and temporal semivariograms can be combined using spatiotemporal anisotropy to estimate the joint semivariogram that can preserve both spatial and temporal effect. The joint semivariogram models developed in our previous effort are adopted in this study for conducting kriging interpolation (Biswas and Kwon 2022).

Based on the formulation shown in Equation 3-16, we can drive NCI using estimation error (kriging variance) under the assumption that a higher estimation error represents an increased need for an RWIS station. Since the optimization is aimed at finding locations that minimize total estimation error, this would mean the optimal RWIS network provides the best monitoring coverage because it has the lowest estimation error. Therefore, the kriging variance is inversely proportional to NCI, and the estimation error can be translated into NCI using the following equation.

$$NCI = \frac{K}{Kriging\ variance} \tag{3-19}$$

Here, K is a proportional factor and is sensitive to the regional attributes and can be established by determining the kriging variance at optimal conditions.

3.7.2 Safety Evaluation of RWIS Network

The collision reduction factor or the percent reduction in collisions is estimated in our previous efforts using the state-of-the-art before-and-after Empirical Bayes (E.B.) method (Sharma 2022). E.B. accounts for the Regression-to-the-Mean (RTM) artifact by incorporating two separate pieces of information; (i) the collision history of the treatment sites and (ii) their predicted collision frequencies obtained from the Safety Performance Function (SPF). The ratio of the observed and expected number of collisions in the post-implementation period is the collision reduction factor of the countermeasure. The overall process was divided into three steps. First, the expected collision frequency in the before period was estimated using the following equations.

$$N_{Expected,B} = w \times N_{Predicted,B} + (1 - w) \times N_{Observed,B} \tag{3-20}$$

$$w = \frac{1}{(1 + k \times N_{Predicted,B})} \tag{3-21}$$

Where, $N_{Expected,B}$ is the expected collision frequency in the before-period, w is the weighted adjustment factor between 0 to 1, $N_{Predicted,B}$ is the predicted collision frequency is the before-period, $N_{Observed,B}$ is the observed collision frequency in the before-period, and k is the negative binomial overdispersion parameter estimated from SPF.

A weighted sum of two separate pieces of information is used in this step. The predicted collisions for each site in the before-period are calculated using the calibrated SPF equation. In contrast, the observed collision frequencies come directly from the collected dataset. The calibrated SPFs are developed for several RWIS stations in Iowa. The calibrated SPF equation is shown below:

$$\mu = e^{(-10.4861\ )}L^{(0.8246)}.V^{(0.2291)} \tag{3-22}$$

Here, the SPF was developed for total collisions regardless of the severity type due to limited dataset. Site specific parameters used for calibration includes - road length, traffic volume (AADT), number of lanes, pavement type, etc. However, only road length and traffic volume has been found statistically significant coefficients and provided meaningful SPF.

Using this equation, the collision frequency in the before-period (μ) can be predicted using road length (L) and traffic volume (V). Additionally, there are various confounding factors, such as improvements in the roadway, general traffic safety trends, and changes in weather conditions that cannot be captured by the SPFs. Therefore, Yearly Calibration Factors (YCFs) are also incorporated into the safety evaluation process.

In the second step, the expected collision frequencies in the after period, $N_{Expected,A}$ is calculated. The calibrated SPF equations were used to estimate an adjustment factor, Adj, that captures the traffic volume variations during the before and after periods.

$$N_{Expected,A} = N_{Expected,B} \times Adj \tag{3-23}$$

The last step involves estimating the effectiveness of the countermeasure. The safety effectiveness or percent collision reduction due to countermeasure implementation is estimated using the following equation. Note that an odds ratio is used to account for potential bias.

$$Percent\ Collision\ Reduction = 100 \times (1 - Odds\ Ratio) \tag{3-24}$$

After quantitatively measuring the impact of RWIS stations on traffic safety, the benefit associated with an RWIS configuration can be evaluated by assessing NCI. By utilizing the safety evaluation output, the collision reduction for each RWIS station can be calculated. The values of NCI for a set of RWIS network configurations are then plotted against the number of collision reduction for corresponding RWIS setup. Here, collision reduction is used as a performance indicator of safety benefits. A higher number of collision reduction is expected to be associated with an RWIS network of lower kriging variance, thus higher NCI value.

Chapter 4

Development of Nation-wide Optimal RWIS Density Guidelines[1,2]

4.1 Introduction

Due to the numerous benefits associated with RWIS information, transportation agencies have invested millions of dollars in deploying RWIS stations to improve the monitoring coverage of winter road surface conditions. However, the design of these networks often varies by region. It is not entirely clear how many stations are necessary to provide adequate monitoring coverage under different conditions. Hence, this chapter focuses on answering the following research question — how many RWIS stations are required for a region with varying environments to provide sufficient coverage by considering spatiotemporal characteristics of road weather variables? In particular, we are interested in investigating how optimized RWIS station densities relate to topographic and weather characteristics. In the initial stage, the study area comprising 20 different states in the US is classified into topographic position index (TPI) and weather severity index (WSI) based zonal classes. A series of geostatistical semivariogram models is then constructed and compared for each TPI and WSI-zones to measure relative topographic variation and weather severity. Subsequently, a heuristic optimization is applied to map the optimum number of RWIS stations across several topographic and weather zones.

4.2 Characterizations of Topography and Weather

As mentioned previously, topography and weather severity-based classifications were conducted to evaluate the relationship between RWIS station density, topographic variability, and weather characteristics for the regions under investigation. TPI was calculated using the DEM data based on Jenness's algorithm (Jenness 2006). Based on TPI values, the study area was classified into three different landform groups (flatland, hilly, and mountainous).

---

[1] Biswas S., M. Wu, S. J. Melles, and T. J. Kwon (2019). Use of Topography, Weather Zones, and Semivariogram Parameters to Optimize Road Weather Information System Station Density across Large Spatial Scales. Transportation Research Record: Journal of the Transportation Research Board, vol. 2673, no. 12, pp. 301-311. https://doi.org/10.1177/ 0361198119846467

[2] Biswas, S., and T. J. Kwon (2020). Developing Statewide Optimal RWIS Density Guidelines Using Space-Time Semivariogram Models. Journal of Sensors, vol. 2020, Article ID 1208692. https://doi.org/10.1155/2020/1208692

On the other hand, the WSI parameter was used for weather-based classifications using an ArcGIS shapefile generated for the United States by Meridian Environmental Technology, Inc. (Mewes 2011). Lower WSI values indicate a less severe weather zone, whereas more severe weather zones are associated with higher WSI values. According to the WSI values, the study area was categorized into four WSI-based classes: less, moderate, high, and extremely high severe weather zones. Details of data description and zonal classification are presented below.

4.2.1. Topographic and Weather Severity Data

The study area was selected based on data availability and completeness of the proposed study which will cover varying topography and weather conditions that can be challenging for driving. Twenty united states were selected for topographic and weather severity analysis named as: California (CA), Colorado (CO), Delaware (DE), Iowa (IA), Illinois (IL), Kansas (KS), Michigan (MI), Minnesota (MN), North Dakota (ND), New York (NY), Ohio (OH), Pennsylvania (PA), Utah (UT), Virginia (VA), Wisconsin (WI), Indiana (IN), Kentucky (KY), Nebraska (NE), Nevada (NV) and Wyoming (WY). Selected states provide a broad enough region, as well as a range of topographic and weather conditions, in which to explore our approach.

Topography Data

Digital Elevation Model (DEM) for twenty US DOTs with a 30 m resolution (28 GB) was downloaded from the United States Geological Society (USGS, https://earthexplorer.usgs.gov/) for topographic characteristic analysis in ArcGIS 10.4.1. The resulting TPI map file has a size of 49 GB.

Weather Severity Data

The ESRI shapefile containing the weather severity index used in this study was generated by Meridian Environmental Technology.

4.2.2. Landform Classification based on TPI and WSI

TPI Based Classification

Topographic features of the twenty US states were studied, quantitatively described, and classified using topographic position index (TPI). The TPI map of our study area is shown in **Figure 4-1**, and the range of values was between – 565 and 5293. As our primary interest in using TPI-based analysis was landform classification over a large extent, the absolute value of TPI was used. A large portion of our study area had TPI values below 75; more specifically, IA, MN, OH, KY, and a large portion of NE and KS. We designated these areas as TPI class 1 (i.e., the light coral colored zone in **Figure 4-1**). In addition, TPI values between 75 and 1500 can be seen at the edges of KY, OH and MN, and another large part of the study area had a TPI range between 1900 and 2100 with a minor area of 1500 to 1900. These zones were categorized as TPI 2 (gray colored zone in **Figure 4-1**) covers a small part or KS and a sizable portion of NE, CO and WY. Large variations in TPI can be seen in the remaining study area, including a large part of CO and WY, where the range in TPI varied from 1900 to 5293 with a minor area under 1900. These remaining areas were classified as TPI class 3.

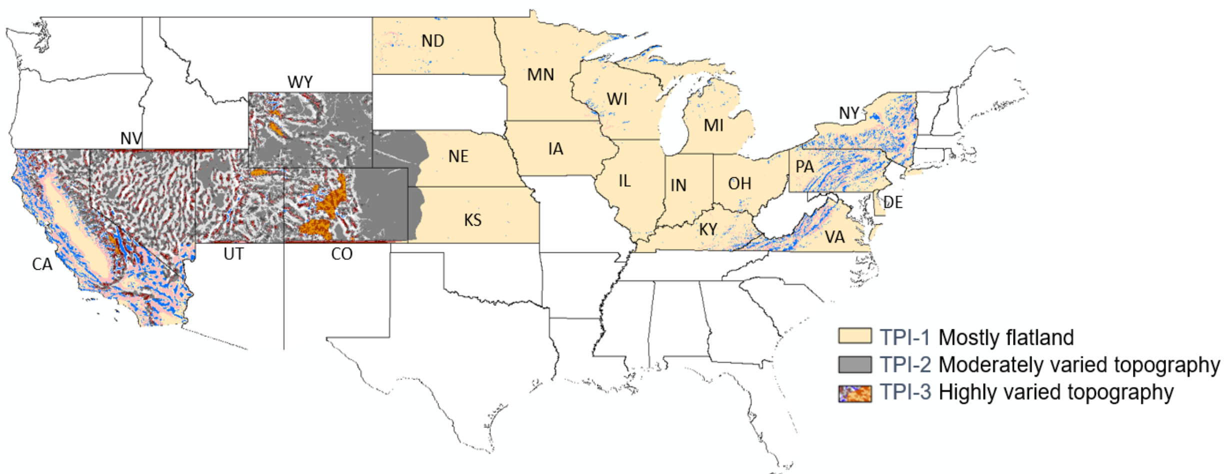

Figure 4- 1: TPI Map of the Study Area

WSI Based Classification

The study area was also classified into four WSI classes (**Figure 4-2**), where WSI ranged from 7.6 to 301.7 Class – WSI 1 (blue coloured zone) includes zones with WSI values less than 25. This area nearly covers all of KY and KS states. The second class – WSI 2 (green colored zone) represents regions with WSI between 25 and 50. OH, IA, NE, southern half of MN, and a small portion of CO are captured by this class. A relatively large region was between 50 to 100 WSI, for which we labeled as class WSI 3. WSI 3 regions cover the northern part of MN, a small portion of OH and CO, and part of WY. The remaining area has a considerable variation in WSI values, from 100 to 301.7. These areas were considered mountainous and were classified into WSI class 4, which is quite similar to TPI class 3.

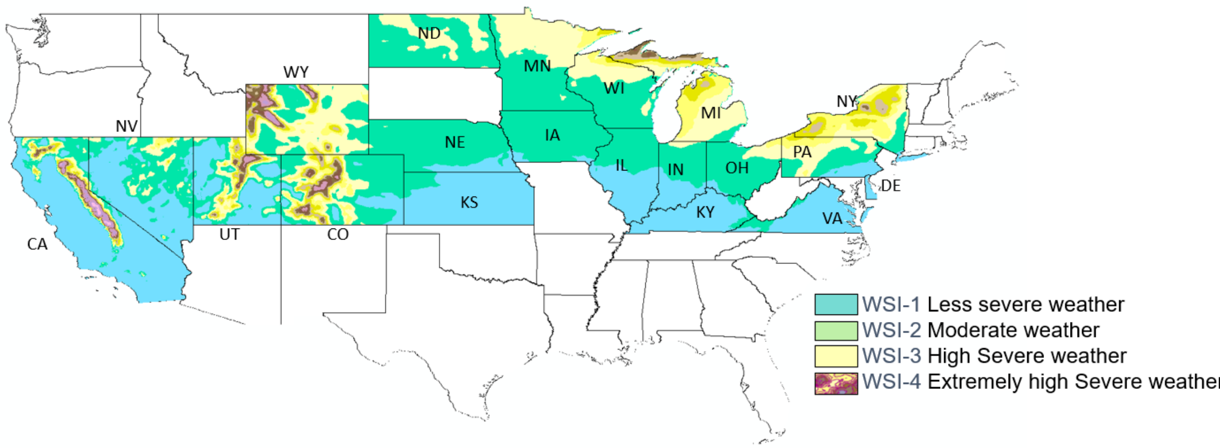

Figure 4- 2: WSI Map of the Study Area

TPI – WSI Combined Map

Figure 4-3 shows the TPI-WSI zones together. The colors represent the several classes of TPI and the contours represent the WSI classes. In general, the severity of weather increases from south to north, except in the mountainous regions of CO and WY. A large part of the study area was under class – TPI 1, which was divided into three WSI classes. Similarly, class – WSI 2 included both TPI 1 and TPI 2 classes.

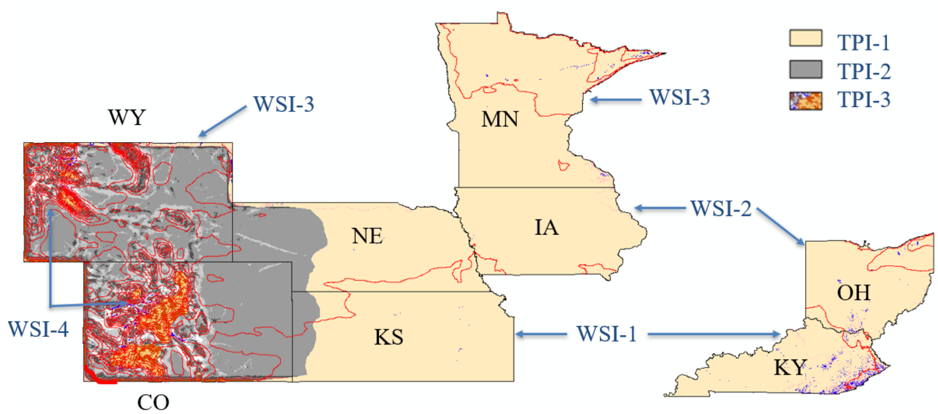

Figure 4- 3: TPI - WSI Map of Eight States

This study examined, quantitatively described, and compared the topographic and weather features of the area under investigation. The parameters used for comparing the topographic and weather characteristics of the study area were TPI and WSI, respectively. Overall, twenty US states were classified into three TPI classes and four WSI classes.

4.3 Research Procedure

Spatiotemporal semivariogram modelling was used in this study to evaluate the spatiotemporal variability of RWIS measurements for TPI and WSI-based classes. RWIS data for the winter season was downloaded, processed, and a space-time matrix was formulated as the input for the spatiotemporal analysis. The dataset was classified based on previously developed TPI and WSI classes, and a separate analysis was conducted for each month and zone, which were aggregated to generate a seasonal spatiotemporal autocorrelation range for the TPI and WSI classes. Optimal RWIS densities were then determined by examining the spatiotemporal semivariogram analysis results. Density per unit area was calculated and compared for different topographic and weather-based zones. The research methodology of this study can be summarized into the following steps:

a. Develop spatiotemporal semivariogram models to examine spatial and temporal autocorrelation of RWIS data.
b. Evaluate the effective spatial and temporal continuity range under different topographic and weather settings.
c. Examine the hypothesis that the spatiotemporal variability of road weather data is dependent on the topographic variation and weather severity of the region.
d. Determine the optimal density of RWIS stations using modified particle swarm optimization (PSO) for different topographic and weather classes.
e. Compare the optimal RWIS density per unit area for different classes.

Figure 4-4 presents an overview of the proposed methodology for RWIS density determination.

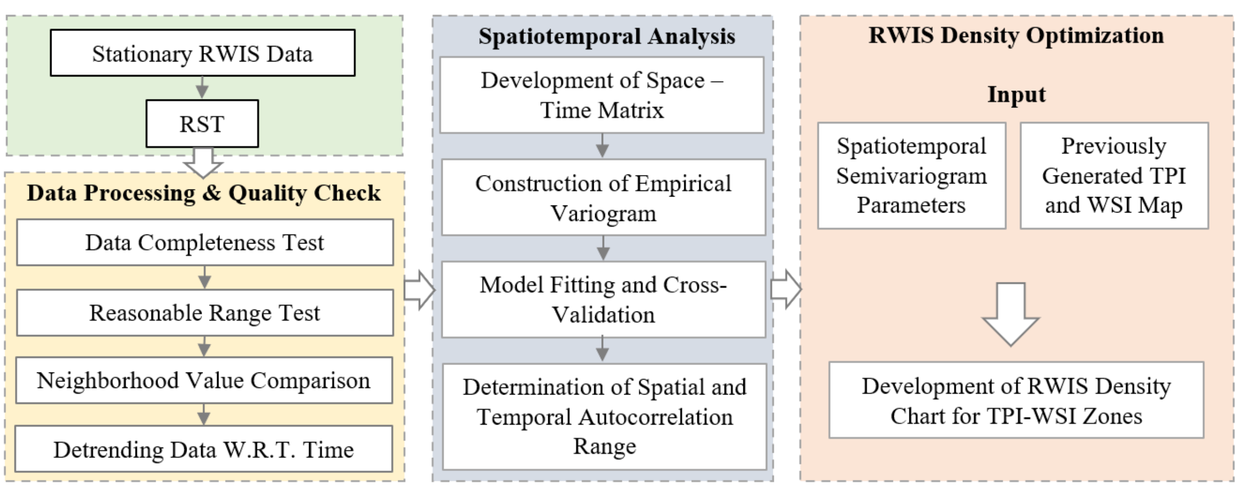

Figure 4- 4: An Overview of the Proposed Methodology

4.4 Study Area and Data Description

4.4.1 Study Area and RWIS Network

The study area for RWIS density optimization was selected based on RWIS data availability and distribution of RWIS stations to cover varying topography and weather conditions. Only eight states had sufficient data, including Colorado (CO), Iowa (IA), Kansas (KS), Minnesota (MN), Ohio (OH), Kentucky (KY), Nebraska (NE) and Wyoming (WY). These eight states provide a broad enough region, as well as a range of topographic and weather conditions needed for our approach. The total available RWIS station count for the states are CO (147), IA (86), KS (56), KY (38), MN (98), NE (70), OH (182) and WY (81), and the study period selected for this project included one winter season (October 2016 to March 2017) to best capture challenging winter driving conditions. The distribution of RWIS stations for the study area is presented in **Figure 4-5**.

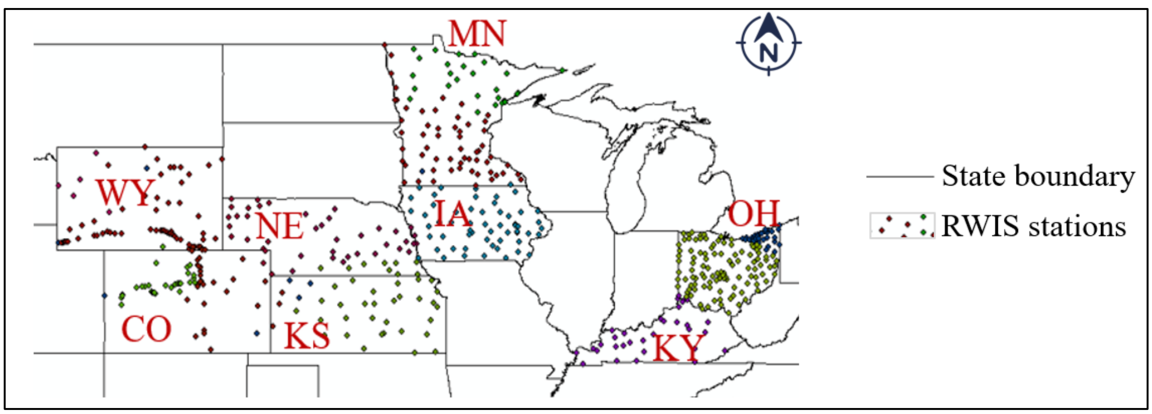

Figure 4- 5: Distribution of RWIS Station for Eight United States

4.4.2 Data Description

The RWIS data sets used were downloaded from two different sources. First, RWIS data for IA, CO and KS were downloaded using the wget script from the WxDE website (Weather Data Environment: https://wxde.fhwa.dot.gov/) using Linux (Shacklette 2007). More than 3300 GZ files were captured and extracted. Twelve algorithms were then used to check the stationary RWIS data generated from WxDE website for quality issues. Among them, IQR (Interquartile Range) spatial and Barnes spatial quality check (both tests verify that observations from similar sensors are close to each other) results were recommended to filter the RST data in this analysis. Upon completion of data quality check, RWIS data for MN, OH, KY, NE and WY were downloaded from IOWA State University (http://mesonet.agron.iastate.edu/RWIS/). Measurements from a typical RWIS station included, but are not limited to, air and surface temperature, dew point temperature, visibility, wind speed, and road surface conditions collected every 15 to 20-minutes. In total, 1026 stations were included in the analysis, and 4368 hours of data were used.

4.4.3 Data Processing

RWIS data were processed to remove the missing and erroneous data using five steps: (a) Data completeness test to identify missing data; (b) Reasonable range test to find erroneous data; (c) Cross-checking RST data with air-temperature data; (d) RST data pattern analysis; and (e) De-trending RST data with respect to time using GAM.

To quickly summarize those five steps, data completeness was checked by identifying the total missing data for each sensor. If the total amount of missing data was over fifteen percent, the associated sensor ID was marked, and the data from that sensor was not used for analysis. Reasonable range was tested based on historical data ranges for the associated region and month. Filtered RST data were then cross-checked with air-temperature data ranges for any possible outliers. An RST data pattern analysis was performed by plotting the day of the month versus the average daily temperature for all selected sensors for each state and month. All selected sensors were expected to show a similar pattern throughout the month. If any unusual pattern was noticed, the RST data for the associated sensors were further investigated. In total, 48 sets of data (six months for eight states) were analyzed using the above-described process. Finally, RST data was de-trended with respect to time using a GAM to incorporate shorter scale variation in the temporal domain, where GAM worked as a generalized linear model with linear predictors. The GAM function was formulated as: $m = \beta_0 + f_1(x_1) + f_2(x_2) + \cdots + f_i(x_i)$. Here, m = variable of interest, β_0 = intercept, $f_i(x_i)$ = smooth function of predictor x_i. The smooth function can be expressed as: $f_i(x_i) = \sum_{n=1}^{m} s(x_n)$ (Wang et al. 2019, Hastie and Tibshirani 1990).

As a precursory step to better understand the data, the descriptive statistics (means and standard deviations) were generated and revealed relatively less variation in average monthly temperatures in the mid-winter months than in the shoulder months. Overall minimum and maximum temperatures for the study area were: -30.3˚C to 51.5˚C (-22.5˚F to 124.7˚F). **Table 4-1** presents the maximum, minimum, average, and standard deviations of RST for the study area. Because erroneous data were detected in Kentucky (November 2016), it was excluded from the analysis.

Figure 4-6 shows the seasonal maximum, minimum, average, and standard deviation of RST for the study area.

Table 4-1. Descriptive Statistics of RST for the Study Area (Winter Months of 2016-17)

States		**CO**	**IA**	**KS**	**MN**	**OH**	**KY**	**NE**	**WY**
Oct-16	**Min**	-6.7	-1.1	0.8	-2.6	-1.5	-7.2	-6.2	-9.4
	Average	15.5	16.9	20.8	12.6	18.3	20.0	16.7	11.9
	Max	37.8	41.5	46.2	41.0	47.0	39.5	44.7	45.1
	StDev	9.0	6.9	8.2	7.0	6.9	6.9	7.7	8.1
Nov-16	**Min**	-29.8	-8.6	-7.6	-9.9	-24.0	-	-12.5	-15.9
	Average	7.6	9.5	12.5	6.0	10.1	-	8.7	5.0
	Max	46.9	38.3	39.5	30.2	35.5	-	34.4	30.6
	StDev	9.2	7.1	7.8	6.2	6.3	-	8.0	8.0
Dec-16	**Min**	-22.6	-29.5	-24.9	-29.9	-19.6	-10.4	-28.1	-29.5
	Average	-1.5	-2.7	0.8	-6.6	1.7	4.5	-3.3	-5.4
	Max	26.6	18.8	22.9	11.7	51.5	21.1	17.8	17.6
	StDev	7.4	6.4	7.3	6.8	5.7	4.8	6.2	6.3
Jan-17	**Min**	-26.9	-24.0	-20.9	-30.3	-19.1	-17.2	-26.9	-29.1
	Average	-0.6	-2.1	2.7	-6.8	2.9	6.4	-2.5	-5.5
	Max	37.8	19.6	28.5	14.2	25.5	21.8	19.9	21.0
	StDev	7.7	6.0	7.4	7.9	6.3	5.1	6.3	6.9
Feb-17	**Min**	-17.7	-15.9	-10.8	-26.0	-22.7	-9.6	-19.4	-23.4
	Average	6.0	5.6	9.8	-1.5	7.1	9.3	4.4	0.9
	Max	37.7	32.4	38.6	27.2	34.5	30.4	36.1	30.7
	StDev	8.9	8.2	9.0	8.1	7.3	5.9	8.0	7.7
Mar-17	**Min**	-17.2	-16.4	-7.3	-22.0	-10.8	-8.4	-11.5	-17.5
	Average	11.0	7.0	13.9	2.5	9.0	12.1	9.4	7.2
	Max	38.3	36.1	48.7	36.3	36.0	31.7	43.7	39.5
	StDev	10.2	7.6	9.5	8.7	7.1	6.5	8.3	9.3

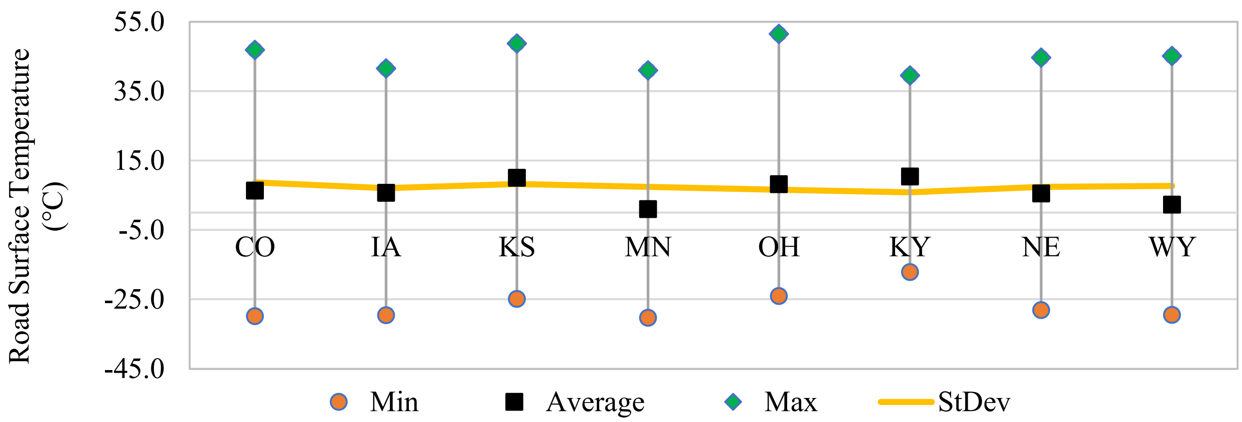

Figure 4- 6: Seasonal Road Surface Temperature Details for Eight States

Spatiotemporal semivariogram modelling was performed using the R statistical package - version 3.2.5 (Pebesma 2004, Graler et al. 2016, R Core Team 2018), and RWIS density optimization was coded in Python. To improve the computational efficiency, all optimizations undertaken in this study were run on the supercomputer "beluga" from the "University of Alberta", managed by Calcul Québec and Compute Canada (https://www.computecanada.ca/). It contains 32 CPUs, each of which runs on 2.4 GHz with 1 GB of allocated memory.

4.5 Spatiotemporal Semivariogram Modelling Results

To maintain a level of granularity to the data, the RWIS data for the study area were processed on a monthly basis from October 2016 to March 2017. Road surface temperature (RST) data were aggregated using twenty-minute intervals for time domain analysis. Space-time matrix was then formulated for each of the TPI and WSI zones. Spatiotemporal autocorrelation of RST for each study zone was then analyzed using spatiotemporal variogram modelling methods using the gstat package in R (Pebesma 2004, R Core Team 2018). Spatial and temporal continuity ranges for the analysis months are presented in Appendix-A. According to Appendix-A, higher spatial and temporal variations occurred when topographic and weather variations increase. Seasonal spatiotemporal analysis results for TPI and WSI zones are presented in **Figure 4-7**.

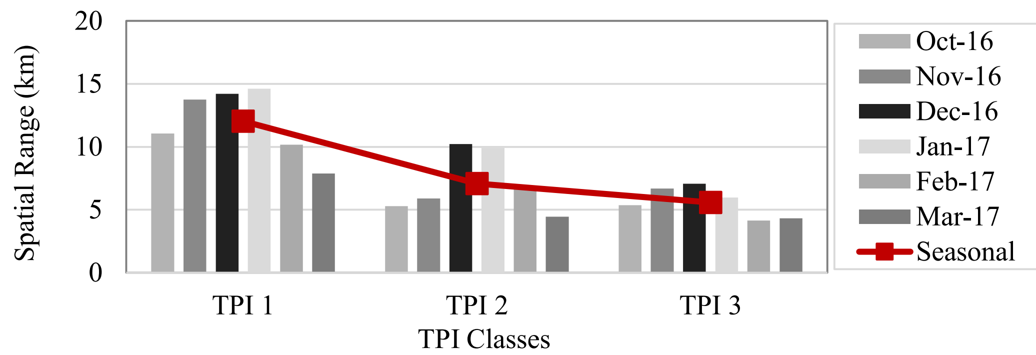

(a)

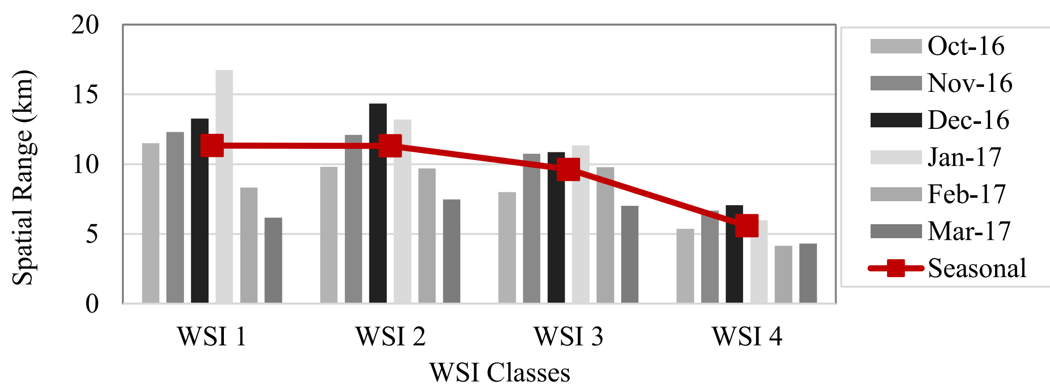

(b)

Figure 4- 7: Spatial Semivariogram Ranges for (a) TPI Class and (b) WSI Classes

According to **Figure 4-7**, relatively higher spatial and temporal ranges were obtained for TPI class 1 (flatland area), followed by class 2 and 3 representing hilly and mountainous areas, respectively. Similar results were obtained for weather-based classes, where regions with less topographic variation and less severe weather have a higher spatial and temporal range (depicted in **Figure 4-8**). The range of autocorrelation decreased with increases in topographic variation and weather severity. In general, there was a trend of higher autocorrelation range during mid-winter months compared to shoulder months.

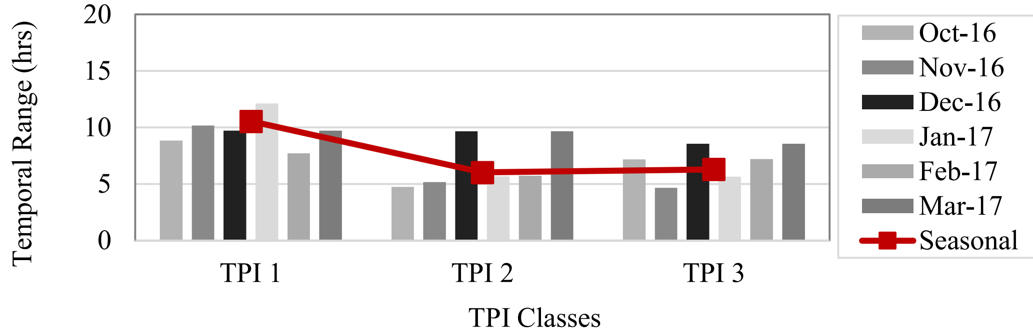

(a)

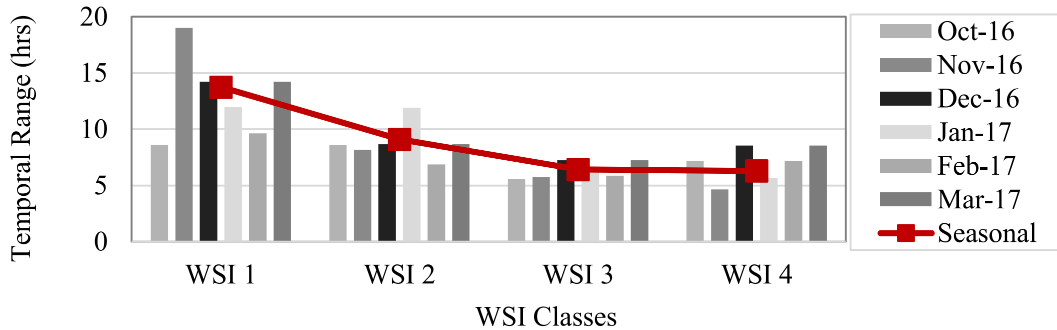

(b)

Figure 4- 8: Temporal Semivariogram Ranges for (a) TPI Class and (b) WSI Classes

The effect of weather severity in the TPI 1 zone—the flatland area—is presented in **Figure 4-9**. In our study area, the flatland region consisted of three weather severity regions and there was a trend for higher autocorrelation range in areas with less weather severity than areas with more severe weather severity regions, especially for the temporal range. The effect of weather for the spatial range was negligible as the total difference is only 1.6 km. From this, we can conclude that topography can serve as a more intuitive measure for RWIS network planning than weather severity. Similar comparisons for other TPI zones were not made as TPI 2 zone consists of WSI 2 and 3 zones, and TPI 3 zone is identical to WSI 4 zone (see **Figure 4-1** and **4-2**).

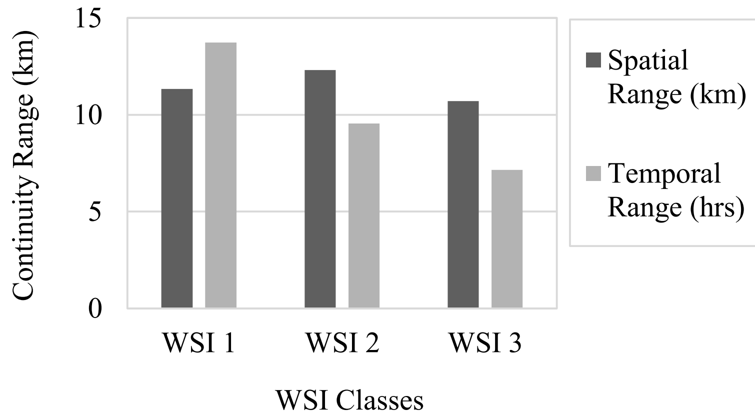

Figure 4- 9: Spatial and Temporal Range for Flatland Area (TPI 1) with Different Weather Severity

4.6 Development of Optimal RWIS Density Guidelines

The spatiotemporal semivariogram analysis results were used as inputs for RWIS density optimization in order to develop RWIS siting guidelines. The RWIS density per unit area for different topographic and weather severity regions was determined from the density optimization outputs. The density optimization results were then used to generate an RWIS density chart for TPI-WSI zones.

The density optimization was conducted using all three semivariogram parameters (range, nugget, and sill). The main focus was the semivariogram range's dependency on the region's topographic-weather characteristics. Spatial parameters of a spatiotemporal semivariogram were used as input for density optimization for topographic and weather severity zones (3 TPI classes and 4 WSI classes). A hypothetical network of 100 km × 100 km was used for density optimization. A 5 km × 5 km prediction grid was then generated in ArcGIS (ESRI 2015) to create the candidate sites for RWIS station placement. The objective function was formulated to minimize the mean ordinary kriging estimation variance and was solved via PSO as described earlier. The algorithm optimized the density of RWIS stations in an iterative process where stations were added one by one into the study area, and the locations were selected based on heuristic attempts to minimize the objective function. The total number of RWIS stations allowed was arbitrarily limited to 100 in this study to ensure the full display of the estimation error variation trend as density changes. The maximum number of iterations was set to 5,000, after which the search process for new RWIS station locations is set to stop. Prediction errors were normalized to make a valid and fair comparison among zonal classes.

According to the density optimization results shown in **Figure 4-10**, topographic and weather severity classes with larger spatial ranges required fewer RWIS stations, except for weather zone 3, which shows a similar trend to weather zone 1. Such findings are in agreement with analyses using TPI classes: WSI 3 zone consists mainly of northern parts of MN, classified as flatland area (TPI 1) and are found to have a lower density of RWIS based on topographic analyses. From this, it can be stated that topographic measures (TPI) provide a more intuitive and direct relationship than WSI in terms of their impacts on RWIS density.

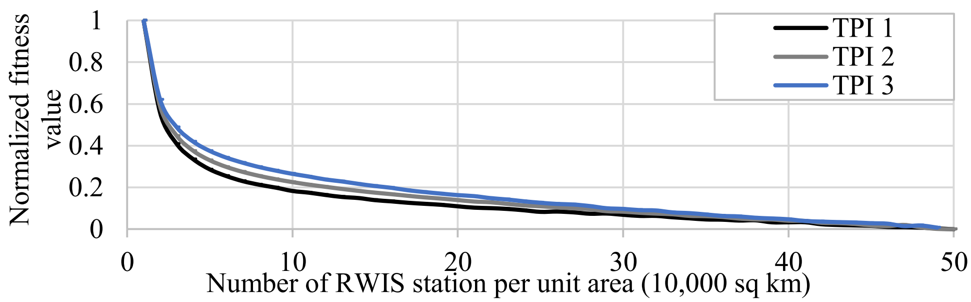

(a)

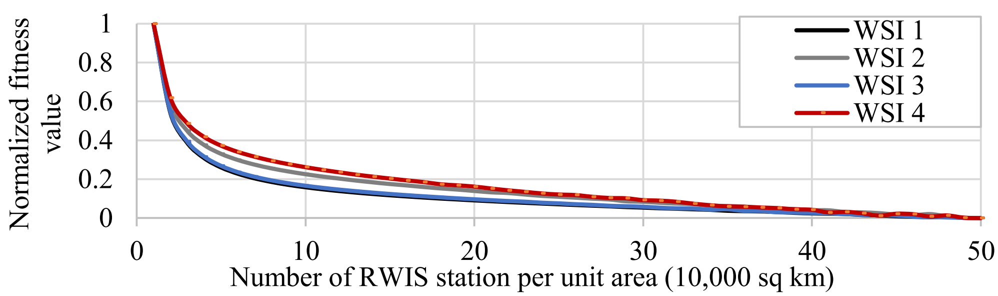

(b)

Figure 4- 10: Normalized Prediction Error as a Function of RWIS Density for (a) TPI Classes and (b) WSI Classes

The number of RWIS stations needed for a 0.1-unit increment of benefit (number of stations needed to reach normalized fitness value of 0.1) was calculated from **Figure 4-10** and presented in **Figure 4-11**. According to **Figure 4-11**, the initial 0.1-unit of incremental benefit requires the highest number of RWIS stations, with each subsequent incremental benefit requiring fewer and fewer additional stations. This trend was expected because the marginal benefit gained from additional RWIS stations should decrease as station numbers increase. A similar trend is observed for both TPI and WSI classes.

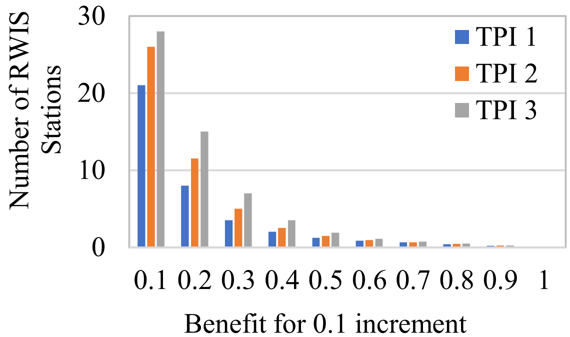

(a)

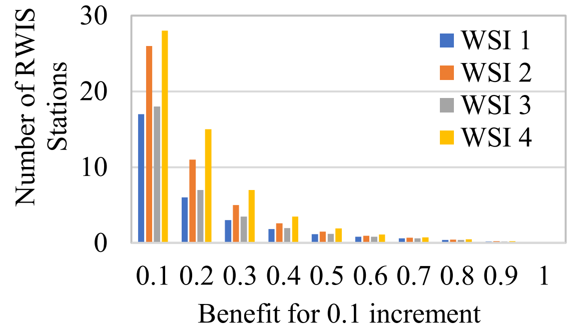

(b)

Figure 4- 11: Number of RWIS Stations for Benefit Increment of 0.1-Unit for (a) TPI Classes and (b) WSI Classes

For determining the optimal RWIS density, marginal benefits (number of additional RWIS stations needed for 0.1-unit incremental benefit) were calculated from **Figure 4-10** and presented in **Figure 4-12**. According to **Figure 4-12**, the number of added RWIS stations for an initial marginal incremental benefit of 0.1-unit was the highest. The number of additional stations decreased for further increments of marginal benefits for both TPI and WSI classes.

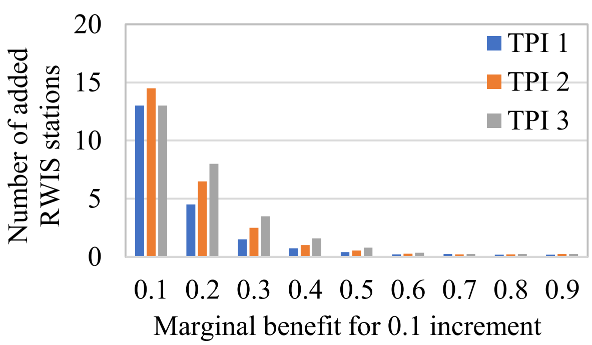

(a)

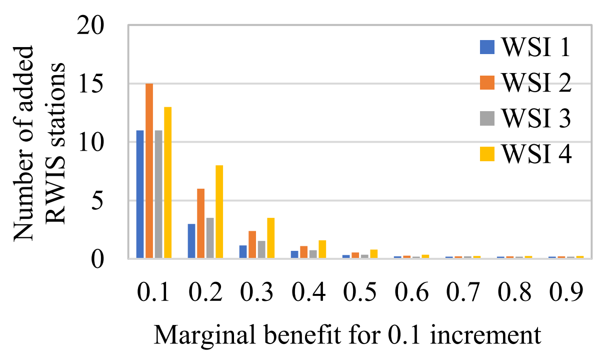

(b)

Figure 4- 12: Added Number of RWIS Stations for Marginal Benefit Increment of 0.1-Unit for (a) TPI Classes and (b) WSI Classes

Looking at **Figure 4-11** and **Figure 4-12**, it can be noted that the marginal benefit decreases significantly after the 0.3-unit increment benefit mark. This was determined as the median of the range and number of associated RWIS stations for 0.3-unit increment of benefit increase was defined as the optimal RWIS density. We then set 0.2-unit and 0.4-unit as the upper and lower bound, respectively. Using this definition, **Figure 4-11** was converted into **Figure 4-13**. According to this figure, RWIS density was the lowest for TPI class 1 and increases with topographic variation. Similarly, less weather severe regions required the fewest number of stations, and the most severe regions required the greatest number of stations; the only exception was WSI 3 for the above-noted reasons.

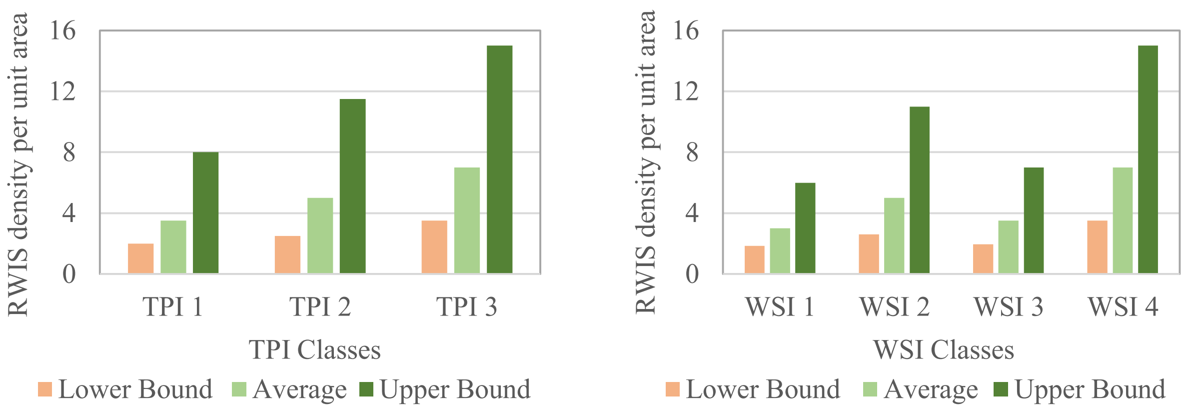

(a) (b)

Figure 4- 13: RWIS Density Comparison for (a) TPI Classes and (b) WSI Classes

The density optimization results were used to generate an RWIS density chart for TPI-WSI zones and is presented in **Table 4-2**. RWIS density for each TPI-WSI region was calculated by combining the topographic and weather effect with equal weightage. According to the result, three to seven RWIS stations are required for a unit area of 10,000 km^2, attesting that the RWIS necessary to provide enough coverage over space and time is about three times more than that over space only. Winter road maintenance agencies can readily use such findings for planning a region-wide RWIS network, especially for regions with limited or no available RWIS stations.

Table 4-2. RWIS Density for TPI-WSI Zones for Unit Area (1/10000 sq km)

RWIS Density for Unit Area		TPI Classes								
		TPI 1			TPI 2			TPI 3		
		LB	Avg	UB	LB	Avg	UB	LB	Avg	UB
WSI Classes	WSI 1	1.93	3.25	7.00	2.18	4.00	8.75	2.68	5.00	10.50
	WSI 2	2.30	4.25	9.50	2.55	5.00	11.25	3.05	6.00	13.00
	WSI 3	1.98	3.50	7.50	2.23	4.25	9.25	2.73	5.25	11.00
	WSI 4	2.75	5.25	11.50	3.00	6.00	13.25	3.50	7.00	15.00

4.7 Statewide RWIS Density Determination

The optimal RWIS density was determined for each of the 14 states using **Table 4-2**. The optimal RWIS density map is presented in **Figure 4-14**.

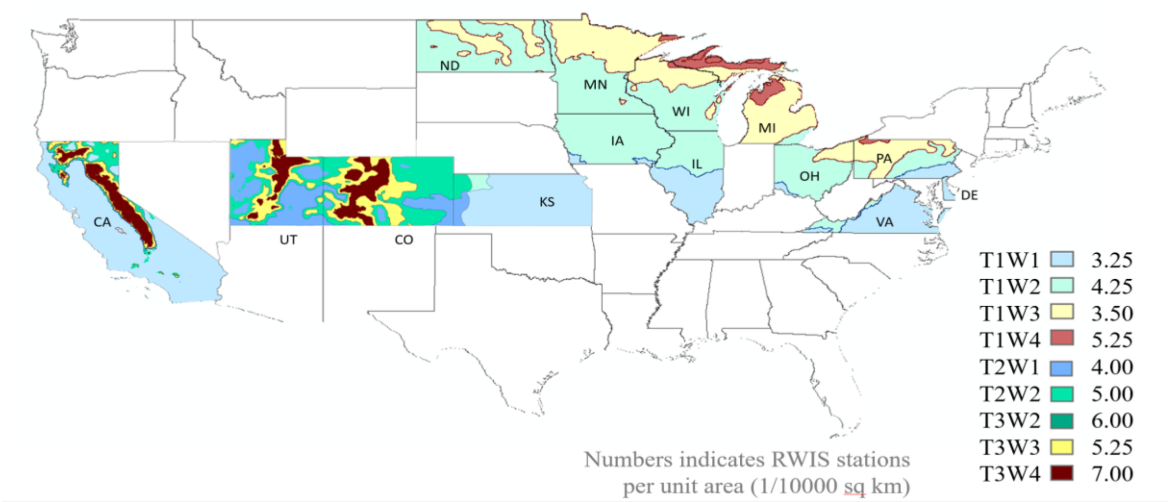

Figure 4- 14: Optimal RWIS Density Map

Nine different TPI-WSI combined zones were identified in the study area. The flatland area (TPI-1 zone) includes four different weather severity zones named T1W1, T1W2, T1W3, and T1W4 (lighter colored blue area in **Figure 4-14**). Weather severity increases in magnitude going from the south to the northern parts of the study area. The optimal RWIS density in these regions varies from 3.25 to 5.25 stations per unit area (1/10000 km^2). The TPI-2 zone, which are hilly areas, combines two different weather severity zones in the study area and were named T2W2 and T2W2.

These areas include a smaller part of Colorado, Kansas, and Utah. Four to five RWIS stations are needed per unit area in these zones. Mountainous areas (TPI-3 zone) include three different weather severity zones named T3W2, T3W3, and T3W4. Very small areas of California, Colorado, and Utah are under theT3W2 and T3W3 zones. Most of the mountainous areas are under extremely high severe weather regions.

The area under each TPI-WSI zone was calculated to determine the optimal RWIS density for each state. **Table 4-3** presents the suggested RWIS density for the 14 states.

Table 4-3. Suggested RWIS Density for the 14 States

States	CA	CO	DE	IA	IL	KS	MI	MN	ND	OH	PA	UT	VA	WI
RWIS density	198	156	2	61	54	73	61	86	75	45	46	127	37	58

The findings from the density analyses show that the number of RWIS stations needed for adequate monitoring coverage of mountainous regions with highly varied climates (i.e., California, Colorado, and Utah) is relatively higher than flat regions with less varied weather. This makes intuitive sense since highly varied regions in terms of weather and topography would typically require more frequent monitoring of road weather and surface conditions during inclement weather events to provide timely and cost-efficient winter road maintenance operations. For example, the suggested RWIS density for Delaware is the lowest as it has the smallest area with relatively less-varying weather and topographic conditions. The values provided are for reference only, and further investigation may be warranted to determine optimal densities based on different weighting schemes (i.e., traffic versus weather) and budgetary constraints.

4.8 Summary

Winter road maintenance is one of the most critical activities for transportation maintenance agencies, especially for cold region countries. The significant and critical information needed to make winter road maintenance decisions requires road condition and weather data, which is often collected, processed, and transmitted by road weather information systems (RWIS). Therefore, for an efficient maintenance program, the monitoring coverage and benefit of RWIS must be maximized through strategic RWIS planning. In this study, we investigated the representativeness of RWIS measurements in two analysis domains – space and time. Spatial and temporal continuity of the variable of interest (RST) were investigated using geostatistical spatiotemporal semivariogram analysis and compared with previously established topographic and weather regions. Lastly, the optimal RWIS density for three TPI and four WSI zones were estimated from the density optimization output.

The key findings of this chapter of the thesis are listed below:

- The spatiotemporal autocorrelation range of RWIS measurements strongly depends on TPI and WSI values.
- The zone with the highest topographic variation (TPI class 3 - mountainous regions) had a shorter spatiotemporal range, whereas zones with lower TPI values (TPI class 1 - flatland regions) had higher ranges.
- The weather severity was determined as another factor influencing the spatiotemporal continuity range of RWIS data. Areas with less severe weather tended to have a higher spatial range (e.g., WSI class 1), whereas areas with more severe weather had a lower range in spatial autocorrelation.
- The desired RWIS density showed a strong dependency on topographical and weather characteristics of the region. Higher RWIS density is required for regions with high topographic variation and high incidence of severe weather, whereas lower RWIS density is needed for less topographically varied regions with less incidence of severe weather to achieve similar levels of monitoring coverage.
- The findings presented in this chapter provide an important basis for strategically locating regional RWIS stations that are most optimal for collecting measurements over space and time.

Chapter 5

Development of Sustainable RWIS Network Planning Strategies[3,4]

5.1 Introduction

This chapter focuses on developing a sustainable RWIS network planning approach: a multi-variable location-allocation model that attempts to answer the second and third research questions: where to strategically prioritize RWIS stations to maximize the short-term monitoring capabilities within budgetary constraints, and how to identify long-term deployment solutions; and what type of RWIS is required for each location. Here, a methodological framework is developed to determine optimal RWIS locations by integrating the effect of critical weather variables: air temperature (AT), road surface temperature (RST), and dew point temperature (DPT). Initially, separate semivariograms are utilized to generate optimal RWIS locations, followed by spatial similarity analysis to determine the similarity among generated solutions. Later, the single semivariogram models are combined to generate the multi-variable semivariogram model. The developed semivariogram model is then used to find the optimal RWIS locations for a given network. Additionally, this study fills the gap in determining the optimal installation choice between Regular RWIS stations and Mini-RWIS stations by developing a bi-level sequential optimization model. Findings from this chapter of the thesis provide valuable insights in enhancing the precision and comprehensiveness of RWIS network planning methodologies.

5.2 Research Procedure

The first phase of this study is data collection, where information about the study area, stationary RWIS data, and traffic data are gathered. In the second step, the collected data is processed by removing missing and erroneous data as per our predefined guidelines (Biswas and Kwon 2020). Next, the processed data is merged into a GIS-based platform for further analysis.

---

[3] Biswas, S., and Kwon, T. J. (2022). Development of a novel road weather information system location allocation model considering multiple road weather variables over space and time. Transportation research record, 2676(8), 619-632.

[4] Biswas, S., and Kwon, T. J. (2023). Strategic Planning for Equitable RWIS Implementation: A Comprehensive Study Incorporating a Multi-variable Semivariogram Model. Journal of Geographical Research, 6(4), 54-72

Moving on to the next stage, a highly effective spatial sampling technique within geostatistical analysis is utilized to determine the spatial autocorrelation of the critical RWIS variables. This technique is designed to enhance the likelihood of capturing spatial variations while minimizing potential biases in the input data. Specifically, semivariogram analysis is conducted here to generate semivariogram clouds for the selected RWIS variables, namely, Air Temperature (AT), Road Surface Temperature (RST) and Dew Point Temperature (DPT).

At the next stage, a model-based approach via kriging is utilized to obtain unbiased estimates with the lowest variance (i.e., uncertainty) to determine the optimal RWIS locations. This step is concluded by generating three sets of optimal RWIS locations and performing a similarity analysis. The main purpose of this step is to determine the necessity of incorporating multiple weather variables into a location allocation model.

In the following step, separate semivariograms were combined to generate a multi-variable semivariogram model. This multi-variable semivariogram model is then applied in different aspects of this study to generate optimal locations, obtain RWIS density, and determine types of RWIS stations. Location analysis is performed by refining our previously developed location optimization framework with dual criteria optimization, combining the effect of both weather factors and traffic criteria. At the next step, the multi-variable semivariogram model is also utilized to generate optimal density. Lastly, a bi-level sequential optimization model is developed to determine not only the location of RWIS, but also the type of RWIS required for each location. The overall research procedures for this section are summarized in **Figure 5.1**.

This entire procedure presented in **Figure 5.1** is illustrated considering four distinct steps as summarized below:

Step – 1: Evaluating the importance of multi-variable semivariogram.

Case Study – Iowa, USA

The initial step aimed to underscore the significance of integrating various weather variables into the location allocation model. This concept is exemplified through a case study conducted in the state of Iowa, USA. Here, geostatistical semivariogram analysis was conducted to generate single-variable semivariograms for AT, RST and DPT. Later, the single-variable semivariograms are utilized to generate optimal location solutions. The optimal solutions generated were subsequently compared to assess spatial similarity among location solutions.

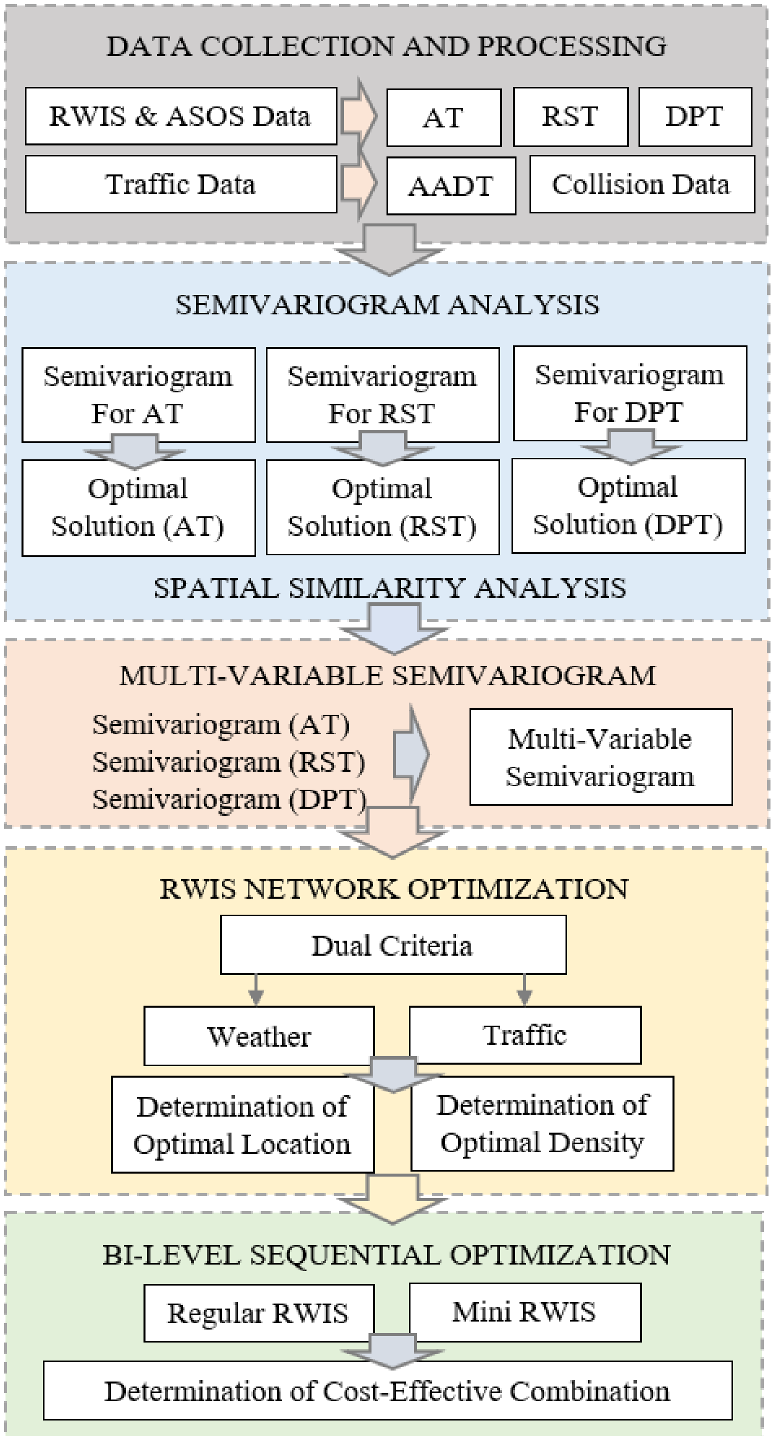

Figure 5- 1: An Overview of the Research Procedure

Step – 2: Development of multi-variable semivariogram.

Case Study – Maine, USA

This step focused on creating a multi-variable semivariogram model, with the aim of establishing a dual criteria location allocation model and a bi-level sequential optimization model. The entire study concept was exemplified through a case study conducted in the state of Maine, USA. Initially, single-variable semivariogram clouds were generated for AT, RST, and DPT. These were then combined to create a multi-variable semivariogram.

Step – 3: RWIS Network Optimization.

Case Study – Maine, USA

In the subsequent step, the developed semivariogram was employed to enhance the RWIS location allocation model, incorporating the impact of weather variables and traffic factors. The refined model was then utilized for RWIS location and density optimization using a case study for the state of Maine.

Step – 4: Designing a bi-level sequential optimization model.

Case Study – Maine, USA

At the last step, the type of RWIS was determined through the development and application of a bi-level sequential optimization model. This step attempts to answer the third research question – what type of RWIS is needed for each optimal location.

The subsequent sections will delve into each step individually.

5.3 Evaluating the Importance of Multi-Variable Semivariogram

5.3.1 Study Area and RWIS Network

To determine the importance of multiple weather variables in the location optimization model, the study concept is illustrated using a case study in the state of Iowa, USA. Iowa is generally a flatland area consisting of rolling plain lands and flat prairies. The altitude of this state is 146 m to 509 m. The total number of RWIS station count for Iowa is 88. The study period selected for this analysis includes a shoulder season month (October 2016) and a mid-winter month (January 2017) to best capture challenging winter driving conditions. The distribution of RWIS stations for the study area is presented in **Figure 5.2**. A randomly generated 10000 square kilometer region within the study area is used as the experimental boundary for location optimization, presented as the red box below, in which there are ten RWIS stations.

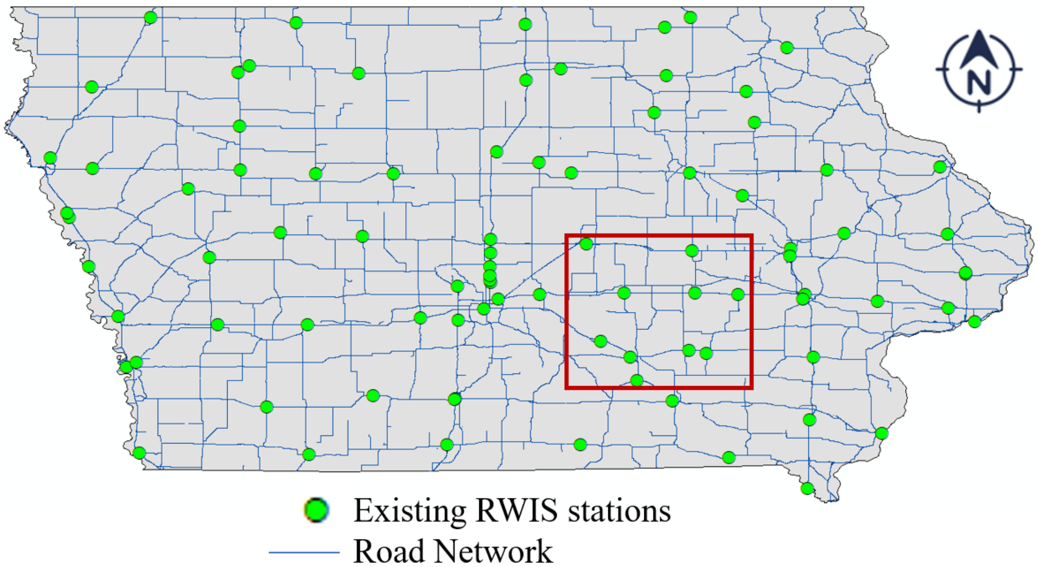

Figure 5- 2: Distribution of RWIS Stations for Iowa

5.3.2 Data Description and Quality Diagnostics

RWIS data for Iowa was downloaded from IOWA State University website (http://mesonet.agron.iastate.edu/RWIS/) as an Excel file. In total, 1488 hours of data was used in this study. The data was processed to remove 'noise' via four steps: (a) Data completeness test to identify missing data; (b) Reasonable range test to find erroneous data; (c) Comparison with neighboring observations; and (d) Detrending processed data with respect to time using GAM. Data processing steps are discussed in detail in section 4.6. Preliminary statistical analysis was then performed using descriptive statistics of the processed data and correlation analysis among weather parameters. Descriptive statistics of AT, RST and DPT are presented in **Table 5-1**. Upon closer inspection of **Table 5-1**, it was revealed that there was relatively less variation in monthly temperatures in the mid-winter month than in the shoulder month for AT and RST, whereas DPT showed the opposite trend. AT varied from -6˚C to 33˚C over the month of October 2016, while the RST and DPT varied from -1˚C to 41˚C, and from -8˚C to 24˚C, respectively. For the month of January 2017, the temperature varied from -27˚C to 20˚C. **Figure 5.3** shows the maximum, minimum, average, and standard deviation of weather data for the study area.

Table 5-1. Descriptive Statistics of AT, RST and DPT for The Study Area

	October 2016			January 2017		
	AT	RST	DPT	AT	RST	DPT
Min	-6.33	-1.10	-7.83	-24.70	-24.00	-26.90
Average	13.64	16.90	9.07	-3.40	-2.10	-6.14
Max	33.10	41.50	23.60	15.00	19.60	11.20
StDev	6.77	6.90	6.91	6.30	6.00	7.42

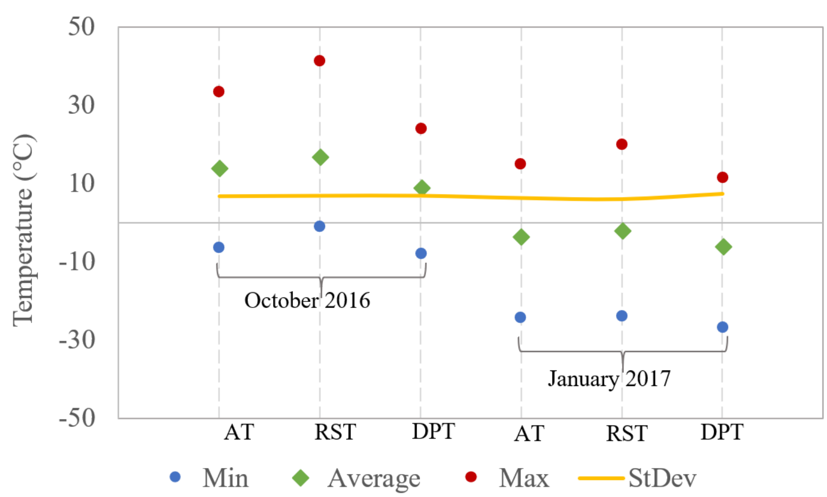

Figure 5- 3: Plot of Variation Found in AT, RST and DPT Over the Shoulder and Winter Months

This was followed by a correlation analysis conducted among the weather variables to find how strongly the two variables were correlated using values between -1 and +1. A correlation coefficient of positive 1 indicates an ideal positive correlation, whereas a negative 1 indicates an ideal negative correlation. Finally, a correlation coefficient near zero indicates no correlation at all (Asuero et al. 2006). For each month, ten RWIS stations were selected randomly, and the correlation coefficient values were generated between each pair of weather variables. These 10 values were then averaged to determine the resultant correlation coefficient. **Table 5-2** below shows the results from this analysis for October 2016 and January 2017.

According to **Table 5-2**, the weather variables were more correlated during the mid-winter month than the shoulder month. The correlation between AT and RST was higher than any other variable pairs, having a correlation value of over 0.9 in both study months. In comparison, the lowest level of correlation was observed between RST and DPT, thereby further attesting to the need to consider their distinctive road weather characteristics later in the location optimization phase. **Figure 5-4** presents a plot comparing the correlation coefficient among AT, RST and DPT of Iowa, which clearly shows that both the similarity and dissimilarity between the three variables changes with month of analysis.

Table 5-2. Correlation Coefficient for AT, RST and DPT for Study Periods

Month of Analysis	Weather Parameter	AT	RST	DPT
October 2016	AT	1		
	RST	0.9134	1	
	DPT	0.7335	0.5117	1
January 2017	AT	1		
	RST	0.9559	1	
	DPT	0.9522	0.8884	1

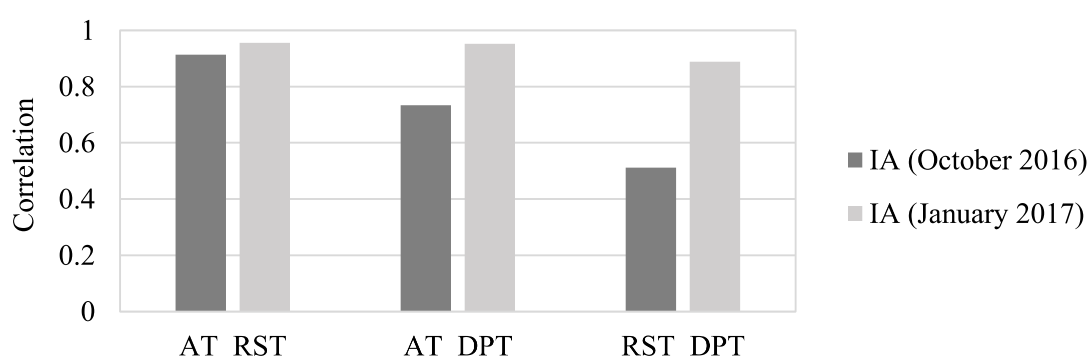

Figure 5- 4: Correlation Coefficients Comparison of Multiple Weather Variables

5.3.3 Spatiotemporal Coverage of Multiple Weather Variables

As evidenced in the previous section where correlation coefficients varied from one variable to another, and over different months, spatiotemporal semivariogram modeling was conducted to gain a deeper understanding of their spatial and temporal variability. For this purpose, RWIS data for the two select months were further processed and aggregated using a one-hour interval for the time domain. A space-time matrix was then formulated as an input for the spatiotemporal analysis. A separate analysis was conducted for each month and each weather parameter, i.e., AT, RST, and DPT. According to previous studies, 30 or more sampling points are needed to construct a reliable semivariogram model (Olea 2006), which we exceeded by employing 88 stations from a robust RWIS network. Semivariogram modeling was performed using the R statistical package - version 3.2.5 (Pebesma 2004, R Core Team 2018). **Figure 5-5** presents the plot of effective spatial, temporal, and joint coverage of RWIS measurements.

According to **Figure 5-5**, higher spatial ranges were obtained for the mid-winter month than the shoulder month. The spatial range is close to 20 kilometers for all weather variables in January 2017, and a 10-to-15-kilometer spatial range was obtained for October 2016. The temporal range was found to be 8.5 to 12 hours for the shoulder month, and 14 to 21.5 hours for the mid-winter month. Such findings make intuitive sense since road weather and surface conditions tend to change more abruptly during shoulder months than during mid-winter months when weather variability is relatively low.

To consider these unique characteristics and implement them in the optimization phase, spatial and temporal semivariograms were combined using spatiotemporal anisotropy to estimate the joint semivariogram as depicted in **Figure 5-5 (c).** The spatiotemporal range for January 2017 was found to be 17 kilometers for all three weather variables, and 7.5 to 10 kilometers was found for October 2016. It can be seen that the seasonal trend is well captured by the joint semivariogram parameters, where a longer range was generated for the mid-winter month compared to the shoulder month. Additionally, the spatiotemporal range was identical for the month of January, which indicates a high correlation among the three weather variables. In contrast, different degrees of correlations were observed for the month of October, possibly due to the presence of weather patterns fluctuations. Based on the recorded results, the parameters of the joint semivariogram are used for RWIS location optimization.

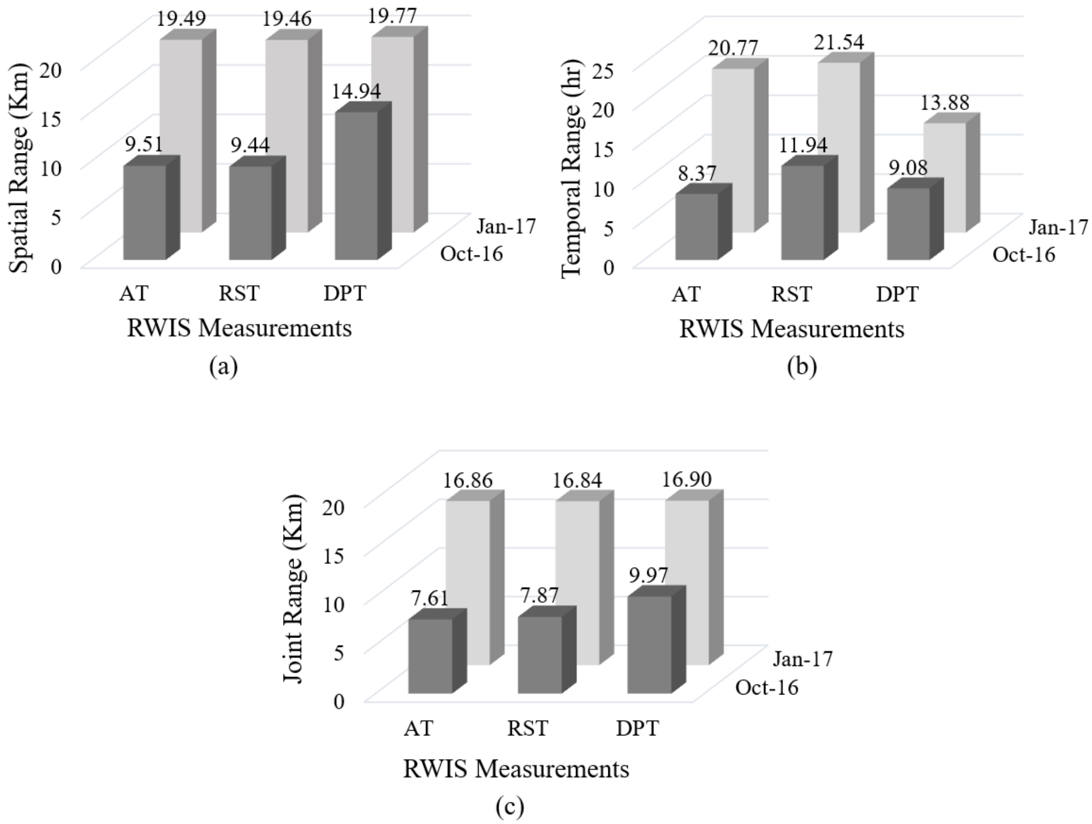

Figure 5- 5: Plot of Effective Spatiotemporal Coverage of RWIS Measurements – (a) Spatial, (b) Temporal and (c) Joint Range

5.3.4 Effect of Road Weather Variables on Optimal RWIS Locations

Optimal RWIS locations were determined by relying on semivariogram analysis results that were obtained in the previous section. To quantitively appreciate each road weather variable's effect on the resulting RWIS locations, the optimization was performed separately for each set of weather variables and month of data using the R statistical package - version 3.2.5 (Pebesma 2004, R Core Team 2018). To reduce the computational complexity associated with the location optimization process and shorten the algorithm runtime, a randomly selected square region (100-kilometer × 100-kilometer) within the study area was used as the experimental boundary for location optimization. A 5 × 5 km prediction grid was generated along the square area in ArcGIS to create the candidate sites for RWIS station placement. The computer used to run the optimization was equipped with 3.60 GHz CPU and 16 GB memory. The average algorithm running time for generating each solution set was approximately 5 to 8 hours. An initial seed value was used for the optimization process in order to generate comparable results. The RWIS network optimization output under different weather variables is presented in **Figure 5-6 (a)** and **Figure 5-7 (b)** for October 2016 and January 2017, respectively. A 10-kilometer buffer was created around the stations arbitrarily to help better recognize the distribution of stations within the rectangle study area. It is evident that the RWIS location solution is substantially different depending on the variable of interest and over the month of analysis.

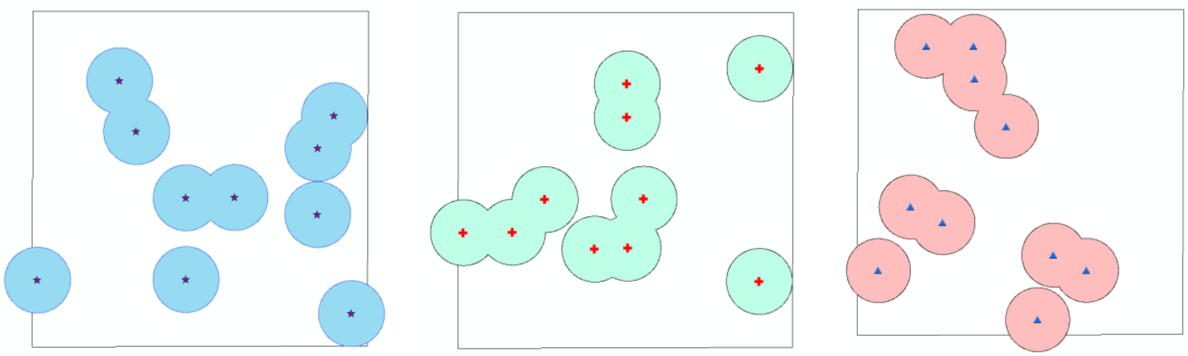

(i) Solution set 1: AT (ii) Solution set 2: RST (iii) Solution set 3: DPT

(a)

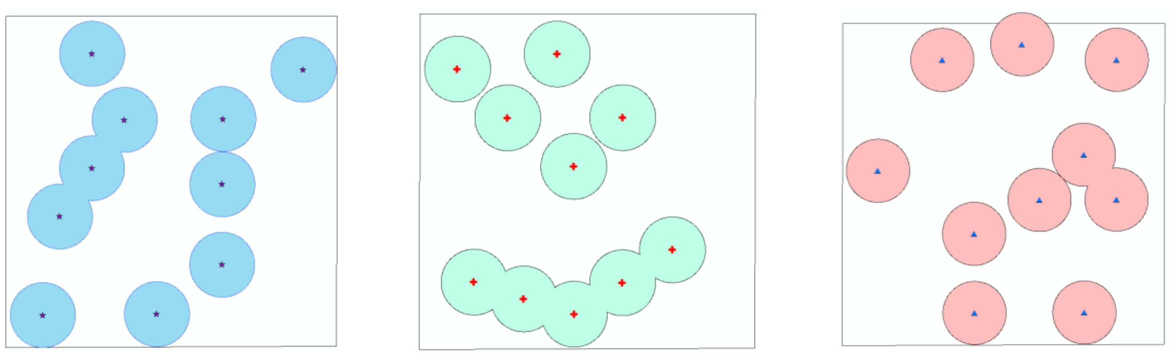

(i) Solution set 1: AT (ii) Solution set 2: RST (iii) Solution set 3: DPT

(b)

Figure 5- 6: Spatial Distribution of Optimized RWIS Locations with respect to Three Variables (a) October 2016 and (b) January 2017

5.3.5 Spatial Similarity Analysis

It is evident from the location allocation output (**Figure 5-6**) that the optimized location solutions are visually different from one another. To quantitatively evaluate the closeness of the optimal RWIS station distributions, a spatial similarity index was developed. For this, a sensitivity analysis was performed to objectively measure the similarity of optimal locations using ArcGIS (ESRI 2015). Initially, buffer polygons were created around the stations up to a maximum of 20 kilometers in linear units. 10 sets of buffer polygon were created for each solution set, which totals up to 60 sets of buffer polygon. The intersecting areas were then determined for each pair of solution sets, each linear unit combination and each month of analysis. The percentage of intersecting area with respect to the study area represents the spatial similarity index, the higher the percentage of intersected area, the more similar the solution sets. **Figure 5-7** presents the results from this analysis.

According to **Figure 5-7**, the percentage of intersecting area with respect to different buffer sizes follows an exponential function. It is clear from the figure that buffer size does not affect the results significantly. In most cases, location solutions generated using the mid-winter month (January 2017) dataset have been found closer than that of the shoulder month (October 2016) dataset. The reason behind this outcome is that the daily fluctuation in weather data is greater during the shoulder months than mid-winter months—higher spatiotemporal autocorrelation of weather data were found in January than October. For a specific buffer size, the percentage of intersecting area between AT and RST solution sets was found to be the highest, followed by in decreasing order, AT and DPT solution sets, RST and DPT solution sets, and AT, RST and DPT solution sets. This phenomenon is quite similar to the correlation analysis results between the weather variables, where the correlation between AT and RST was the highest, followed by AT and DPT, and RST and DPT. This analysis indicates that spatial similarity of location solutions can be examined by creating buffer polygons regardless of the size implemented.

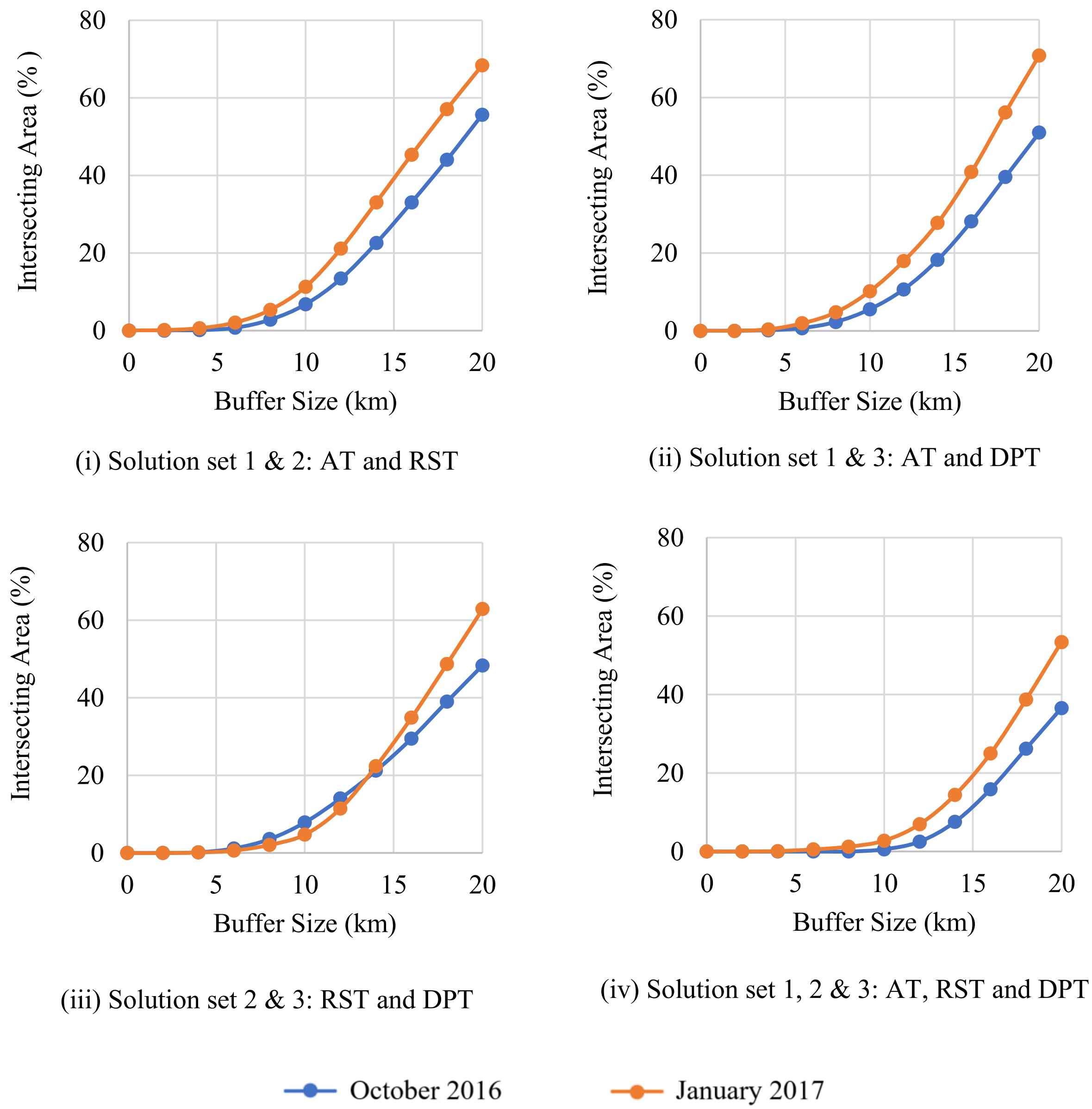

Figure 5- 7: Similarity among Optimal RWIS Station Placements

5.3.6 Location Allocation for the Entire Iowa State

In the previous section, it was confirmed using the hypothetical square region that the generated locations were dependent on weather variables. Based on this finding, the proposed location optimization method was expanded to cover the entire Iowa state. To achieve a comparable result as the existing RWIS locations, a constrained optimization was performed with respect to the road network using the shoulder month dataset. Although the existing number of RWIS stations is 88, the total number of all new stations has been set to 61 for location optimization purposes. The number 61 was chosen based on optimal RWIS density guideline (Chapter 4, **Table 4-3**), where the number of RWIS stations per unit area was generated given the topographic variation and weather severity of regions. In terms of computational efficiency, the average running time for each set of optimization algorithm was approximately 78 hours. **Figure 5-8** represents the plot of the objective function value as a function of the number of iterations; **Figure 5-9** shows existing and optimized RWIS locations with multiple weather variables. From **Figure 5-9**, it is evident that the optimal locations are different and largely dependent on the underlying spatiotemporal autocorrelation structure considered during the optimization process. The spatial similarity analysis was also conducted to objectively assess the difference between the three solution sets generated. The results show that spatial correlation between RST and DPT was lower than AT and RST, which is consistent with our hypothetical test results. These findings, undoubtedly, provide a steppingstone for the development of a multi-objective RWIS location allocation model by considering the varying degrees of representativeness of multiple weather variables.

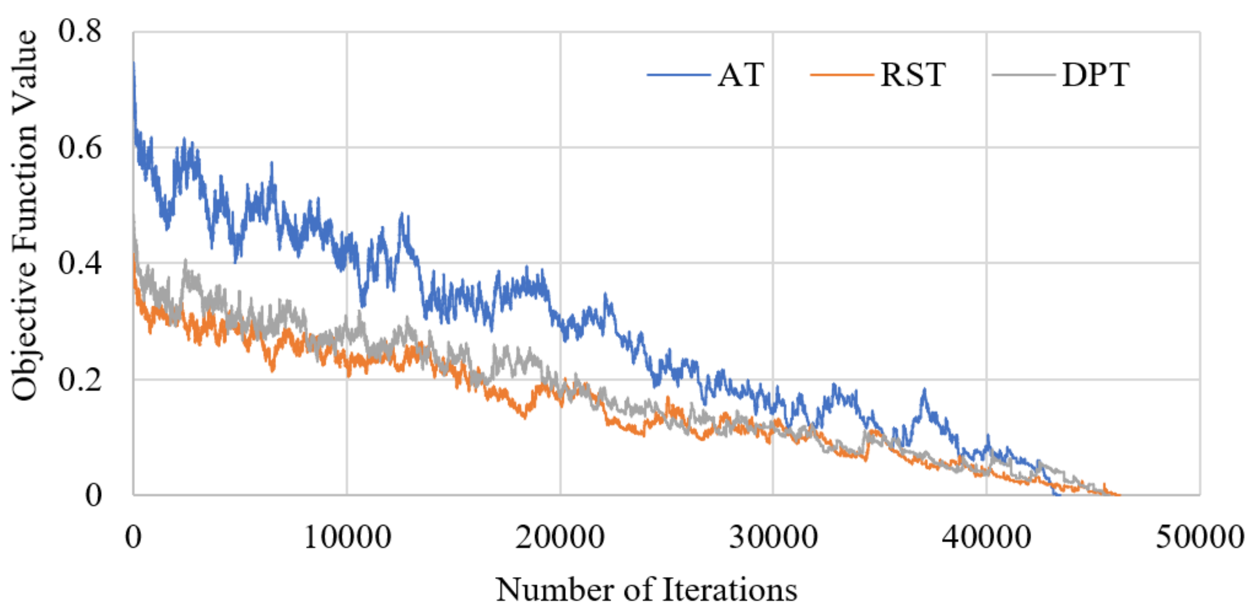

Figure 5- 8: Plot of Objective Function with respect to Number of Iterations

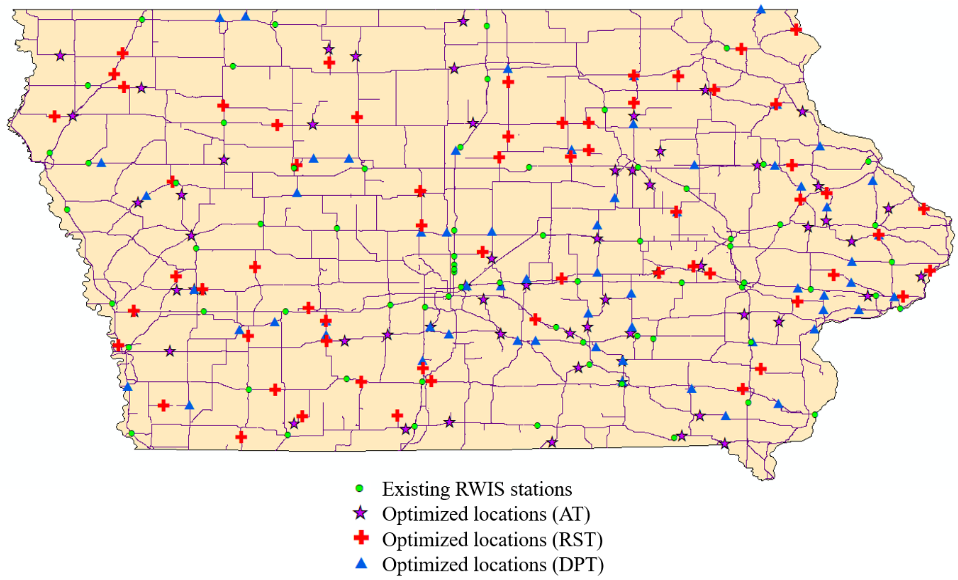

Figure 5- 9: Existing and Optimized RWIS Locations of Iowa Generated with Three Variables for October 2016

This subsection of this chapter investigated and confirmed the difference in solutions generated from AT, RST, and DPT. Their closeness was further quantified and objectively validated using spatial similarity index. The main goal of this single-variable location optimization was to prove the hypothesis that, location solutions generated by individual weather variables may not lead to the same results; therefore, revealing the need for developing multi-criteria location allocation optimization. These findings direct the resurgent need to consider the effects of multiple weather variables collectively in the optimization framework by developing a multi-variable semivariogram model.

5.4 Development of Multi-Variable Semivariogram

5.4.1 Study Area and RWIS Network

To develop the multi-variable semivariogram, the study concept is illustrated using a case study in the state of Maine, USA. Located in the northeastern region of the United States, Maine is positioned as the easternmost state, sharing its border with Canada. Maine exhibits diverse geographical features, encompassing distinctive regions such as uplands, coastal lowlands, mountains, and piedmont areas. Severe winter conditions, including heavy snowfall and freezing temperatures, result in the formation of slippery road surfaces and reduced visibility, consequently rendering winter driving a demanding and challenging task (Kahl et al. 1991, Greenleaf 1829).

There are 10 RWIS stations in Maine, with the majority of them strategically positioned along the interstate highway. Due to the limited number of existing stations, RWIS data from a neighboring state, NH (New Hampshire), is also utilized in this analysis. Additionally, ASOS (Automated Surface Observing System) data from both states are also included after conducting data representativeness tests. In the process of assessing the representativeness of NH data for the state of ME, an analysis was conducted on the variation patterns of selected weather variables in both states. According to the assessment, it can be inferred that NH's RWIS and ASOS data are reliable for representing Maine's weather.

The study period selected for this analysis includes three consecutive winter seasons between 2019 and 2022. Within these three years, RWIS and ASOS data collected over a span of five winter months (November to March) are utilized in this analysis. The distribution of RWIS and ASOS stations for the study area is presented in **Figure 5-10**.

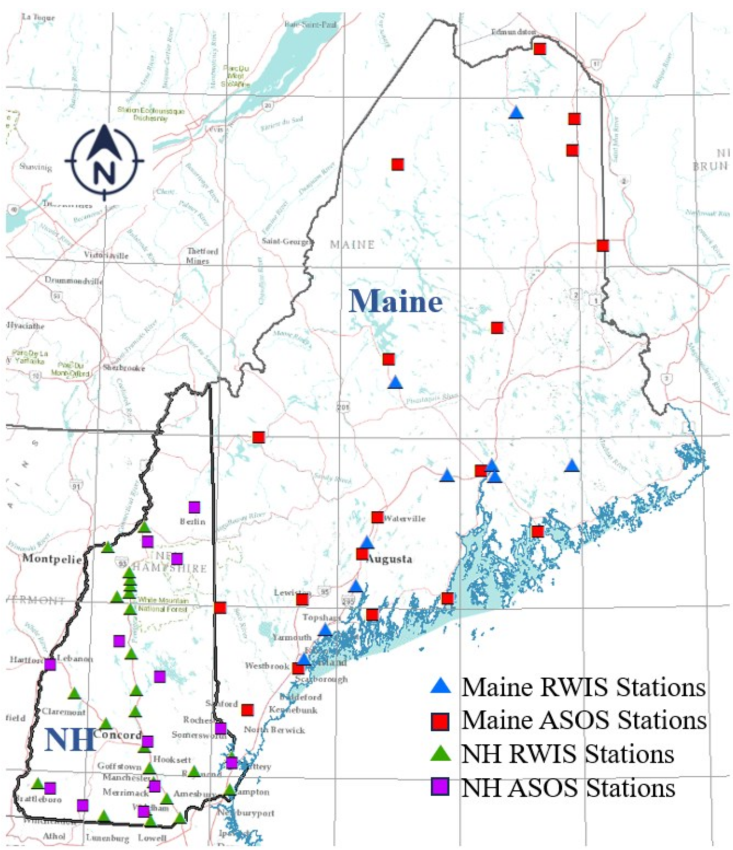

Figure 5- 10: Distribution of RWIS and ASOS Stations for Maine and NH

5.4.2 Data Description

This study utilized a comprehensive dataset obtained from the Maine DOT with supplemented data from the adjacent state NH to compensate for Maine's lack of RWIS data. The dataset includes state boundary information, road network data, stationary RWIS data, and traffic data. Furthermore, the study incorporated information regarding candidate RWIS sites, which serve as potential locations for future installations of RWIS stations.

RWIS and ASOS Data

Stationary RWIS data for Maine was collected from Maine DOT (https://www.maine.gov/mdot/). RWIS data for NH and ASOS data for Maine and NH were downloaded from Iowa State University (http://mesonet.agron.iastate.edu/RWIS/) and WxDE website (Weather Data Environment: https://wxde.fhwa.dot.gov/). State-wide RWIS data in the form of Excel files were downloaded, containing measurements from multiple parameters including air and surface temperature, visibility, wind speed, and road surface conditions. Likewise, ASOS data encompasses similar weather variables, excluding RST. These measurements are collected at intervals of approximately 15 to 20 minutes. In total, 25 RWIS stations from NH, 10 RWIS stations from Maine, 33 ASOS stations in NH, and 18 ASOS stations in Maine were included in the analysis. A total of 10,800 hours of data was incorporated in the analysis.

The weather data underwent a predefined processing procedure to eliminate missing and erroneous data. These steps included data completeness test, reasonable range test, cross-checking RST data with AT and DPT data, and pattern analysis of weather data (Biswas and Kwon 2020). Using this procedure, a total of 60 sets of data were analyzed.

Traffic Data

To calculate the accident/crash rate, AADT and collision data were collected for the same 5-year period as RWIS and ASOS data. Then, for the purpose of evaluating collisions during the winter season, only collisions occurring between November and March were considered. Furthermore, to identify collisions caused by adverse weather conditions, several factors were taken into account. These factors included: (i) the contributing factor of the accident, such as road surface conditions like wet, icy, snowy, slushy, etc., (ii) the surface condition during the accident, encompassing ice/frost, snow, slush, mud, dirt, and gravel, and (iii) the type of roadway, focusing on non-intersection collisions. By considering these factors, the study aimed to determine the collision rate (CR) associated with adverse weather conditions.

To create the CR distribution map, the study employed Equation 3-15 to calculate CR values for square polygons of different sizes generated from Maine's road network data. Subsequently, the CR values are normalized on a scale from 0 to 1. Smaller polygon sizes resulted in a significant number of polygons with zero CR values, leading to a random CR distribution map that made hotspot identification challenging. After an extensive search process to select the optimal polygon size, the CR map generated with 20 km by 20 km polygons was selected as the most suitable, providing a comprehensive representation of CR and better visualization of high-crash areas. The CR distribution map for Maine with 20 by 20 km square polygons is depicted in **Figure 5-11**.

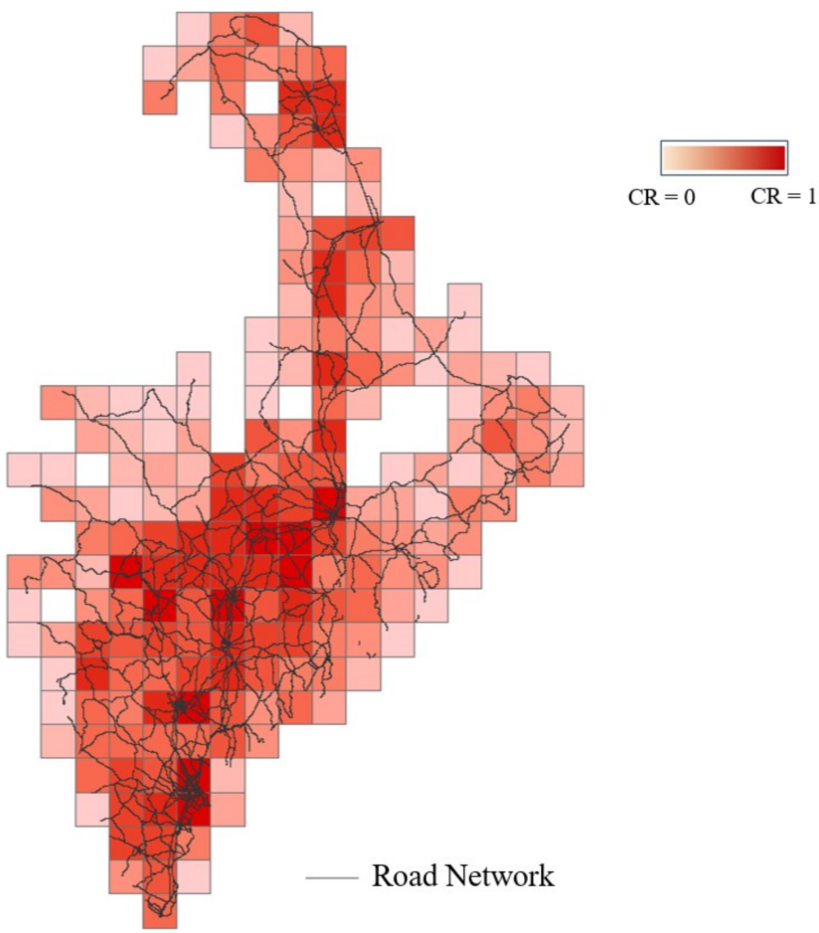

Figure 5- 11: Crash Rate (CR) Distribution Map for the State of Maine

5.4.3 Data Processing

RWIS and ASOS data were processed to remove the missing and erroneous data using four steps: (a) Data completeness test to identify missing data, (b) Reasonable range test to find erroneous data, (c) Cross-checking RST, AT and DPT data to identify outliers, and (d) weather data pattern analysis.

Data completeness was checked by identifying the total missing data for each sensor. If the total missing data is more than 15%, the associated sensor ID was marked and the data from that sensor was not used for analysis. Reasonable range was tested based on historical data ranges for the associated region and month. Filtered weather data were then cross-checked with each other to identify data ranges for any possible outliers. A set of data pattern analysis was performed by plotting the day of the month versus the average daily temperature for all selected sensors, and each month of analysis. All selected stations were expected to show a similar pattern throughout the month. If any unusual pattern was noticed, the weather data for that associated station was further investigated for the time period of the unusual pattern. In total, 60 sets of data (three winter seasons for seven sets of stations) were analyzed using the above-described process.

The descriptive statistics of the processed data are summarized in **Table 5-3**, providing insights into the minimum, average, maximum, and standard deviation values for the data collected from weather stations. Upon closer examination of **Table 5-3**, it can be observed that the AT exhibits a range of -34.0ºC to 26.3ºC throughout the study period, with an average value ranging from -1.2ºC to -2.3ºC. The RST varies between -25.9ºC and 32.1ºC, with an average value of 0.12ºC. Furthermore, the DPT ranges from -41.9ºC to 21.8ºC, with average values of -6.0ºC to -6.48ºC. It is noteworthy that the standard deviation is slightly higher for DPT compared to AT and RST. These statistics provide a comprehensive overview of the temperature variations across the study period and highlight the relative variability among the different variables.

Table 5-3. Descriptive Statistics of Weather Station Data for Maine and NH

Station	Maine ASOS		NH RWIS			NH ASOS	
Weather Variable	AT	DPT	AT	RST	DPT	AT	DPT
Minimum Temperature	-30.61	-41.89	-29.50	-25.90	-33.00	-34.00	-40.00
Average Temperature	-2.32	-6.46	-1.18	0.12	-6.48	-1.22	-5.97
Maximum Temperature	24.39	19.00	26.30	32.10	21.80	25.00	21.00
Standard Deviation	7.04	7.77	6.82	6.87	7.58	7.10	7.72

5.4.4 Multi-variable Semivariogram Model

To assess the spatial structure of key road weather and surface condition variables, semivariogram modeling was integrated into this study. The gstat package in R (R. C. Team. 2018, Pebesma 2004) was utilized for this purpose. Initially, semivariogram clouds were generated for each weather variable, enabling an examination of the spatial autocorrelation among the recorded sample points. Each point within the cloud represents the variance between a pair of measurements (Johnston et al. 2001, ESRI. ArcGIS, Version 10.4.1). Subsequently, the semivariogram clouds for the weather variables were combined to form a unified semivariogram cloud. By binning the cloud points together, an empirical semivariogram model was constructed that incorporated the spatial autocorrelation of all essential weather variables. **Figure 5-12** represents the multi-variable semivariogram model developed in this research. Here, the spatial range of autocorrelation was determined to be 145 kilometers, with a sill value of 3.55 and a nugget value of 0.01.

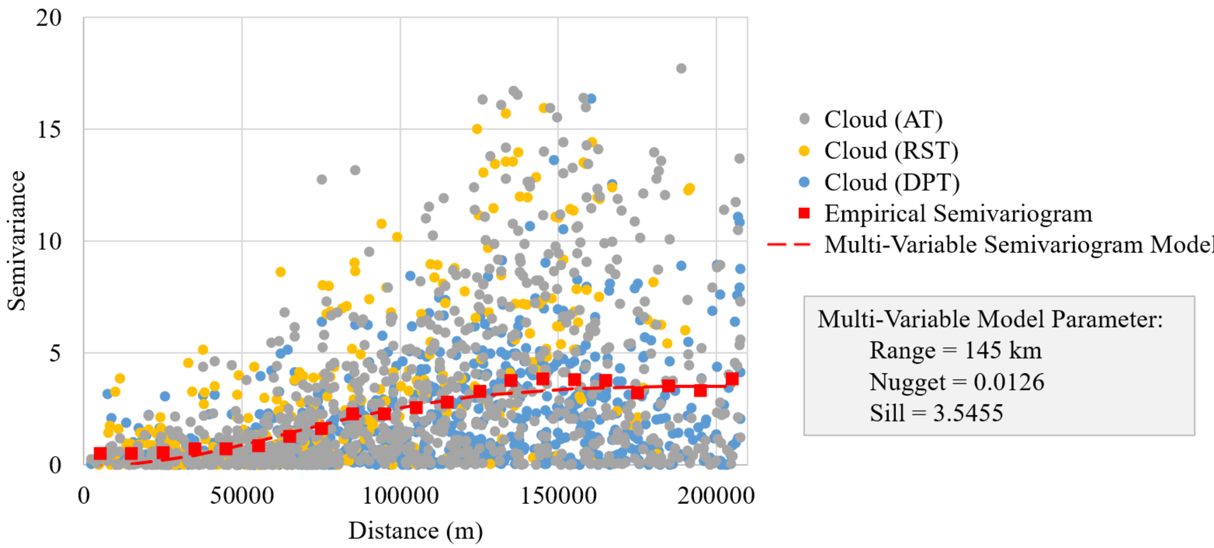

Figure 5- 12: Multi-Variable Semivariogram Model with Model Parameters

The use of a multi-variable semivariogram model was expected to yield a more accurate location solution by capturing the variability of multiple weather variables. To evaluate the validity of this hypothesis, single-variable semivariogram models were also employed in the location-allocation algorithm to compare against multi-variable-based solutions. This study utilized R statistical packages to generate separate semivariogram models for AT, RST, and DPT. These models were subsequently employed to determine location solutions for the state of Maine.

Recall that the location optimization process leverages the SSA (Spatial Simulated Annealing) algorithm. The primary objective was to maximize spatial coverage by minimizing estimation variance, represented by a value referred to as 'criterion'. The optimization process involves selecting locations that minimize the 'criterion' value. The resultant solution with the lowest 'criterion' value indicates maximized monitoring coverage. To demonstrate the superiority of the multi-variable model compared to single-variable models, optimization outputs from both approaches were compared.

Figure 5-13 illustrates the location solutions for eight stations (selected based on planning approaches) and optimization schedules for the three single and multi-variable cases. The optimization schedule displayed the 'criterion' value progression, indicating that the multi-variable model has a notably lower 'criterion' value compared to the single-variable models. This suggests that the multi-variable model offers enhanced monitoring coverage. The parameters of the multi-variable semivariogram model were then used as inputs in the location optimization process.

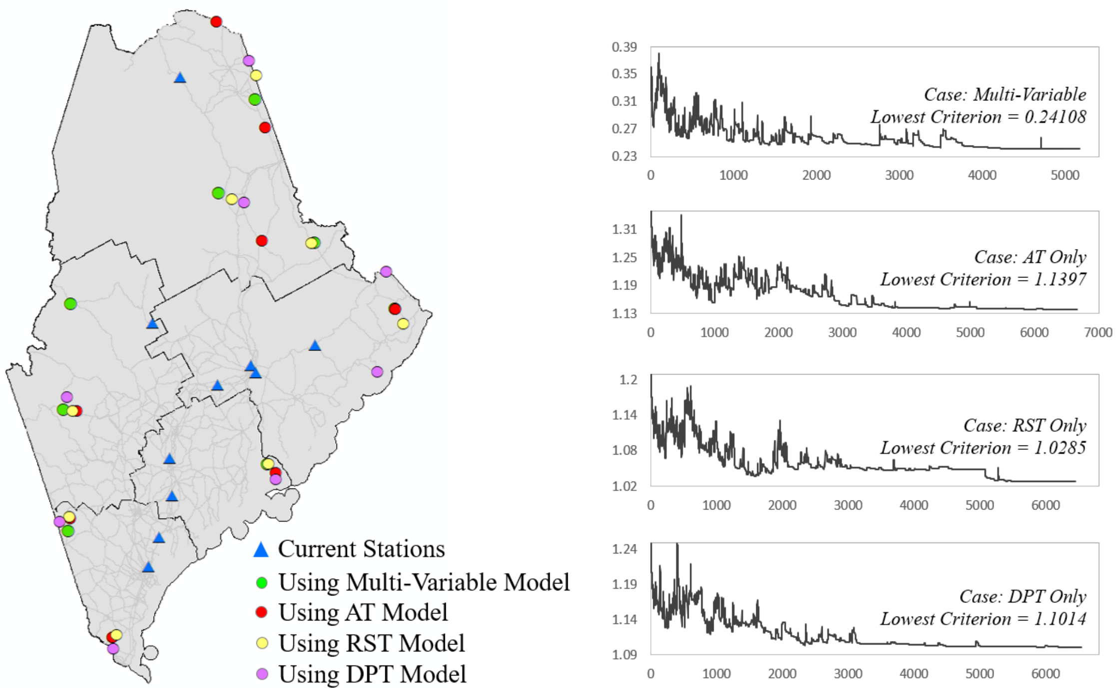

Figure 5- 13: Comparison of Single-Variable and Multi-Variable Model for Network Optimization

5.5 RWIS Network Expansion

Using the multi-variable semivariogram model developed in the previous step, the study proceeds to assess the effects of spatial demarcation on RWIS planning by constructing various design scenarios. In previous studies, we developed an innovative RWIS location modeling framework where the problem was formulated as an integer programming problem. The objective was to minimize spatial inference error, in other words, maximize spatial coverage across the road network. These spatial inference errors capture the necessity of installing RWIS stations to enhance monitoring capabilities, ultimately improving the effectiveness of winter road maintenance operations (Biswas and Kwon 2020). In this step, we refined the previously developed location optimization model by incorporating the influence of multiple critical weather variables as well as the distribution of traffic demand.

This study focused on two specific tasks for expanding the RWIS network. A detailed description of the specific tasks is given below.

Task – 1: Selection of Priority Locations

A total of 18 potential RWIS locations in Maine have been identified by Maine's regional officers. Our first task was to select 8 priority locations from this pool of predetermined sites. The intent of this analysis was to prioritize RWIS locations based on the constraint that a limited number of RWIS installations can be installed per year. **Figure 5-14** illustrates the predetermined and existing RWIS stations. The state is divided into five maintenance zones by gray lines. According to **Figure 5-14**, there are two potential locations identified in zone-1 and zone-2, three locations in zone-3, four locations in zone-4, and seven locations in zone-5.

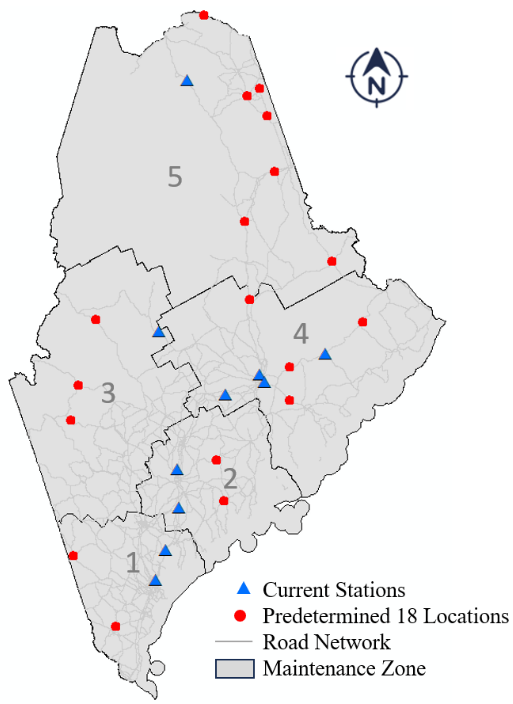

Figure 5- 14: Distribution of Current and Predetermined Locations

Both weather and traffic factors were considered to identify priority locations. The aim was to serve a wide range of road users while also effectively capturing weather variability. The weather criteria were incorporated by utilizing multi-variable semivariogram parameters, while the traffic parameters were considered by incorporating CR. In the optimization algorithm, equal weightage was assigned to both weather and traffic factors. This approach aimed to maximize the overall benefit by considering both weather conditions and traffic demands. This resulted in the generation of priority locations, represented by green circles **in Figure 5-15**.

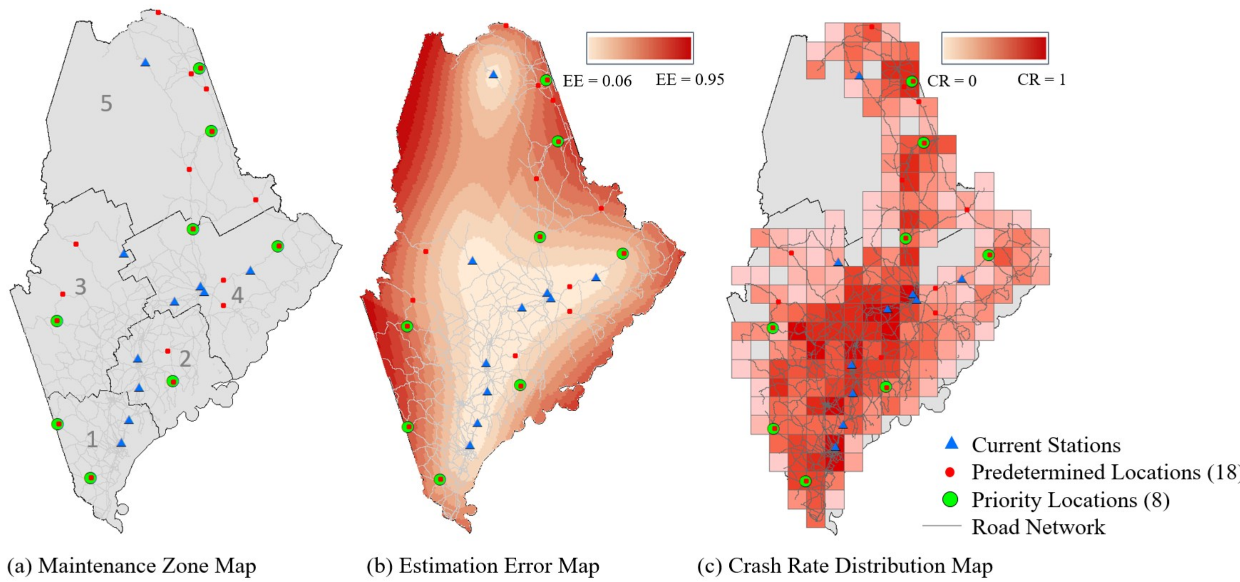

Figure 5- 15: Visualization of Priority Locations

Figure 5-15 presents the eight priority locations for RWIS installation with a maintenance zone map, an estimation error (EE) map, and a CR distribution map. The priority locations are evenly distributed throughout the network. The EE map shows varying shades of red, indicating estimation error values computed using ordinary kriging. The kriging interpolation technique utilizes semivariogram parameters to estimate values at unsampled locations, while also providing an assessment of the uncertainty in the estimation, also known as estimation error. The presence of an RWIS station at a particular location result in a lower EE value. As the distance from the station increases, the estimation for unknown locations becomes associated with higher error. This indicates a greater requirement to install a new RWIS station in those areas to bridge the spatial gap and reduce estimation uncertainty. In the optimization process, additional RWIS stations are strategically positioned to minimize EE values and improve network effectiveness. The CR distribution map displays lower CR values in light-colored squares and higher CR values in dark-red squares. The new station locations strike a balance between weather variability and accident-prone areas, with strategic placement near high-traffic and hotspot locations. Location information of the first 8 priority locations is presented in Appendix B.

Task – 2: Clean-Slate Optimization

At this step, the candidate locations from Task 1 were expanded to encompass all non-interstate corridors in Maine. This extended study corridor includes interstate, freeway, expressway, major collector, principal arterial, and minor arterial roads. The purpose of this analysis was to objectively assess how to best utilize available resources by addressing gaps in the statewide data collection and road weather forecasting network. A constrained optimization process was conducted to determine the optimal locations for RWIS placement, referred to as clean-slate optimization. Three consequent scenarios were considered during the clean-slate optimization process.

i. *Generate the first 8 optimal locations*

   Here, 8 optimal locations were generated through clean-slate optimization to compare with 8 priority locations that were identified in task – 1.

ii. *Generate the second 10 optimal locations*

   To match the 18 predetermined candidate sites, 18 optimal locations were generated, consisting of 10 new sites and 8 initial locations. The aim of this step was to create a direct alignment between the optimal locations and the predetermined candidate sites, ensuring a clear correspondence between the two sets.

iii. *Generate the third 6 optimal locations*

   The RWIS network expansion plan of Maine DOT aims to install 8 new stations annually for three consecutive years. By the end of this expansion plan, a total of 24 stations will be installed. In this step, an additional 6 optimal stations were generated to reach a total of 24 additional sites (8 + 10 + 6). The outcomes of this step will provide the RWIS planners with a complete set of optimal locations for extending their network.

During the process of determining optimal locations for the three mentioned scenarios, a series of sensitivity analyses were carried out to assess the impact of various weight distributions in kriging-based RWIS location optimization. This step yielded multiple location solutions depending on the weight assigned to weather (W) and traffic (T) factors. These location solutions offer flexibility to network planners and decision-makers, allowing them to choose installation sites based on their specific requirements. For each scenario, a total of 7 sets of weight distributions were considered as follows:

Set-1: 0%W, 100%T;
Set-2: 20%W, 80%T;
Set-3: 40%W, 60%T;
Set-4: 50%W, 50%T;
Set-5: 60%W, 40%T;
Set-6: 80%W, 20%T;
Set-7: 100%W, 0%T.

To generate each set of solutions for each scenario, an average of three to five trials were conducted to find a conclusive outcome. In total, clean-slate optimizations were performed over one hundred times. To enhance computational efficiency, a portion of the optimizations in this study were executed using the advanced research computing system called the 'Digital Research Alliance of Canada' (https://alliancecan.ca/en) from the University of Alberta. This system utilized GPUs from the supercomputers "Cedar" and "Graham," each equipped with 12 to 32GB HBM2 memory. The subsequent sections present comprehensive explanations of various clean-slate optimization scenarios and their outcomes.

Scenario – i: Generate first 8 optimal locations

In order to determine the first eight optimal locations, multiple solutions were generated for seven sets of weight distributions, as mentioned earlier. The distribution of the first eight optimal locations for all seven sensitivity analysis scenarios are provided in Appendix – C. For the sake of brevity, we will focus on discussing the three most significant cases: (a) traffic only, (b) equal weightage for weather and traffic, and (c) weather only, as presented in **Figure 5-16**. For set-1, selection of locations was based on the ranking of CR values. **Figure 5-16** (a) illustrates the distribution map of CR, highlighting eight square polygons with higher CR values. It is evident that most of these locations are in close proximity to the interstate and downtown area. **Figure 5-16** (c) displays the optimal locations along with the EE map (set-7). In this case, the objective was to fill the spatial gap in order to effectively capture weather phenomena. The resultant solution exhibits a uniform distribution of locations, effectively capturing the weather patterns. Lastly, for set-4, optimal locations were determined by considering dual criteria, as depicted in **Figure 5-16** (b). Here, the selected locations aimed to strike a balance between capturing weather variability and addressing accident-prone areas. Consequently, we observe some stations located in proximity to hotspot areas, while the overall distribution also captures weather variability by placing stations in areas with higher EE (or areas with high uncertainty).

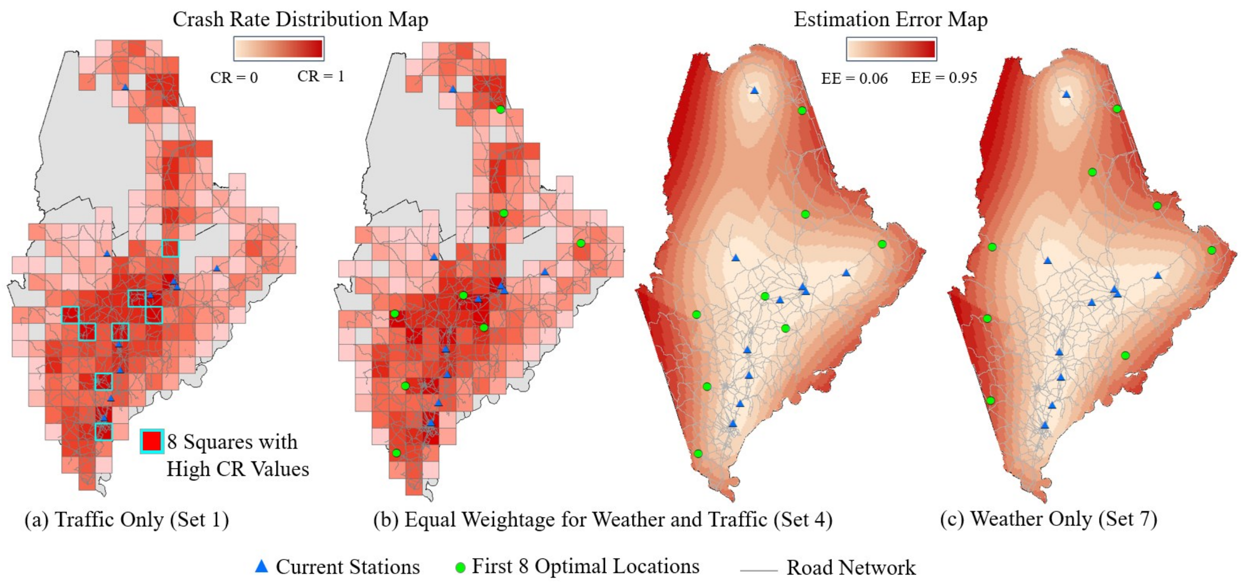

Figure 5- 16: Distribution of First 8 Optimal Locations for (a) Traffic Only Criterion, (b) Dual Criteria, and (c) Weather Only Criterion

A comprehensive sensitivity analysis was conducted to assess the sensitivity associated with the optimal locations generated for the seven sets of weight distributions. This analysis aimed to capture how the optimal locations are influenced by different weightage assigned to the weather and traffic factors. To conduct the sensitivity analysis, the EE and CR values for all seven sets of solutions were extracted from the EE map and CR map, respectively, using ArcGIS. **Figure 5-17** displays the results of the sensitivity analysis.

The analysis reveals that higher percentages of the weather factor prioritize locations with higher EE values, while higher percentages of the traffic factor prioritize accident-prone locations with higher CR values. These findings validate the effectiveness of the optimization process and offer insights into the influence of factor weightage on location selection.

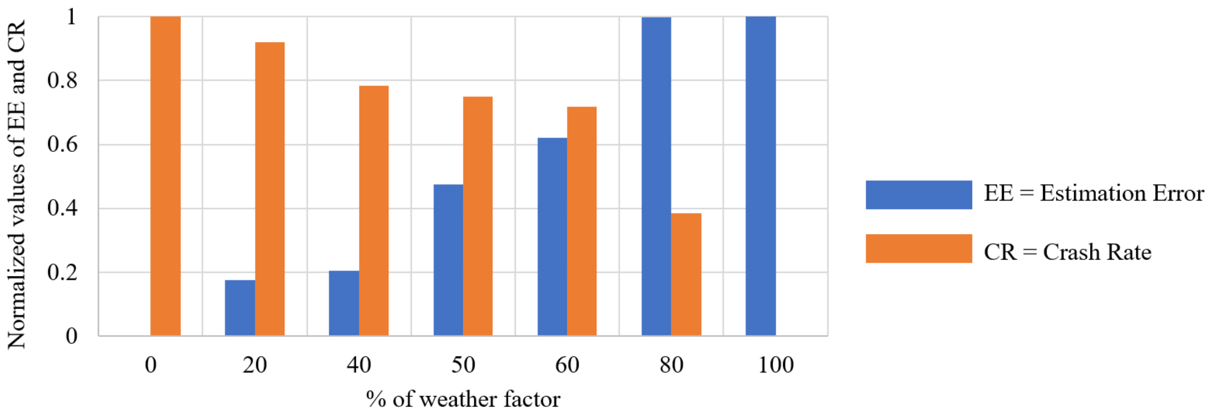

Figure 5- 17: Sensitivity Analysis Result for First 8 Locations: Normalized EE and CR values for 7 Sets of Optimal Location

Scenario – ii: Generate the second 10 optimal locations

In the case of determining the second set of ten optimal locations, the initial eight optimal locations for the dual criteria were treated as existing stations, along with the current RWIS stations. Similar to scenario-i, solutions were generated for seven sets of weight distributions, and the three most significant cases are presented in **Figure 5-18**. The distribution of second ten optimal locations for all seven sensitivity analysis scenarios are provided in Appendix – D.

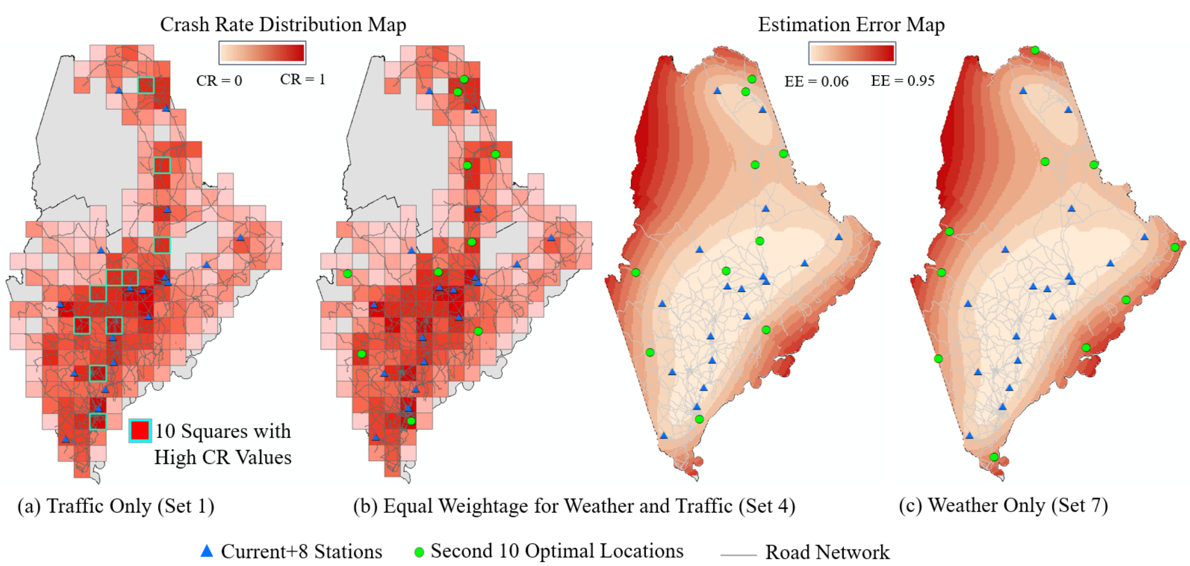

Figure 5- 18: Distribution of Second 10 Optimal Locations for (a) Traffic Only Criterion, (b) Dual Criteria, and (c) Weather Only Criterion

Figure 5-18 (a) highlights the top ten square polygons with higher CR values, while the weather-only criterion strategically places RWIS stations in locations with higher EE values to accurately capture weather phenomena. In the case of the dual scenario, the location solution achieves a balance between capturing weather variability and addressing hotspot areas.

Figure 5-19 presents the sensitivity analysis results for Scenario-ii, showing a near identical pattern to the previous case, demonstrating the clear influence of factor weightage on optimal location selection.

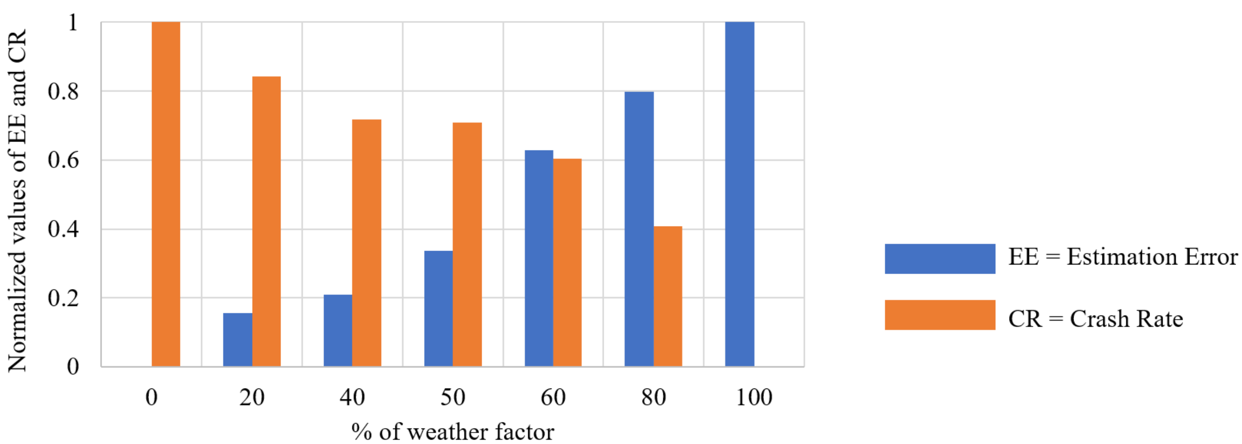

Figure 5- 19: Sensitivity Analysis Result for Second 10 Locations: Normalized EE and CR Values for 7 Sets of Optimal Location

Scenario – iii: Generate the third 6 optimal locations

To determine the third set of optimal locations, the first eight and second ten optimal locations for the dual criteria were considered as existing stations, along with the current RWIS stations. Following the methodology employed in previous scenarios, solutions were generated for seven sets of weight distributions. The distribution of third six optimal locations for all seven sensitivity analysis scenarios are provided in Appendix – E. The findings of the three most significant cases are presented in **Figure 5-20**.

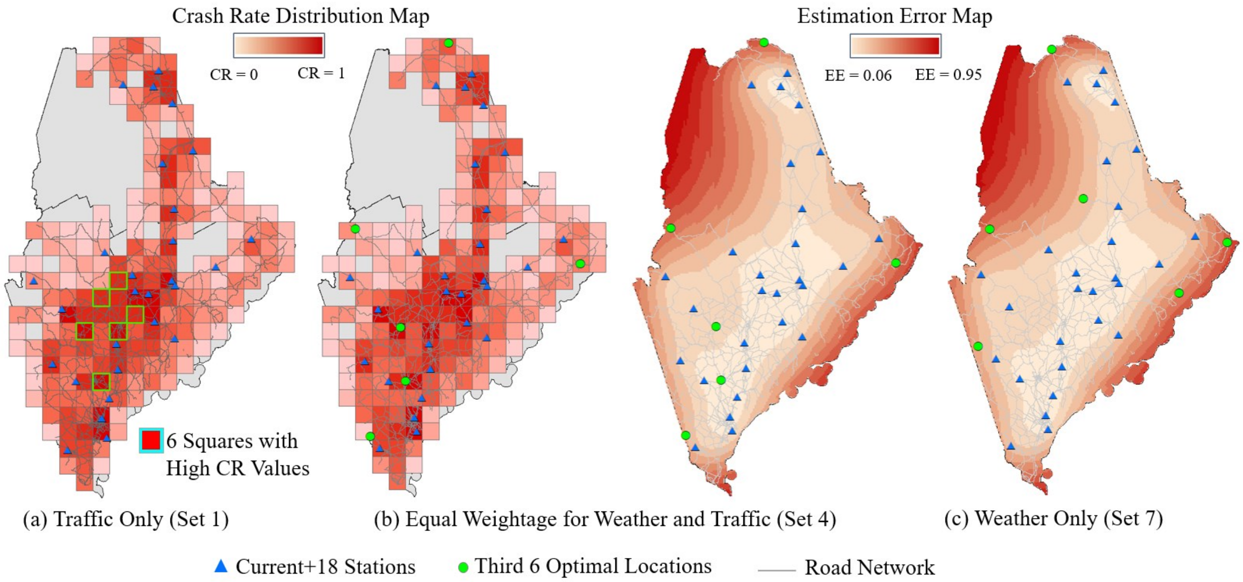

Figure 5- 20: Distribution of Third 6 Optimal Locations for (a) Traffic Only Criterion, (b) Dual Criteria, and (c) Weather Only Criterion

Here, in **Figure 5-20** (a), the top six square polygons with higher CR values are emphasized, and the weather-only criterion strategically positions RWIS stations in locations with higher EE values to increase interpolation accuracy. **Figure 5-21** displays the sensitivity analysis results for Scenario-iii, which is the same as the two previous cases. This further confirms the location weight dependency.

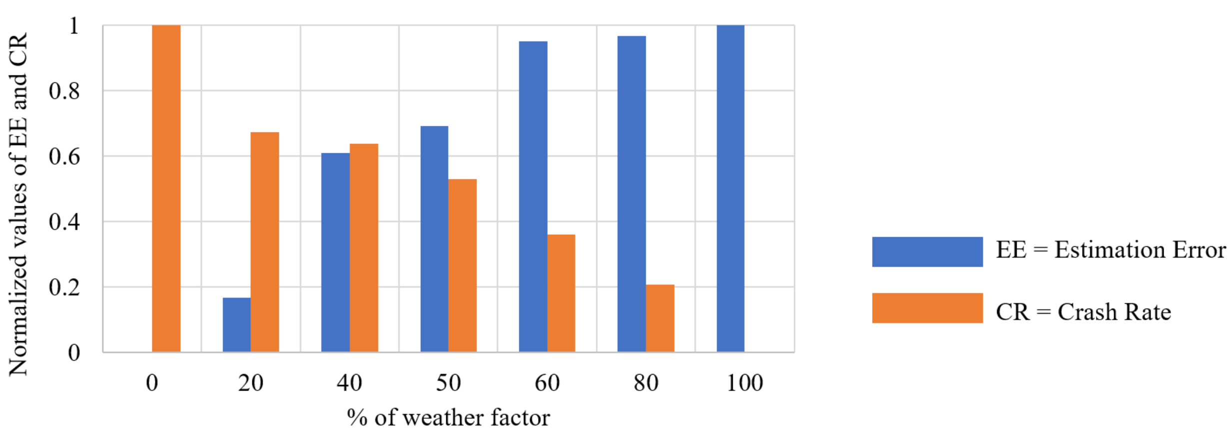

Figure 5- 21: Sensitivity Analysis Result for Third 6 Locations: Normalized EE and CR values for 7 Sets of Optimal Location

Overall, the sensitivity analysis provides valuable insights into the impact of varying weightage on the selection of optimal locations. These findings underscore the importance of carefully considering and adjusting the weightage assigned to different factors when determining optimal RWIS locations.

Performance Analysis of RWIS Network

After identifying the optimal locations through clean-slate optimization, the study embarked on a comparative analysis with the 8 priority and 18 predetermined locations within Maine's five maintenance zones. Within this framework, the density of RWIS stations was determined based on the length of roads in each zone and the number of existing and new RWIS stations. The analysis was also aimed not just at validating the predetermined locations but also delved into an equity assessment to ensure that the RWIS stations are distributed fairly across the five distinct zones.

The results, presented in **Table 5-4**, indicate that the RWIS densities for both the priority and optimal locations remain consistent across eight stations. This consistency provides evidence supporting the validity of the selected priority locations. When comparing the 18 predetermined and 18 optimal locations, similar numbers of stations are observed in most regions, with minor differences between Zone 1 and 5. The evaluation of standard deviation values unveils that the predetermined case is characterized by a slightly higher variability (1.29), contrasting with the more streamlined standard deviation found in the optimal case (0.979). From an equity perspective, this numerical difference underscores a more refined alignment of the RWIS stations within the optimal solution, reflecting a concerted effort to evenly balance the distribution across different zones. Consequently, the optimal case not only illustrates the efficacy of the selected locations but also emphasizes a more harmonized and equitable distribution of RWIS stations across the maintenance zones.

Table 5-4. RWIS Density Comparison between Priority and Predetermined Locations with Optimal Locations

Maintenance Zone		**1**	**2**	**3**	**4**	**5**
Road Length (1000 km)		2.25	1.73	1.62	2.05	1.63
8 Priority Locations	Priority and Existing RWIS	4	3	2	6	3
	Density per 1000 km of Road	1.78	1.74	1.23	2.93	1.84
First 8 Optimal Locations	Optimal and Existing RWIS	4	3	2	6	3
	Density per 1000 km of Road	1.78	1.74	1.23	2.93	1.84
18 Predetermined Locations	Predetermined and Existing RWIS	4	4	4	8	8
	Density per 1000 km of Road	1.78	2.32	2.47	3.90	4.91
First 8 + Second 10 Optimal Locations	Optimal and Existing RWIS	5	4	4	8	7
	Density per 1000 km of Road	2.23	2.32	2.47	3.90	4.29

The impact of incorporating additional RWIS stations into Maine's network was also evaluated by analyzing the 'objective function' values associated with each set of solutions during the optimization process. The findings, depicted in **Figure 5-22**, quantify the percentage improvement in monitoring coverage. The infusion of the first 8 and second 10 stations show substantial improvement, while the improvement for the third set of 6 stations is relatively lower, indicating that the network is nearing saturation. The monitoring improvement for optimal locations surpasses that of the proposed locations. This is because the entire road network of Maine was utilized as a study corridor for the optimal case, leading to more favorable outcomes. While the improvement for 8 priority locations is slightly lower than the optimal case, the second set of 10 locations demonstrates similar improvements. These findings confirm the effectiveness and validity of the predetermined locations proposed by Maine DOT in optimizing the RWIS network.

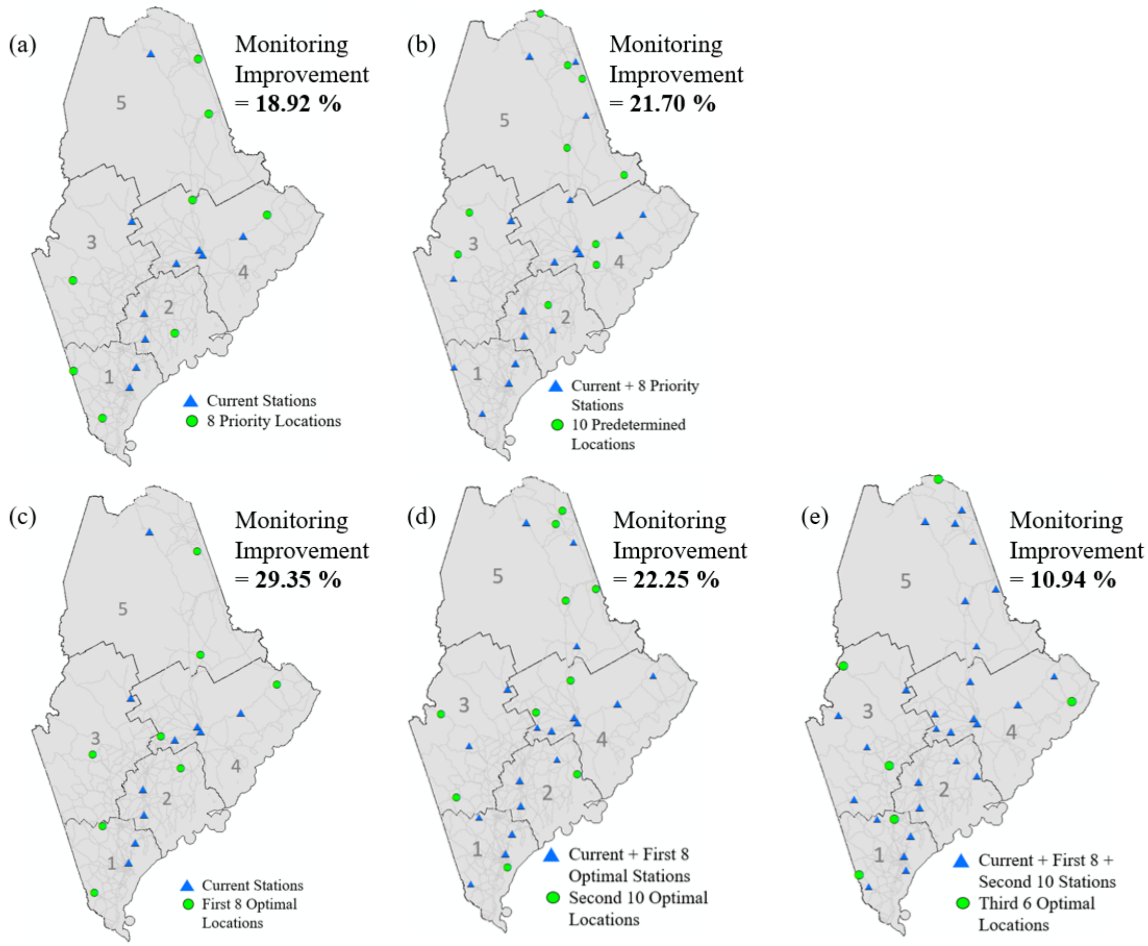

Figure 5- 22: Enhanced Network Monitoring: The Impact of Additional RWIS Stations

5.6 Bi-Level Sequential Optimization Model

Following the density and location optimization of RWIS stations, this study introduces a novel bi-level sequential optimization model to determine both locations and types of RWIS stations (R-RWIS and M-RWIS) to enhance the efficiency and effectiveness of the RWIS network deployment. The procedure for development of bi-level sequential optimization is below.

Definition of variables

- Monitoring Stations (R-RWIS and M-RWIS): A combination of k *(1, 2, . . . , R)* number of R-RWIS and k' *(1, 2, . . . ,M)* number of M-RWIS with location attribute $X = [x_1, \ldots, x_k]$ and $X' = [x'_1, \ldots, x'_{k'}]$ respectively.

- Candidate sites: N, with location attribute $i \in 1, 2, \ldots, N$; which is the total number of grid cells along the road network.

- Weather factor: Variable of interest for R-RWIS is $z(i|X)$, which is the estimation of $z(i)$ given observations at X. Similarly, variable of interest for M-RWIS is $z'(i|X')$, which is the estimation of $z(i)$ given observations at X'.

- Traffic factor: Decision variables, $y_{k,i}$ and $y_{k',i}$ [1 if an RWIS station is assigned to cell i, 0 otherwise]. μ_i^{-1} is the inverse of accident / crash rate.

Objective function for allocating k number of R-RWIS

$$C_R = Min\ \varphi(X) = [\tfrac{1}{N}.\textstyle\sum_i \left(\sqrt{\sigma^2\ [z(i|X)]}\right).\omega + \tfrac{1}{R}.\sum_i(\mu_i^{-1}.\sum_k y_{k,i}).(1-\omega)\ ];\ \forall i,\ \forall k \qquad (5\text{-}1)$$

Subject to:

$0 \le \omega \le 1$

$y_{k,i} \in \{0, 1\};\ \forall i\ ,\ \forall k$

Here, C_R is the criterion value (objective function value) for R-RWIS.

Objective function for allocating k' number of M-RWIS

$$C_M = Min\ \varphi(X') = [\tfrac{1}{N}.\textstyle\sum_i \left(\sqrt{\sigma^2\ [z(i|X')]}\right).\omega + \tfrac{1}{M}.\sum_i(\mu_i^{-1}.\sum_{k'} y_{k',i}).\ (1-\omega)];\ \forall i,\ \forall k' \qquad (5\text{-}2)$$

Subject to:

$0 \le \omega \le 1$

$y_{k',i} \in \{0, 1\};\ \forall i\ ,\ \forall k'$

Here, C_M is the criterion value (objective function value) for M-RWIS.

Replaceable and non-replaceable R-RWIS

Non-replaceable number of R-RWIS was determined by comparing the criterion value of R-RWIS (C_R) and M-RWIS (C_M) as presented in **Figure 5-23**. C_M is expected to be higher than that of C_R

for a certain number of RWIS, as it is evident that R-RWIS provides better monitoring coverage than M-RWIS. As the number of RWIS increases, the marginal benefit decreases. At a point, it becomes close to zero. At this step, the criterion values, $C_{M,}$ is determined where the marginal benefit is close to zero. This value is then compared to C_R to determine the number of R-RWIS that are replaceable (k_{Repl}) with M-RWIS and the number of non-replaceable R-RWIS (k_{NRepl}) following this equation:

$$k_{Optimal} = k_{Repl} + k_{NRepl} \tag{5-3}$$

Here, $k_{Optimal}$ is the optimal density of R-RWIS which was determined in section 4.4 (RWIS Density Determination for Maine). By comparing the criterion values, non-replaceable R-RWIS number has been found as 12, while using Equation 13, the replaceable R-RWIS number has been found as 18. This indicates that the network should have 12 R-RWIS in the network and any number from the other 18 R-RWIS can be replaceable with equivalent number of M-RWIS.

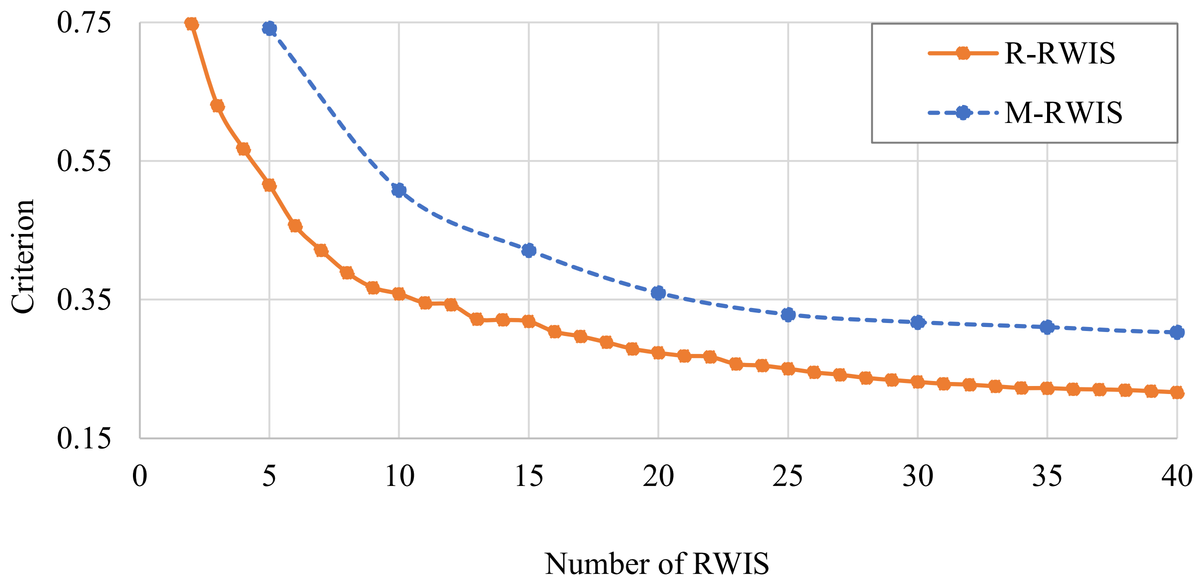

Figure 5- 23: Comparison of criterion for R-RWIS and M-RWIS

Comparable Combinations of R-RWIS and M-RWIS

At the next step, the combinations of R-RWIS and M-RWIS are determined, so that each combination will provide equal monitoring coverage. Here, k number of R-RWIS and k' number of M-RWIS is determined by using two loops as depicted in **Figure 5-24**. For k number of R-RWIS, value of k should be within a range of k_{NRepl} to $k_{Optimal}$ as presented in Equation 5-4. While determining the k' number of M-RWIS, k'_{eqv} should be determined in such a way that the criterion for each replaceable number of R-RWIS is equivalent to the criterion of M-RWIS as shown in Equation 5-5. In that way, equal monitoring coverage can be obtained.

$$\text{For } k\text{: } k = [k_{NRepl}, \ldots, k_{Optimal}] \tag{5-4}$$

$$\text{For } k' : C_R\ (k = k_1, k_2, \ldots, k_{Repl}) = C_M\ (k' = k'_{eqv}) \tag{5-5}$$

By following the same procedure, we can obtain several combinations of R-RWIS and M-RWIS that are able to provide equal monitoring coverage of the network.

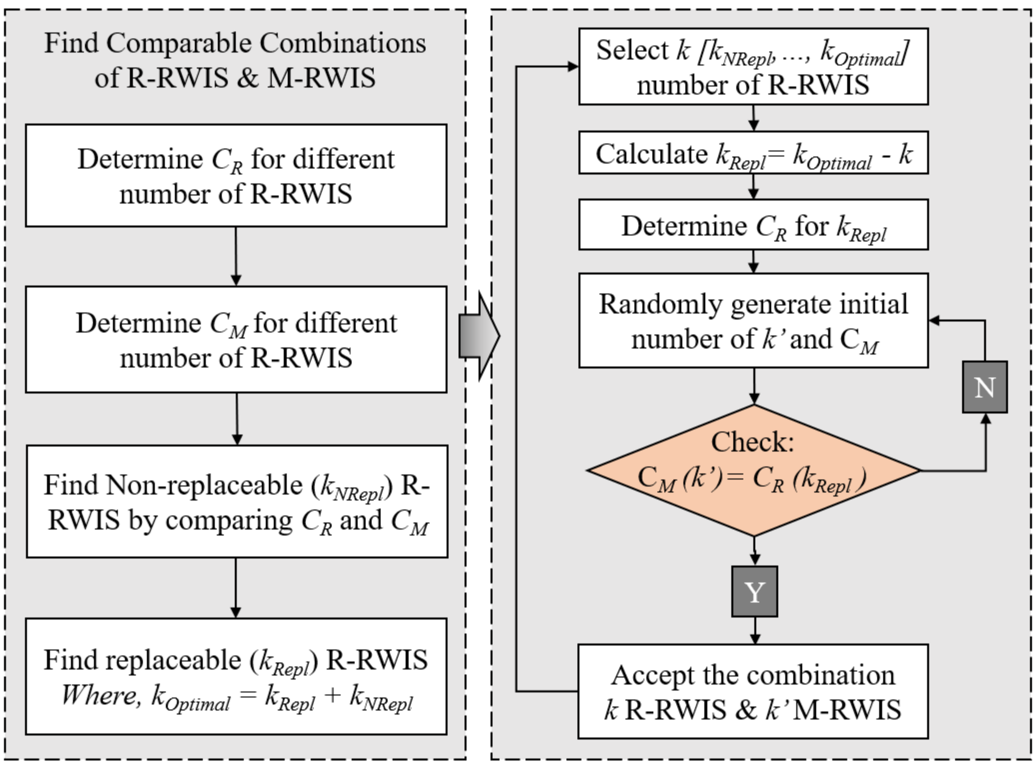

Figure 5- 24: Flow chart for bi-level sequential optimization

For example, the non-replaceable number of R-RWIS has been determined as 12 for the state of Maine, and the density of R-RWIS has been found to be 30. Thus, the following combinations can be generated that provide equal monitoring coverage.

Combination 1 – 30 R-RWIS

Combination 2 – 25 R-RWIS + 5 R-RWIS (equivalent number of M-RWIS)

Combination 3 – 20 R-RWIS + 10 R-RWIS (equivalent number of M-RWIS)

… … …

Combination N – 12 R-RWIS + 18 R-RWIS (equivalent number of M-RWIS)

Equivalent number of M-RWIS is generated in an iterative process by checking the criterion value of R-RWIS and M-RWIS. For example, to replace 5 R-RWIS from a network, 10 M-RWIS is needed to ensure equal coverage. Thus, '25 R-RWIS + 10 M-RWIS' can be considered as a comparable combination of '30 R-RWIS'. Similarly, 30 M-RWIS is required to replace 15 R-RWIS, thus another combination would be '15 R-RWIS + 30 M-RWIS'. A number of comparable combinations are provided in Appendix – F.

Cost-Effective Combination

After generating a set of comparable combinations, the cost-effective combination is determined by applying cost function for all the combinations. The objective function for determining cost-effective combination is as below:

$$Min\ (C_T) = k \times (I_k + C_m \times \frac{1-(1+r)^{-n}}{r}) + k' \times (I_{k'} + C_{m'} \times \frac{1-(1+r)^{-n'}}{r}) \quad (5\text{-}6)$$

Where, C_T = total monetary cost

I_k and $I_{k'}$ are installation costs of each R-RWIS and M-RWIS.

C_m and $C_{m'}$ are yearly maintenance cost/ station for R-RWIS and M-RWIS.

r is discount rate, which is assumed as 8% for this study.

n and n' are lifespan of R-RWIS and M-RWIS.

Several combinations are generated and examined to identify the most cost-effective option, as summarized in **Figure 5-25**.

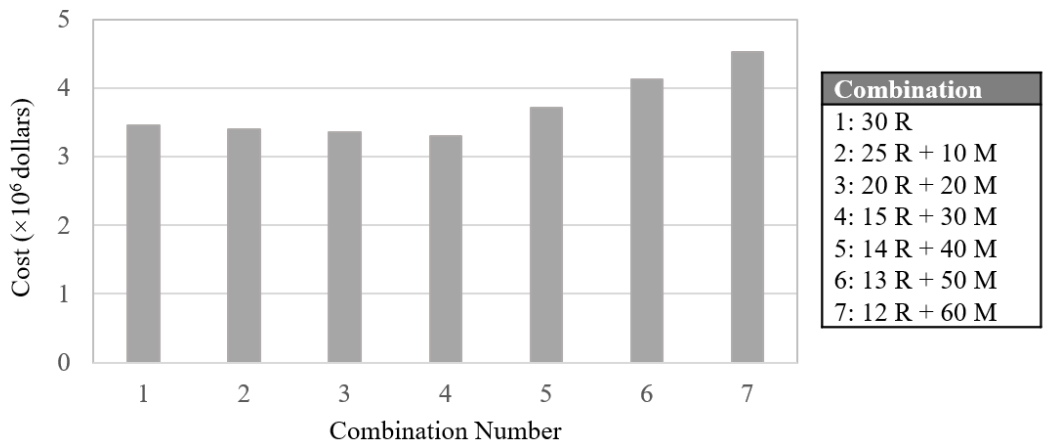

Figure 5- 25: Cost comparison for comparable combinations

According to **Figure 5-25**, the first combination is for only R-RWIS, while from the second combination an incremental number of R-RWIS is replaced by M-RWIS. By comparing the cost of the combinations, it can be noticed that cost can be minimized by replacing a certain number of R-RWIS. For the state of Maine, a combination with 15 R-RWIS and 30 M-RWIS can be determined as the cost-effective combination. The distribution of stations is presented in **Figure 5-26**.

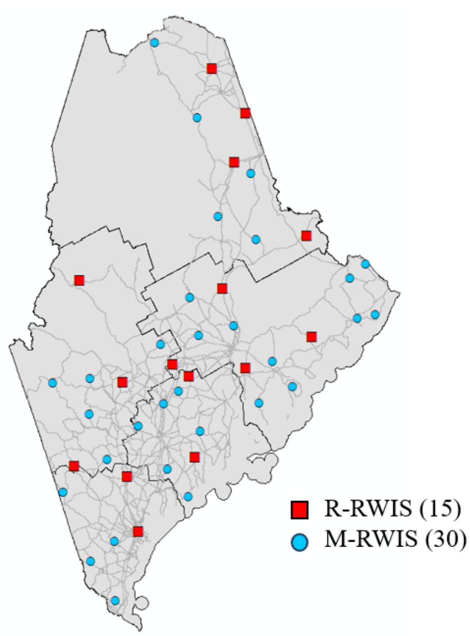

Figure 5- 26: Cost-effective combination (15 Regular RWIS and 30 Mini-RWIS)

The innovative bi-level sequential optimization algorithm developed in this study stands as the inaugural contribution in the literature capable of determining not just the station locations but also the specific type of RWIS required at each location. This additional step marks a substantial advancement in RWIS network planning by enhancing the overall effectiveness of RWIS deployment with a combination of Regular and Mini-RWIS.

The location solutions developed in this research were integrated into a prototype web-based RWIS location visualization platform for demonstrating the proposed models and the resulting solutions, as detailed in the following section.

5.7 Web-Based Visualization Tool

A prototype web-based application has been developed to enable the visualization of the location solutions derived from this research. This application, named LoRWIS (https://sites.google.com/view/lorwis/states/Maine), exhibits the location solutions alongside the distribution of existing RWIS throughout the Maine network. It offers options to display solutions for various scenarios, encompassing various combinations of weather and traffic factors, offering a comprehensive yet user-friendly presentation of the location planning data.

The web platform, as depicted in **Figure 5-27**, features an interactive map that enables users to visualize and interact with multiple layers of generated data. By clicking on any point on the map, users can view specific details like location coordinates and switch between bird's eye and street views. The platform also offers various heatmaps for crash rates and estimation error maps from different optimization scenarios.

The platform also facilitates easy navigation through different RWIS locations and optimization outcomes. It showcases prioritized sites for new installations and allows users to examine different scenarios, balancing weather and traffic data. Likewise, the tool simplifies the evaluation of potential Regular and Mini-RWIS sites, offering a straightforward yet robust tool to compare alternatives and pinpoint the most favorable solution.

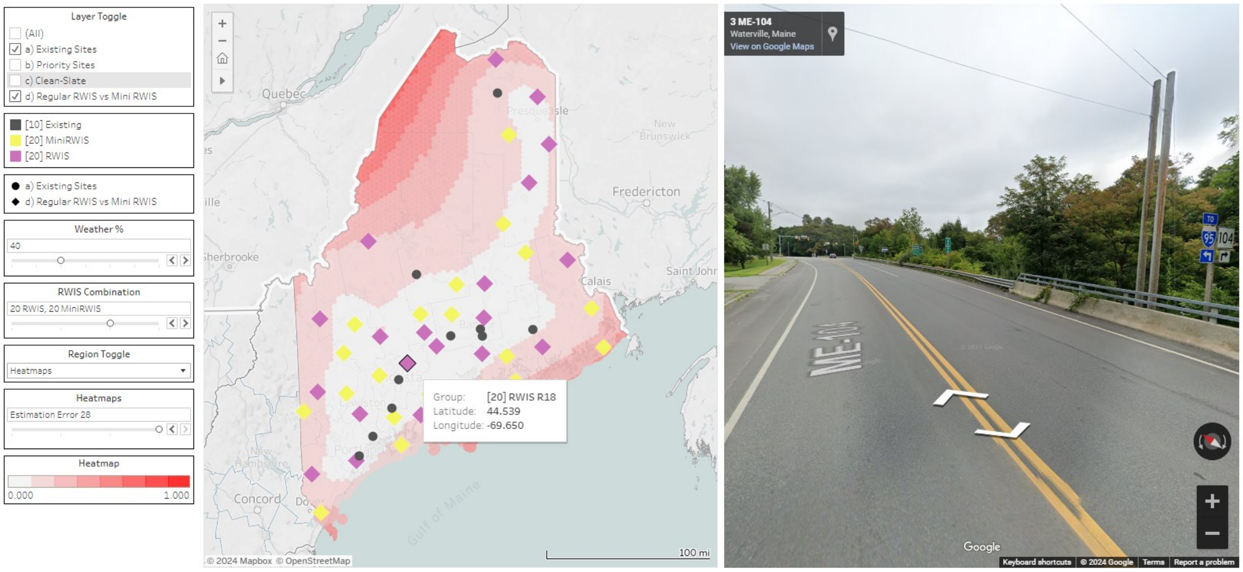

Figure 5- 27: Features of the web-based application; LoRWIS (https://sites.google.com/view/lorwis/states/Maine)

5.8 Summary

This section demonstrates the importance of incorporating the effect of multiple weather variables in optimizing the placement of RWIS. By refining the location-allocation algorithms and utilizing a multi-variable semivariogram model, we have developed a novel optimization framework for determining optimal solutions for RWIS network expansion, a valuable contribution to the field. The refined location allocation framework was applied in regional RWIS network planning for the state of Maine, where we carried out a comprehensive state-wide gap analysis to determine the most suitable locations. To further assess the selection of optimal locations, a sensitivity analysis was conducted to examine the effects of assigning different weightings to weather variability and traffic factors. Lastly, a novel bi-level sequential optimization was developed in this study to determine not only the location but also the type of RWIS stations that are needed in each location.

The key contribution of this research is listed below:

- This research has made significant strides in the optimization of RWIS station placement by introducing an innovative multi-variable semivariogram model that considers essential road weather variables. The comparative study between single and multi-variable semivariogram models demonstrates that employing the multi-variable approach leads to more precise location solutions by effectively capturing the variability of multiple weather variables, resulting in significantly improved monitoring coverage compared to single-variable models.

- Through the application of this refined framework to Maine's existing RWIS network, we modelled prioritized strategic locations for installing RWIS stations, ensuring equitable and balanced distribution across various zones, and statewide coverage. The location solutions generated are currently being adopted by Maine DOT for future implementations, demonstrating the practicality and robustness of our approach.

- A total of 24 locations were generated using the optimization model for the annual installation of RWIS stations, aligning with the requirements of Maine DOT. These generated locations serve as evidence of the validity and effectiveness of the proposed locations. Additionally, the sensitivity analysis allowed us to assess the impact of different weightings for weather and traffic factors on the selection of optimal station locations. This information empowers decision-makers to tailor the model according to specific monitoring requirements.

- An empirical optimal density model was developed tailored for the state of Maine. The developed model presents the ideal number of RWIS stations required to ensure comprehensive monitoring coverage. Furthermore, the methodology for attaining optimality with a specific number of existing stations is elucidated, accompanied by the recommendation of additional station numbers for ensuring optimality.

- This research introduced an innovative bi-level sequential optimization model aimed at determining both the location and type of RWIS stations, including Regular and Mini-RWIS. This approach enhances the overall effectiveness of RWIS network deployment. A combination of Regular and Mini-RWIS is presented utilizing the developed model, ensuring equivalent monitoring coverage of the network. Ultimately, the cost-effective solution was identified.

- The solutions developed in this project were integrated into LoRWIS (https://sites.google.com/view/lorwis/states/Maine), a prototype web-based RWIS location visualization platform for demonstrating the proposed models and the resulting solutions.

Chapter 6

Quantitative Assessment of Optimal RWIS Network[5]

6.1 Introduction

Optimal RWIS network can be defined as an RWIS configuration where the total number of stations (RWIS density) are determined based on a well-established guideline and the locations are allocated systematically assuming that it will provide the maximum monitoring coverage of the network. This chapter examines and quantifies the benefits of an optimized RWIS network by introducing a performance indicator, named network coverage index (NCI). NCI, introduced in this study, has the capability to assess the performance of the RWIS network and quantitatively evaluate its influence on traffic safety.

While developing the optimal RWIS location solution, it was implicitly assumed that each solution set is associated with a unique spatial configuration tied to an objective function value or sum of kriging variance that represents RWIS' monitoring capability. The solution set associated with the lowest objective function value (lowest kriging variance) would be considered the solution with the highest network coverage and thus assumed to be most beneficial (Biswas and Kwon 2022). Based on this presumption that network coverage is a vital parameter for determining the goodness of an RWIS configuration, there is a resurgent need to extend this effort by investigating if it could also be used to explain its impact on traffic safety – a worthwhile attempt that has never been made in existing literature pertaining to quantifying the safety benefits of RWIS location solutions.

Therefore, the primary objectives of this chapter are: (a) to investigate the relationship between a newly created measure called network coverage index (NCI) and network configuration of RWIS, and (b) quantitatively assess the impact of NCI on the transportation system based on collision reduction potential. The findings of this chapter will provide a clearer understanding of the benefit of an optimal RWIS solution and its impact on the transportation system.

---

[5] Biswas, S., Sharma, D., & Kwon, T. J. (2022). Safety Impact Assessment of Optimal RWIS Networks—An Empirical Examination. Sustainability, 15(1), 327.

6.2 Research Procedure

The methodological framework is built upon our previous efforts in RWIS location-allocation, where the kriging variance is used as a performance indicator for monitoring coverage. The first phase of this study was the database development by aggregating and integrating various data sets into GIS. Two datasets were developed, one to determine the NCI (a more detailed description is to follow) and another to evaluate safety.

After extracting the RWIS station data, a quality check was performed using the following methods: data completeness test, reasonable range test, and a neighborhood value comparison. Following this, detrending was performed with respect to time using Generalized additive model (GAM) (Wang et al. 2019, Hastie et al. 1990), followed by geostatistical analysis. Spatiotemporal analysis was performed by constructing empirical semivariograms from the processed data, which optimizes parameter estimations for unsampled locations and captures the possible autocorrelation associated with the RWIS variables. Joint semivariogram models were then developed by combining spatial and temporal semivariograms to evaluate the spatiotemporal variability of RWIS measurements (Biswas and Kwon 2022).

Based on parameters obtained from the joint semivariogram, kriging interpolation was used to estimate values at unsampled locations and their estimation error or kriging variance. Kriging variance was then utilized to determine the NCI for respective RWIS networks. The procedure was repeated for each set of RWIS configurations to investigate its impact on the NCI.

In terms of safety evaluation, 12 years (2008 to 2019) of inclement winter weather collision data were extracted, among which collisions due to poor road surface conditions were isolated for safety evaluation. Additionally, only major network roads, i.e., Interstate, State, and U.S. highways were considered due to maintenance departments prioritizing major roads for treatment. RWIS stations included in the safety evaluation were selected based on three review criteria: (a) data review to ensure that sufficient before and after period collision data were available, (b) geometry review to ensure that no major design nor construction activities occurred near the RWIS stations, and (c) operation review to ensure that minimal operation gaps were present in the data. The processed data were employed to calibrate the safety performance functions (SPFs) and yearly calibration functions (YCFs). Next, Empirical Bayes (E.B.) analysis was applied to determine the collision reduction associated with each of the selected RWIS stations (Sharma 2022).

Upon processing the data, the impact of NCI on collision reduction was assessed in order to evaluate the goodness of the RWIS location solutions. Research procedures for this study are summarized in **Figure 6-1**.

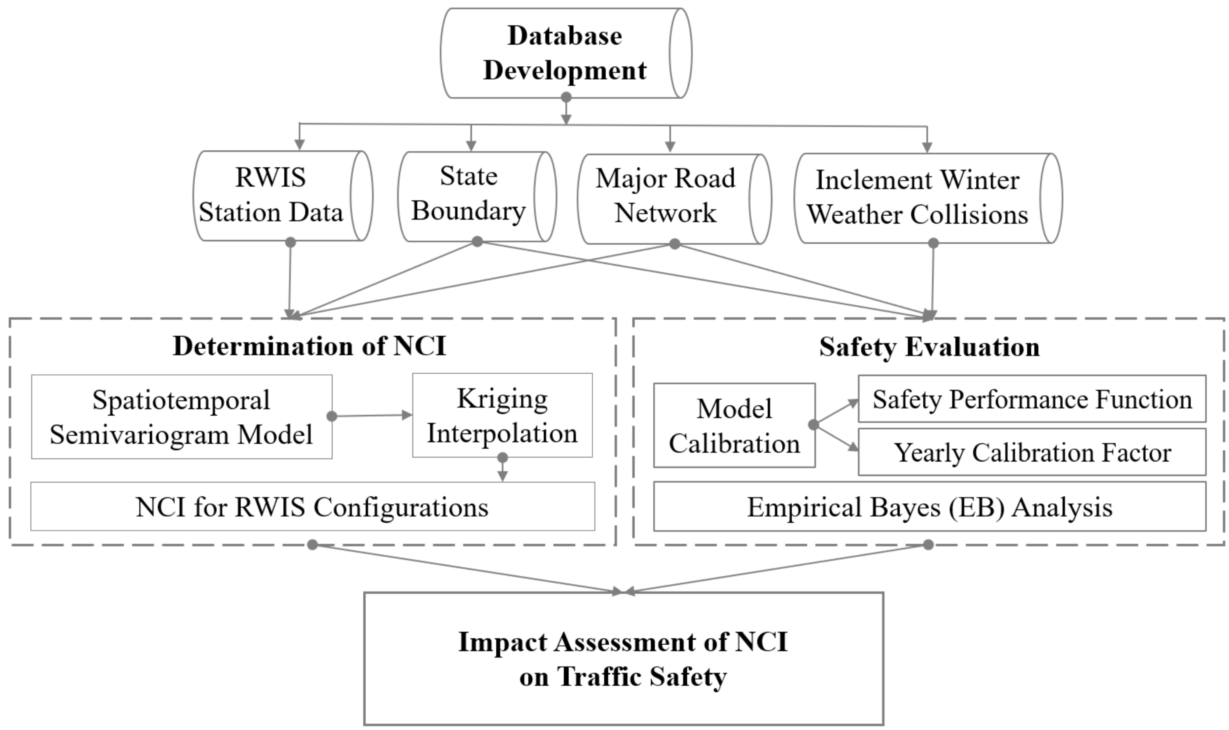

Figure 6- 1: Methodological flowchart

The network coverage index (NCI) was used to rate the monitoring capabilities of a defined RWIS configuration for a specific region. It is a surrogate measure that ranges between 0 and 1, where 0 represents no monitoring coverage, and 1 represents complete network coverage.

6.3 Study Area and Data Description

Study Area

Iowa—the selected study area—is a flatland region consisting of rolling plains and flat prairies. This state was categorized as a moderate-severe weather region (Biswas et al. 2019) where the adverse winter negatively impacts the transportation system. In regions like this, RWIS information plays a critical role, where the information it provides increases the responsiveness of winter road maintenance activity. The RWIS network of this state consists of 86 stations. **Figure 6-2** represents the distribution of RWIS stations along with the major road networks in Iowa.

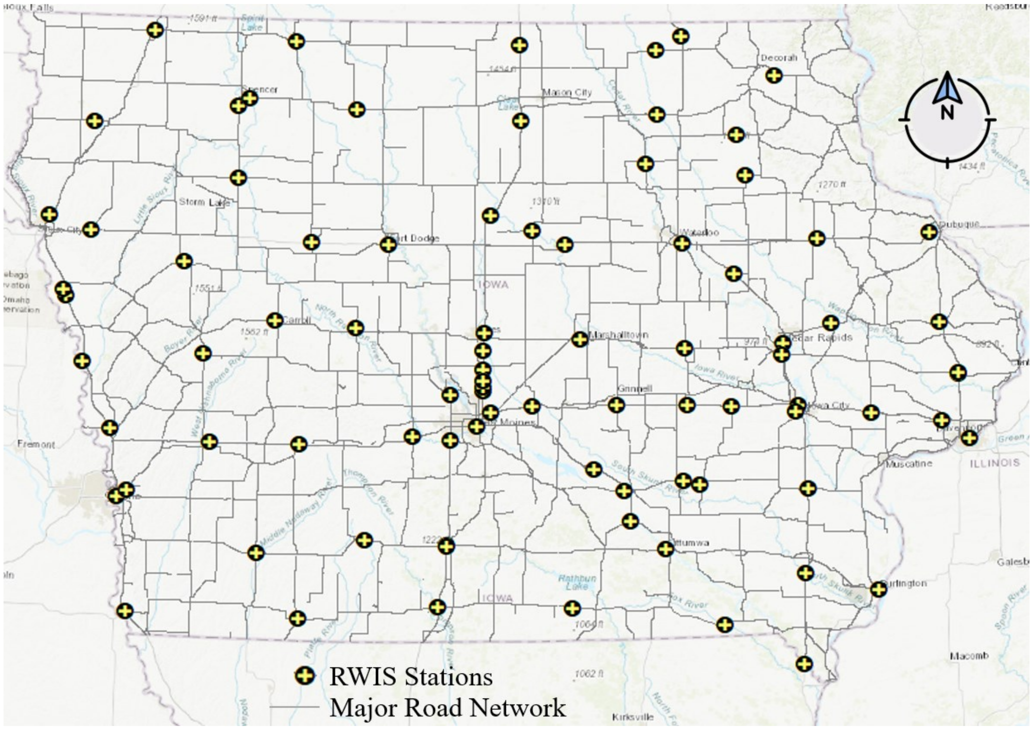

Figure 6- 2: RWIS network and major roads in the state of Iowa

Data Description and Integration

The RWIS data used in this study was downloaded from Iowa State University's website (http://mesonet.agron.iastate.edu/RWIS/). Variables that were recorded include air and surface temperature, dew point temperature, visibility, wind speed, road surface conditions, etc., collected at 15 to 20-minute intervals. Winter season data (October 2016 to March 2017) was processed based on the quality check procedures discussed in the methodology section. Among these various RWIS measurements, road surface temperature (RST) was considered to be the most critical as it has a significant influence on the formation of ice and road surface friction, both of which are crucial factors for winter road maintenance (WRM) operations (Hatamzad 2022). Post-processing for the semivariogram analysis was done using the R statistical package – version 3.2.5 (Pebesma 2004, R Core Team 2018). Here, spatial and temporal semivariograms were constructed by considering space and time attributes separately. The output variograms (spatial and temporal) were then combined into a joint semivariogram using spatiotemporal anisotropy parameters (StAni), allowing us to preserve both spatial and temporal features. StAni represents the number of space units equivalent to one time unit. In this study, joint semivariograms for a mid-winter month were utilized for kriging variance determination. The continuity ranges of autocorrelation are presented in **Figure 6-3**. The spatial range of the variable of interest (RST) was found to be around 20 km for the month of January, while the temporal range was approximately 21.5 hours. The resultant joint semivariogram range was found to be 17 km in this case, which is lower than the spatial range. This finding makes intuitive sense since both spatial and temporal attributes are preserved in the joint semivariogram. The readers are referred to our previous work for a detailed investigation on joint semivariogram analysis for multiple weather variables (Biswas and Kwon 2022).

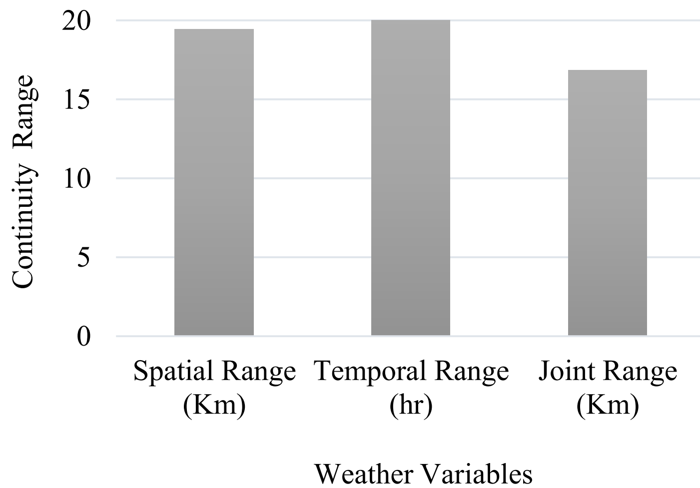

Figure 6- 3: Spatial, temporal, and joint semivariogram parameters of RST for January 2017

The parameters of the joint semivariogram were used in this study to evaluate the impact of RWIS configurations on NCI. The state of Iowa was used as the experimental boundary for determining the kriging variance. In addition, the major road network of this state was used as a constraint as to where the kriging estimation will be conducted; meaning that the observed RWIS measurements were used to estimate the unsampled location that lies on the major road network of Iowa. State boundary and major road network shapefiles were integrated within ArcGIS (ESRI 2015) to create a 5 km × 5 km grid surface of unsampled locations for what the kriging estimations were generated for. Afterwards, the variance was translated into NCI for the impact assessment of the RWIS network. The following section discusses the findings of the analysis.

6.4 Results and Discussion

This study focuses on quantifying the benefit of optimal RWIS network by evaluating the collision reduction potential of various RWIS configurations. In our previous study, the methodological framework for determining the optimal RWIS network was based on the concept that every location solution or RWIS configuration is associated with an objective function value (kriging variance). The optimal location solution has the lowest objective function value, and it is assumed to provide the maximum network monitoring coverage. In this study, the RWIS network coverage index (NCI) was determined for a set of RWIS configurations to establish a link between NCI and safety benefits. Kriging estimation error was used here to determine the NCI, while percent collision reduction was used as a performance indicator to quantify its benefit. The findings of this study are described below:

6.4.1 Dependency of NCI on RWIS Configuration

The relationship between kriging variance and NCI can be derived from the concept that NCI is inversely related to kriging variance. Hence, a proportional factor should be introduced to construct the relationship as defined previously in Section 3.7.

It was assumed that an optimal RWIS density provides full network coverage of Iowa with an NCI value of 1. According to one of our previous studies, the optimal number of RWIS stations for Iowa is 61 (Biswas and Kwon 2020). Hence, at best, 'K' in Equation 3-19 is equal to the kriging variance associated with this optimal number, and the maximum number of RWIS stations is capped at 61 because kriging variance cannot, or at least theoretically, go below optimal. Kriging variance is calculated using the joint semivariogram model developed in our previous study through a series of geostatistical analyses, where both spatial and temporal aspects were preserved (Biswas and Kwon 2022). Here the estimation variance was determined for an increasing number of RWIS stations. As the number of RWIS stations increases, the monitoring capability is expected to improve. This phenomenon is represented in **Figure 6-4** by the decrease in kriging variance as the number of stations increases.

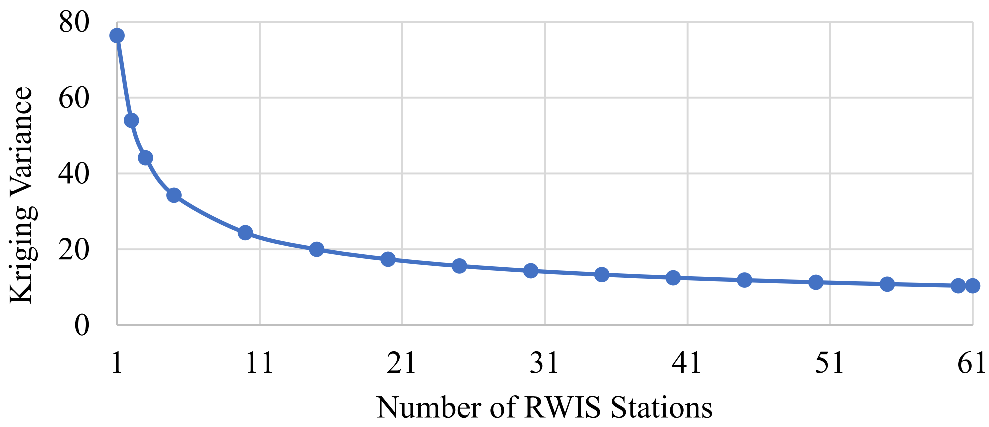

Figure 6- 4: Plot of kriging variance for different number of RWIS stations

From **Figure 6-4**, the value of kriging variance associated with the optimal scenario is 10.36 – the number at which the greatest rate of change on kriging variance happens to occur. At this point, full monitoring coverage can be achieved with an NCI value of 1. Thus, the proportional factor, K = 10.36 is used to update the equation as follows.

$$NCI = \frac{10.36}{Kriging\ Variance} \tag{6-1}$$

NCI values for different RWIS configurations can be achieved using Equation 6-1, which changes **Figure 6-4** to **Figure 6-5**. According to **Figure 6-5**, the monitoring coverage increases as the number of RWIS stations increases. In contrast, the marginal benefit gained with each additional RWIS decreases. The combination of these two effects results in the graph being concave shaped.

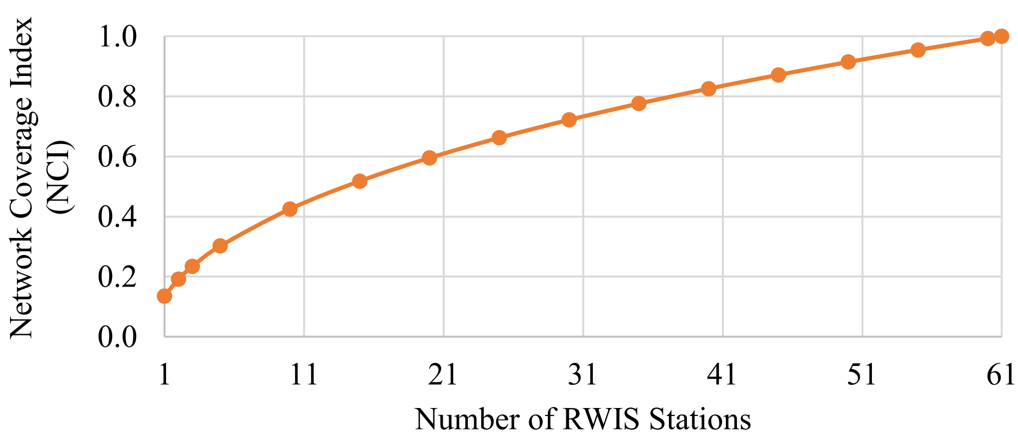

Figure 6- 5: Plot of NCI for different number of RWIS stations

NCI and kriging variance for different RWIS configurations is presented in **Figure 6-6.**

(a) Scenario 1
Number of RWIS Station = 5
Kriging Variance = 34.29
NCI = 0.30

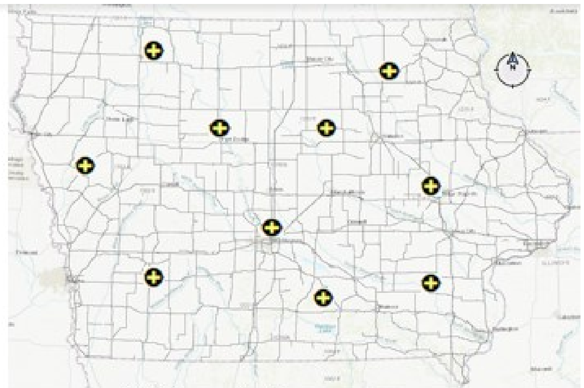

(b) Scenario 2
Number of RWIS Station = 10
Kriging Variance = 24.37
NCI = 0.43

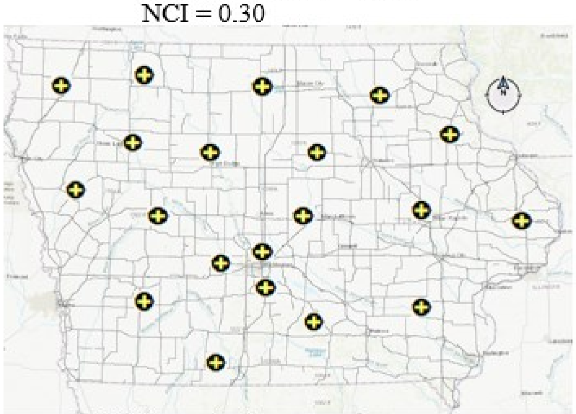

(d) Scenario 4
Number of RWIS Station = 20
Kriging Variance = 17.40
NCI = 0.60

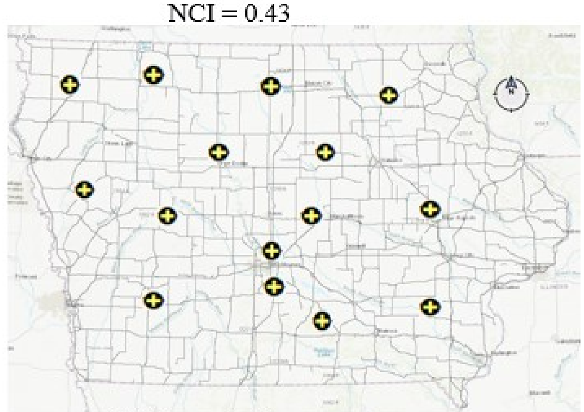

(c) Scenario 3
Number of RWIS Station = 15
Kriging Variance = 19.99
NCI = 0.52

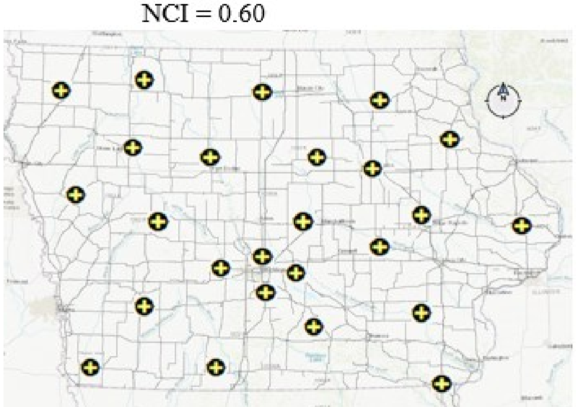

(e) Scenario 5
Number of RWIS Station = 25
Kriging Variance = 15.64
NCI = 0.66

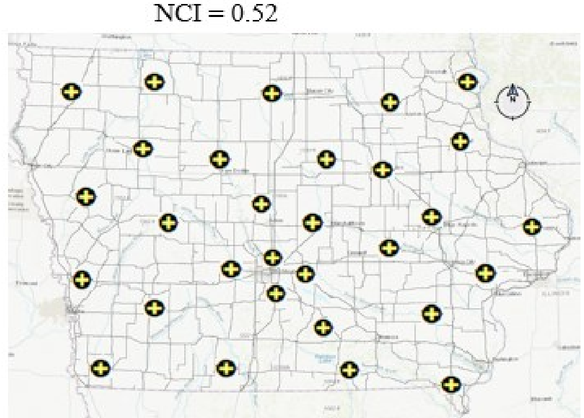

(f) Scenario 6
Number of RWIS Station = 30
Kriging Variance = 14.35
NCI = 0.72

Figure 6- 6: NCI and kriging variance for different scenario

Figure 6-6 demonstrates how monitoring coverage changes with an increase in the number of stations. An example of this is the difference between scenarios one and six. Only 30% (NCI=0.3) of optimal coverage could be provided as a result of having only five stations. In contrast, due to the increase in the number of stations in scenario six, the coverage level increased to 70%. Furthermore, the scenario with 5 RWIS stations generated an estimation error of 34.29, while a much smaller value (14.35) is obtained from the 30 stations scenario. It is clear from the above discussion that the NCI strongly depends on the density of the RWIS network. Thus, NCI is used in the subsequent section as a performance indicator to determine traffic safety benefits.

6.4.2 Impact Assessment of Iowa's RWIS Network

Our recent study examined the safety benefits of RWIS stations in Iowa using before-and-after Empirical Bayes (E.B.) method (Sharma 2022). This method requires collision data before and after the implementation of the countermeasure. The study period was isolated to 2008 – 2019 and according to the operation information of the RWIS stations of Iowa, 30 stations were implemented within the study period. The selected 30 stations were filtered using a review criterion including data review, geometry review and operation review as discussed previously. This study considered 2 years of only winter months, (i.e., November to March) of before implementation and after implementation periods in the analysis. Thus, stations with inadequate data sizes or shorter operational periods, were removed from the analysis. Secondly, geometric changes near RWIS stations during the before and after period were reviewed to identify major construction activities within the study period. Stations near major geometric changes were removed from analysis as variations in road geometry can lead to unexpected changes in collision behavior. Lastly, operational issues associated with stations were identified by assessing the frequency of data collection. Stations having issues with data collection were removed from the analysis as they have a negligible effect on WRM, as the data provided was insufficient. At the end of the review, 11 out of 30 stations were eliminated from analysis. Of the remaining stations, 7 stations along with associated service area and treatment sites were selected and are presented in **Figure 6-7**.

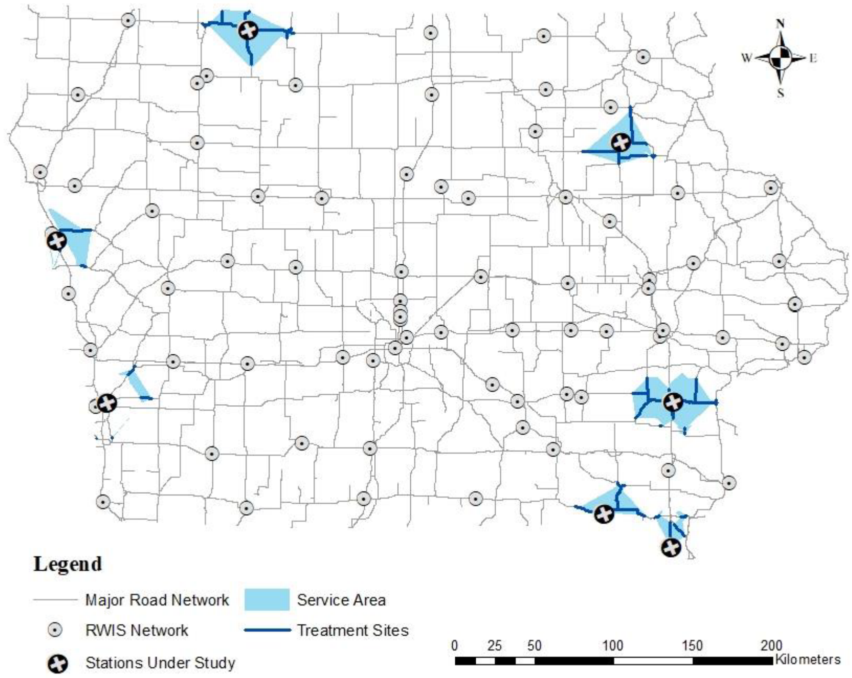

Figure 6- 7: Map of Iowa showing various elements used in the safety evaluation study

The effect of a countermeasure (RWIS station) can be assessed by observing the change in collision frequency for a number of sites that are under the influence of that RWIS station. Here, a 30 km radius around an RWIS station was assumed as the influence region and accessible roads within this distance from the facility were considered its service area. For several cases where multiple stations were implemented close to each other, the service area under one station will overlap the service area of another station. Such stations were also removed from the analysis to avoid selecting sites that could be under the influence of another station. At this stage, 12 RWIS stations were eliminated from the analysis because the influence regions for these stations were partially or completely overlapped with another station. Hence, 7 stations were selected for the safety evaluation that has a significant influence region with a reasonable number of sites. According to the analysis result, the collision reduction potential for an RWIS station varies from 31.53% to 88.23%, with an average reduction of 65% in winter weather collisions (Sharma 2022). The number of collision reductions varies from 4.73 to 27.61, with an average collision reduction value of 15. Since the total number of sites in each station ranges from 4 to 22, we can divide the number of collisions reduced by the number of sites to quantify the safety benefit of an individual station—an average value of 1.06. **Table 6-1** depicts the collision reduction potential for different stations.

Table 6- 1. Average Collision Reduction Calculation Based on Safety Evaluation

Station ID	Collision Reduction (%)	Number of Collision Reduction	Total Sites	Collision Reduction Per Site
RCCI4	59.49	5.4	7	0.7714
RCLI4	83.11	8.81	12	0.7342
RETI4	31.53	21.22	22	0.9645
RSOI4	83.8	4.73	4	1.1825
RAGI4	88.23	14.03	12	1.1692
RAII4	46.87	27.61	19	1.4532
RMYI4	63.35	22.93	20	1.1465
Average =	65.20	14.96	-	1.0602

By utilizing the average traffic safety benefit associated with RWIS stations, the collision reduction potential for each of the RWIS configuration is determined and plotted against the associated kriging variance as presented in **Figure 6-8**. While determining the anticipated collision reduction for different RWIS networks, it is assumed that each additional station will contribute the same amount to collision reduction.

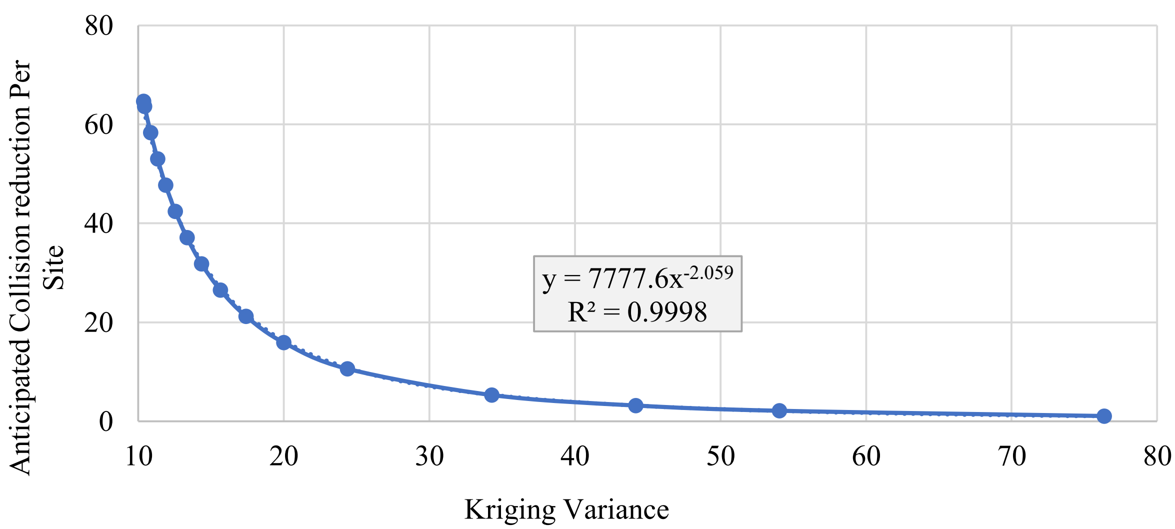

Figure 6- 8: Plot of collision reduction potential with kriging variance

According to **Figure 6-8**, error variance, which is an indicator of monitoring capability, has a strong effect on traffic safety. The primary intention of this plot is to acknowledge that enhanced monitoring coverage has the potential to improve traffic safety. The dependency of collision reduction potential on kriging variance can be expressed with a power function as presented in Equation 6-2 with an R-square value of 0.99. The output of this finding presents strong evidence that optimal RWIS locations, which is associated with minimized kriging variance, can provide superior transportation system (traffic safety) benefits.

$$Collision\ Reduction\ Potential = \frac{7777.6}{Kriging\ Variance^{2.059}} \tag{6-2}$$

In the last step, the dependency of safety effectiveness of RWIS network on NCI was determined by plotting it against the associated collision reduction potential (**Figure 6-9**). The findings revealed that NCI is highly correlated with collision reduction. An RWIS configuration with a higher NCI value was proven to be more effective for transportation safety than an RWIS network with a lower NCI value. For example, an RWIS network with 80% network monitoring coverage provides 40 collision reduction per site per analysis period (2 years).

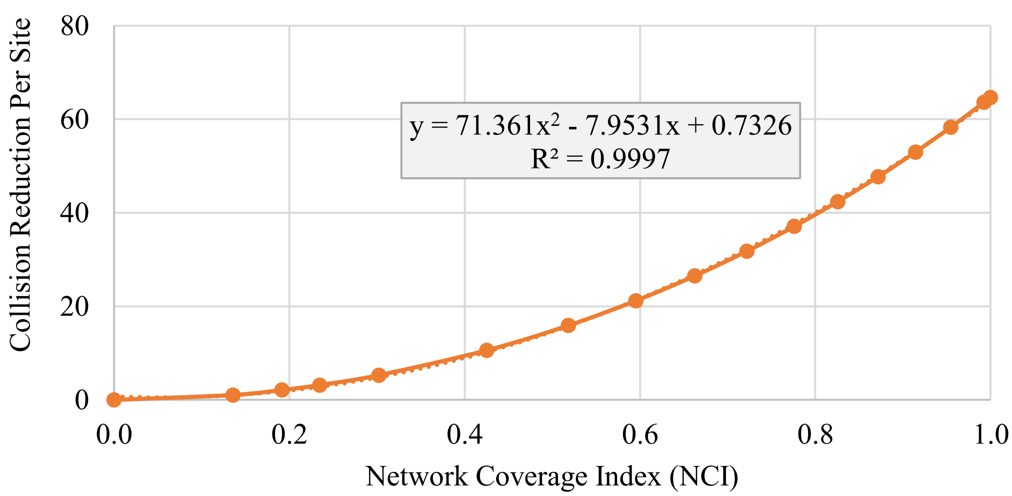

Figure 6- 9: Plot of collision reduction potential with NCI

The dependency of collision reduction potential on NCI can be expressed as a polynomial function in Equation 6-3 with an R-square value of 0.99.

$$Collision\ Reduction\ Potential = 71.36 * NCI^2 - 7.95 * NCI + 0.73 \quad (6\text{-}3)$$

It is evident from the above findings that an RWIS location solution with lower estimation error (higher NCI) will provide a significantly safer transportation network than another solution with higher estimation error (lower NCI). This result in turn justifies the previously developed location allocation strategy (Biswas and Kwon 2022), where optimal RWIS location was selected based on lowest estimation error. It is apparent that the optimal location solution is more beneficial in terms of safety effectiveness.

6.5 Summary

RWIS play an essential role in improving transportation safety, mobility, and winter road maintenance operations. Acknowledging their significant operational and environmental benefits, many North American transportation agencies have invested millions of dollars in deploying RWIS stations to strengthen the monitoring coverage of winter road surface conditions. To maximize the benefits of such systems, RWIS stations should be located systematically at a specific number of selected locations, which is referred to as the optimal RWIS network. Our previous research provided a solid foundation for planning an optimal RWIS network. However, the goodness of the RWIS locations has never been examined, particularly the effect RWIS location solutions have on transportation safety. The key findings of this study are:

- The Network coverage index (NCI), a measure of monitoring capability, is intensely tied to the RWIS network configuration. A direct relationship between NCI and kriging variance has also been established in this study.

- The collision reduction potential of an RWIS network has been found to be proportional to and highly correlated with NCI. An RWIS configuration having higher NCI has a higher potential to reduce traffic collision, thus maximizing safety effectiveness.

- The findings documented in this study concluded that optimal RWIS locations, which are associated with the lowest kriging variance (highest NCI), maximizes the overall benefits on transportation systems.

Chapter 7

Conclusions and Future Research

7.1 Introduction

Road Weather Information Systems (RWIS) play an essential role in transportation maintenance operations by keeping roadways clear of ice and snow for improved safety and mobility of the traveling public. To maximize the benefits of such systems, transportation agencies strive to answer the key questions: how many RWIS stations do we need? Where should we place the RWIS stations? What type of stations are needed for each location? This thesis attempted to answer these critical RWIS network planning questions by proposing an advanced geostatistical approach alongside optimization methods considering critical weather variables. The first step in our proposed process involved classifying the study area based on topographic and weather severity characteristics. Together, this makes up the environmental characteristics of the region and was captured in our study area that included regions of flatland or varied terrain and with different severities of winter weather.

To answer the first research question, the spatial and temporal continuity of RWIS measurements was investigated using geostatistical spatiotemporal semivariogram analysis and compared to different topographic and weather regions. Optimal RWIS density for each topographic and weather severity zones were then determined based on the developed semivariogram parameters using a popular mathematical programming approach – PSO algorithm.

Regarding the second research question, an advanced location optimization model was developed by combining the effects of three key RWIS variables – AT, RST, and DPT. The location allocation problem was solved using a popular mathematical programming approach, the SSA algorithm, as this algorithm has proven to be effective in solving various facility location optimization problems. An initial attempt was carried out, determining the importance of incorporating multiple weather variables into location allocation models.

At the next step, a multi-variable semivariogram was developed in order to refine the location allocation model and to develop a bi-level sequential optimization model, answering the second and third research questions respectively. Lastly, the benefit associated with the optimal RWIS network was quantified by developing a network monitoring factor, NCI.

This chapter outlines the potential contribution of this research followed by a number of recommendations for future research.

7.2 Major Contributions

This study represents a sophisticated approach to RWIS network planning and deployment strategies by developing a methodological framework for optimizing the density and location of RWIS networks for any given regions based on its topographic and weather characteristics. The findings reveal a strong correlation between optimal RWIS density and these regional characteristics demonstrating that RWIS data from one region can inform deployment requirements for similar regions. In addition, a multi-variable geostatistical model is developed to enhance both the RWIS location allocation and bi-level sequential optimization models. This provides RWIS planners with a more robust decision-support tool for both short-term and long-term RWIS network planning. Lastly, this thesis evaluates the impact of an optimized RWIS network on transportation systems, highlighting its significance in enhancing overall transportation safety and efficiency.

The followings are the major contributions of this thesis:

- **Correlation Analysis between RWIS and Regional variables:** This thesis developed an innovative methodological framework to quantify the spatiotemporal coverage of RWIS measurements, significantly enhancing the understanding of the spatiotemporal variability of key road weather variables. The major contribution is the identification of higher spatial and temporal autocorrelation continuity ranges during mid-winter months and in flatland areas with less varied weather, which informs the strategic placement of RWIS stations to achieve efficient monitoring coverage (less varied topography require comparatively fewer RWIS stations to achieve a certain level of monitoring coverage compared to hilly or mountainous regions)

- **Development of Region-wide RWIS Density Guidelines:** A series of RWIS density curves were generated alongside an optimal RWIS chart, providing transportation authorities with a decision support tool for planning an RWIS network without the need for road weather and surface conditions data. The desired RWIS density shows a strong dependency on topography and weather characteristics of the region under investigation.

The density guidelines and map would provide decision-makers with a reference to help plan an optimal RWIS network within any climate and/or geographical region of interest.

- **Formulation of a Multi-Variable Semivariogram-Based RWIS Location Allocation Framework:** This research developed an innovative multi-variable semivariogram model, which is seamlessly integrated into an advanced RWIS location allocation framework. By capturing the variability of multiple critical weather variables, this combined model significantly enhanced the precision of location solutions. This advancement represents a substantial leap forward in existing literature, offering a comprehensive tool for transportation agencies to determine optimal RWIS locations. Furthermore, the model aids in prioritizing sites within budgetary constraints and supports optional long-term planning, thereby resulting in significantly improved monitoring coverage compared to single-variable models.

- **Investigation of Safety Effectiveness of Optimal RWIS networks:** Given the challenges in quantifying the benefits of RWIS information due to a limited understanding of how RWIS data is utilized, this thesis developed a unique methodological framework. By employing advanced geostatistical analytics and location-allocation models, this framework directly assesses the safety impact of optimal RWIS location solutions. This contribution addresses the existing gap by providing a robust method to evaluate the effectiveness of RWIS networks, thereby enhancing the understanding of their role in improving traffic safety.

- **Development of a Bi-Level Sequential Optimization Model:** This thesis introduced a pioneering bi-level sequential optimization model for RWIS station planning, effectively determining both the location and type of stations. By providing empirical evidence that single-variable models are suitable for Mini-RWIS and multi-variable models are appropriate for Regular-RWIS, the framework elegantly determines the optimal combination of station type and location. By balancing monitoring coverage with budgetary constraints, this approach not only enhances the overall efficiency and effectiveness of RWIS network deployment but also maximizes resources by delivering a quantitative framework to determine the most appropriate type and location for each station.

- **Development of a Web-Based Visualization Tool:** A prototype web-based application has been developed to enable the visualization of location solutions derived from this research. This interactive user-friendly online application, named LoRWIS (https://sites.google.com/view/lorwis/states/Maine), displays the proposed location solutions and the distribution of existing RWIS stations throughout the study network. By effectively actualizing the research outcomes, LoRWIS offers dynamic representations of various location solutions. It is noteworthy that the Maine DOT is leveraging LoRWIS for their RWIS deployment planning, and the locations generated from this thesis are set to be implemented over the next two years, further validating the practicality and effectiveness of the proposed methods and solutions.

7.3 Future Research

The following is a list of recommendations on the possible extensions of this research.

- The geographic study area included in this research consisted largely of flatlands, with few hilly and mountainous regions due to data availability issues. Hence, more case studies consisting of wider geographic regions should be conducted for a better understanding of the relationship between spatial range of autocorrelation in RST and the topographic and weather features to develop a more robust quantitative relation between these parameters. In addition, the study period for TPI and WSI-based zonal classification was limited to one winter season including six months from October 2016 to March 2017. Thus, larger temporal ranges could be considered to improve the level of confidence in the outcomes.

- The optimal density guideline developed in this study incorporates the effect of topography and weather severity in determining the optimal number of RWIS needed for a region. As a future research path, sensitivity analysis could be conducted to investigate how the resulting optimal densities would change with respect to some of the factors considered in the analysis, especially the coefficients used to generate WSI (or even a winter severity index model) and TPI classification schemes.

- In this study, ordinary kriging is utilized to develop the concept of network optimization model. Hence, universal kriging or kriging with external drift could be applied considering meteorological parameters (wind speed and direction, precipitation, humidity, cloud cover, vegetation cover, etc.) to better capture the dependency of RST data (or other key parameters, including road surface condition index) on local meteorological parameters.

- The multi-variable semivariogram model, developed in this research accounted the effect of the most critical RWIS variables – AT, RST and DPT. Hence, this model can be refined by exploring additional road weather variables and investigating their interactions. Moreover, investigating the impact of different weighting schemes for individual weather variables within the model may provide insights into optimizing the trade-off between variables.

- The study area incorporated to enhance the location allocation model is Maine, which is a flatland area. Hence, including a larger and more diverse sample size in this research could enhance the methodology's robustness and reliability. For instance, application of the proposed methodological framework in various geographical settings and climate conditions would increase the adaptability of the model. Additionally, this study incorporated data spanning three winter seasons. Therefore, employing extended periods of weather data will enhance the model's adaptability.

- The impact of optimal RWIS network into the transportation system has been assessed using a case study for Iowa, which is a flatland area with moderate weather conditions. Hence, the benefit of optimal RWIS network should also be determined for other regions including hilly and mountainous regions for a comprehensive and conclusive output.

- In addition to the traffic safety benefit, transportation mobility and winter road maintenance (WRM) benefits also need to be evaluated. One potential approach to determine mobility benefit could be based on AADT (Annual Average Daily Traffic) for a predefined coverage area before and after the installation of RWIS station. Similarly, the WRM benefit may also be determined based on the maintenance cost for the before and after-period of RWIS deployment.

Reference

Agah, M., & Pape, C. Road Weather Information Systems (RWIS) Data Integration Guidelines. *AURORA Program. Estados Unidos*. 2002.

Ahmed, S. O., R. Mazloum and H. Abou-Ali. Spatiotemporal interpolation of air pollutants in the Greater Cairo and the Delta, Egypt. Environmental research, 2018. 160, 27-34.

Ahmed, S.; Kumar, D.; Bhat, A. N. Application of Geostatistics in Optimal Groundwater Monitoring Network Design, Groundwater Dynamics in Hard Rock Aquifers, 2008. pp 179-190.

Ahrens, C. D. 2009. Meteorology Today: An Introduction to Weather, Climate, and the Environment. Brooks/Cole, Cengage Learning, Inc., Belmont, CA.

Andrey, J. C., B. E. Mills, and J. Vandermolen. Weather information and road safety. Institute for Catastrophic Loss Reduction (ICLR), Toronto, Ontario, Canada, 2001. Paper Series – No. 15.

Asuero, A. G., A. Sayago, and A. G. Gonzalez. The correlation coefficient: An overview. Critical reviews in analytical chemistry, 2006. 36(1), 41-59.

Biswas S.; Wu, M.; Melles, S. J.; Kwon T. J. Use of Topography, Weather Zones, and Semivariogram Parameters to Optimize Road Weather Information System Station Density across Large Spatial Scales. Transportation Research Record: Journal of the Transportation Research Board, 2019. vol. 2673, no. 12, pp. 301-311. https://doi.org/10.1177/ 0361198119846467

Biswas, S.; Kwon, T. J. Developing Statewide Optimal RWIS Density Guidelines Using Space-Time Semivariogram Models. Journal of Sensors, vol. 2020, Article ID 1208692. https://doi.org/10.1155/2020/1208692

Biswas, S.; Kwon, T. J. (2022). Development of a Novel RWIS Location-Allocation Model Considering Multiple Road Weather Variables over Space and Time. Transportation Research Record: Journal of the Transportation Research Board, 2022. Vol. 2676(8), pp. 619–632. https://doi.org/10.1177/03611981221084678

Bohling, G. Introduction to geostatistics and variogram analysis. Kansas Geological Survey, Vol. 1, 2005, pp. 1-20.

Boon, C.B. and Cluett, C. (2002). Road weather information systems: enabling proactive maintenance practices in Washington State. Research paper prepared for Washington state transportation commission. March 2002.

Boselly, S. E., G. S. Doore, J. E. Thornes, C. Ulbery, and D. D. Ernst. 1993. SHRP-H-350: Road Weather Information Systems Volume 1: Research Report. Strategic Highway Research Program, Washington, DC.

Brus, D. J. and G. B. Heuvelink. Optimization of sample patterns for universal kriging of environmental variables. Geoderma, 2007. 138(1-2): 86-95.

Canadian Strategic Highway Research Program (2000). “Anti-Icing and RWIS Technology in Canada”, C-SHRP Technical Brief #20, July 2000.

Chapman, L. and J. E. Thornes. The influence of traffic on road surface temperatures: Implications for thermal mapping studies. Meteorological Applications, 2005. 12:371-380.

Epps, Jon. A. and Ardila-Coulson, Maria. (1997). Summary of SHRP Research and Economic Benefits of Snow and Ice Control, Prepared for FHWA, Washington D.C.,December 1997. (FHWASA-98-015).

Eriksson, M. and J. Norrman. Analysis of station locations in a road weather information system. Meteorological Applications, Vol. 8, No. 4, 2001, pp. 437–448.

ESRI. ArcGIS version 10.4. 1. 2015.

Farahani, R. Z., SteadieSeifi, M., & Asgari, N. (2010). Multiple criteria facility location problems: A survey. Applied mathematical modelling, 34(7), 1689-1709.

Fetzer, J., Caceres, H., He, Q., & Batta, R. (2018). A multi-objective optimization approach to the location of road weather information system in New York State. *Journal of Intelligent Transportation Systems*, 22(6), 503-516.

Fu, L., Moreno, L.M., Shah, Q.A., and Lee, C. (2005). Effects of Winter Weather and Maintenance Treatments on Highway Safety A final report submitted to MTO, March 2005.

Galarus, D., and Angryk, R. (2018). Beyond accuracy–A SMART approach to site-based spatio-temporal data quality assessment. Intelligent Data Analysis, 22(1), 21-43.

Gething, P. W., P. M. Atkinson, A. M. Noor, P. W. Gikandi, S. I. Hay and M. S. Nixon. A Local Space–Time Kriging Approach Applied to a National Outpatient Malaria Data Set. Computers & Geosciences, 2007. 33(10): 1337-1350.

Goovaerts, P. Geostatistics for Natural Resources Evaluation. Oxford University Press, New York. 1997.

Graler B., E. Pebesma and G. Heuvelink. Spatio-temporal interpolation using gstat. RFID Journal, 2016. 8(1), 204-218.

Gu, L., M. Wu and T. J. Kwon. An Enhanced Spatial Statistical Method for Continuous Monitoring of Winter Road Surface Conditions. Canadian Journal of Civil Engineering, (ja), 2019.

Gustavsson, T. 1990. Variation in Road Surface Temperature Due to Topography and Wind. Theoretical and Applied Climatology, Vol. 41, No. 4, pp. 227–236.

Hatamzad, M.; Pinerez, G. C. P.; Casselgren, J. Intelligent cost-effective winter road maintenance by predicting road surface temperature using machine learning techniques. Knowledge-Based Systems, 2022. 247, 108682.

Hastie, T. J. and R. J. Tibshirani Generalized Additive Models. Chapman & Hall/CRC, 1990.

Heuvelink, G. B., D. J. Brus and J. J. de Gruijter. Optimization of sample configurations for digital mapping of soil properties with universal kriging. Developments in Soil Science, 2006. 31: 137-151.

Hu, D., H. Shu, H. Hu and J. Xu. Spatiotemporal regression Kriging to predict precipitation using time-series MODIS data. Cluster Computing, 2017. 20(1), 347-357.

Jenness, J. (2006). Topographic position index (TPI) v. 1.2. Flagstaff, AZ: Jenness Enterprises.

Jin, P., A. Walker, M. Cebelak and C. Walton. (2014). Determining strategic locations for environmental sensor stations with weather-related crash data. Transportation Research Record: Journal of the Transportation Research Board, No. 2440, Transportation Research Board of the National Academics, Washington, D.C., 2014, pp. 34-42.

Kennedy, J. and R. Eberhart. Particle Swarm Optimization. In IEEE International Conference on Neural Networks.1995. pp. 1942–1948. doi:10.1109/ICNN.1995.488968.

Kennedy, J. and R.C. Eberhart. A Discrete Binary Version of the Particles Swarm Algorithm. In Systems, Man, and Cybernetics, Computational Cybernetics and Simulation, IEEE International Conference. 1997. pp. 4–8. doi:10.1109/ICSMC.1997.637339.

Kwon, T. J. and L. Fu. Evaluation of alternative criteria for determining the optimal location of RWIS stations. Journal of Modern Transportation, Vol. 21, No. 1, 2013, pp. 17–27.

Kwon, T. J., and L. Fu. RWIS network planning: Optimal density and location. 2016. (No. Aurora Project 2010-04).

Kwon, T. J., L. Fu and S. J. Melles. Location optimization of road weather information system (RWIS) network considering the needs of winter road maintenance and the traveling public. Computer-Aided Civil and Infrastructure Engineering, Vol. 32, No. 1, 2017, pp. 57–71.

Kwon, T. J. and L. Fu. Spatiotemporal variability of road weather conditions and optimal RWIS density—an empirical investigation. Canadian Journal of Civil Engineering, Vol. 44, No. 9, 2017, pp. 691–699.

Kwon, T. J., and Fu, L. Performance evaluation of road surface temperature forecasts. Canadian Journal of Civil Engineering, 2021. 48(5), 532-539.

Kirkpatrick, S., C. D. Gelatt and M. P. Vecchi. Optimization by simulated annealing. Science, 1983. 220(4598): 671-680.

Li, L., J. Zhang, W. Qiu, J. Wang and Y. Fang. An ensemble spatiotemporal model for predicting PM2. 5 concentrations. International journal of environmental research and public health, 2017. 14(5), 549.

Mackinnon, D., and Lo, A. 2009. Alberta transportation road weather information system (RWIS) expansion study. Alberta Transportation, Edmonton, Alta.

Manfredi, J., T. Walters, G. Wilke, L. Osborne, R. Hart, T. Incrocci, and T. Schmitt. Road Weather Information System Environmental Sensor Station Sitting Guidelines. Publication No. FHWA-HOP-05-026. Federal Highway Administration. 2005.

Manfredi, J., T. Walters, G. Wilke, L. F. Osborne, R. Hart, T. Incrocci and C. Schmitt. Road Weather Information System Environmental Sensor Station Siting Guide, Version 2.0. No. FHWA-HOP-05-026. United States Department of Transportation, 2008.

Matthews, L., J. Andrey, I. Minokhin and M. Perchanok. Operational Winter Severity Indices in Canada–From Concept to Practice. Presented at 96th Annual Meeting of the Transportation Research Board, Washington, D.C., 2017.

Matthews, L., J. Andrey, D. Hambly and I. Minokhin. Development of a flexible winter severity index for snow and ice control. Journal of Cold Regions Engineering, Vol. 31, No. 3, 2017, p. 04017005.
Mewes, J. J. Mapping weather severity zones (No. CR10-02). 2011.

Mokarram, M., G. Roshan and S. Negahban. Landform classification using topography position index (case study: salt dome of Korsia-Darab plain, Iran). Modeling Earth Systems and Environment, 2015. 1(4): 40.

Network, R. E. S. S. T. E. Analyzing spatio-temporal data with R: Everything you always wanted to know–but were afraid to ask. Submitted to Journal de la Société Française de Statistique, 2016.

Olea, R. A. A six-step practical approach to semivariogram modeling. Stochastic Environmental Research and Risk Assessment, Vol. 20, No. 5, 2006, Pp. 307-318.

Olea, R. A. Geostatistics for engineers and earth scientists. Springer Science & Business Media, New York, 2012.

Pebesma, E.J. Multivariable geostatistics in S: the gstat package. Computers & Geosciences, Vol. 30, 2004, pp. 683–691.

Pebesma, E. and B. Graeler. Spatial and spatio-temporal geostatistical modelling, prediction and simulation. 2012.

Pebesma, E. and Gräler, B. Introduction to Spatio-Temporal Variography. 2018.

Pebesma, E., B. Graeler and M. E. Pebesma. Package 'gstat', The Comprehensive R Archive Network (CRAN), 2019.

Pilli-Sihvola, E., P. Leviakangas, and R. Hautala. Better winter road weather information saves money, time, lives and the environment. 19th Intelligent Transport Systems World Congress, ITS 2012.

Poli, R., J. Kennedy and B. Tim. Particle swarm optimization. Swarm Interlligence, 1: 33–57. 2007. doi:10.1007/s11721-007-0002-0 Particle.

Qin, J., Ni, L.L., and Shi, F. (2012). Combined Simulated Annealing Algorithm for the Discrete Facility Location Problem. The Scientific World Journal Volume 2012, Article ID 576392.

R Core Team. R: A language and environment for statistical computing. R Foundation for Statistical Computing, Vienna, Austria, 2018. URL https://www.R-project.org/.

Revelle, C. S., H. A. Eiselt and M. S. Daskin. A bibliography for some fundamental problem categories in discrete location science. European Journal of Operational Research, 2008. 184(3): 817-848.

Sato, N., J. E. Thornes, T. Maruyama, A. Sugimura, and T. Yamada. 2004. Road Surface Temperature Forecasting: Case Study in a Mountainous Region of Japan. Sixth International Symposium on Snow Removal and Ice Control Technology, June 7–9, Spokane, WA.

Seif, A. Using Topography Position Index for Landform Classification (Case study: Grain Mountain). Bulletin of Environment, Pharmacology and Life Sciences (Bull. Env. Pharmacol. Life Sci), 2014. 3: 33-39.

Seif, A. Landform Classification by Slope Position classes. Bull. Env. Pharmacol. Life Sci, 2014. 3: 62-69.

Shacklette, M. Linux Operating System. Handbook of Computer Networks: LANs, MANs, WANs, the Internet, and Global, Cellular, and Wireless Networks, 2, 78-90. 2007.

Sharma, D.; Safety Effects of Road Weather Information Systems (RWIS)–A Large-Scale Empirical Investigation. M.Sc Thesis. University of Alberta. 2022.

Shekhar, S., H. Xiong and X. Zhou Encyclopedia of GIS. Springer, New York, 2008.

Shi, Y. Particle swarm optimization: developments, applications and resources. In Proceedings of the 2001 congress on evolutionary computation (IEEE Cat. No. 01TH8546), 2001. (Vol. 1, pp. 81-86). IEEE.

Solana-Gutiérrez, J. and S. Merino-de-Miguel. A Variogram Model Comparison for Predicting Forest Changes. Procedia Environmental Sciences, Vol. 7, 2011, pp. 383-388.

Strong, C.K., Ye, Z., and Shi, X. 2010. Safety effects of winter weather: the state of knowledge and remaining challenges. Transport Reviews, 30(6): 677–699. doi:10.1080/01441640903414470.

Usman, T., L. Fu and Miranda-Moreno, L. F. (2012). A Disaggregate Model for Quantifying the Safety Effects of Winter Road Maintenance Activities at an Operational Level Accepted for publication in the Journal of Accident Analysis and Prevention, February 2012. DOI 10.1016/j.aap.2012.02.005.

Van Groenigen, J. W. and A. Stein. Constrained optimization of spatial sampling using continuous simulated annealing. Journal of Environmental Quality, 1998. 27(5): 1078-1086.

Van Groenigen, J. W., W. Siderius and A. Stein. Constrained optimisation of soil sampling for minimisation of the kriging variance. Geoderma, 1999. 87(3-4): 239-259.

Wang, H., H. Sun, C. Li, S. Rahnamayan and J. S. Pan. Diversity enhanced particle swarm optimization with neighborhood search. Information Sciences, 223: 119–135. Elsevier Inc. 2013. doi:10.1016/j.ins.2012.10.012.

Wang, X., L. Gu, T. J. Kwon and T. Z. Qiu. Determining the Spatiotemporal Coverage of Road Weather Information Systems–A Case Study in Alberta, Canada. Transportation Research Record: Journal of the Transportation Research Board, 2019. (No. 19-00551).

Weiss, A. Topographic Positions and Landforms Analysis (Conference Poster). ESRI International User Conference. San Diego, CA, 2001. pp. 9-13.

White, S. P., J. E. Thornes and L. Chapman. A Guide to Road Weather Information Systems. Version 2. SIRWEC, University of Birmingham, UK. 2006, pp. 1–83.

Ye, Z., Strong, C., Fay, L., and Shi, X. Cost benefits of weather information for winter road maintenance. Montana State University, Western Transportation Institute, 2009.

Yeh, M; Lin, Y.P.; Change, L.C. Designing an optimal multivariate geostatistical groundwater quality monitoring network using factorial kriging and genetic algorithms. Environmental Geology 2006. 50: 101–121.

Yuan, Z., Zhou, X., & Yang, T. (2018, July). Hetero-convlstm: A deep learning approach to traffic accident prediction on heterogeneous spatio-temporal data. In Proceedings of the 24th ACM SIGKDD International Conference on Knowledge Discovery & Data Mining (pp. 984-992).

Zaefferer, M., Naujoks, B., & Bartz-Beielstein, T. (2013). A Gentle Introduction to Multi-Criteria Optimization with SPOT.

Zhao, L., Chien, S., Meegoda, J., Luo, Z., & Liu, X. (2016). Cost–benefit analysis and microclimate-based optimization of a RWIS network. Journal of Infrastructure Systems, 22(2), 04015021.

Zwahlen, H.T., Russ, A., and Vatan, S. 2003. Evaluation of ODOT roadway/ weather sensor systems for snow and ice removal operations: Part I: RWIS. FHWA/OH-2003/008A. Ohio Department of Transportation.

Appendix A

SPATIAL AND TEMPORAL CONTINUITY RANGE

Topographic zones	**Weather severity zones**

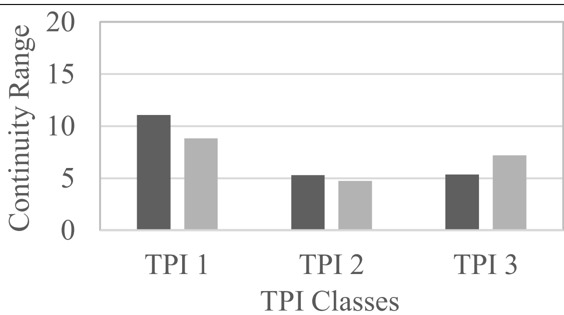

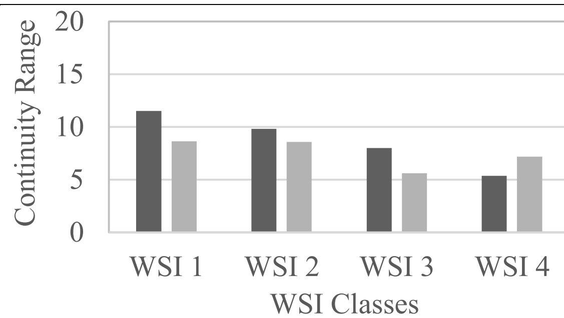

Analysis Period: October 2016

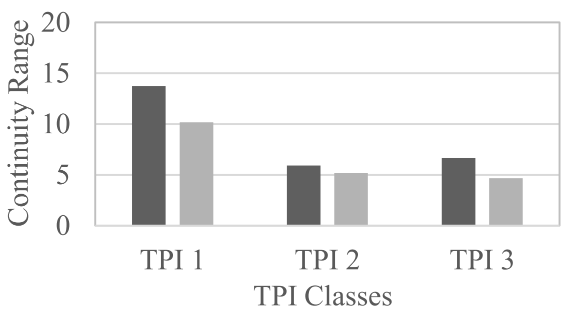

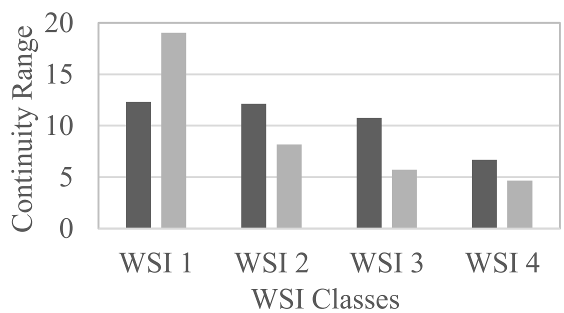

Analysis Period: November 2016

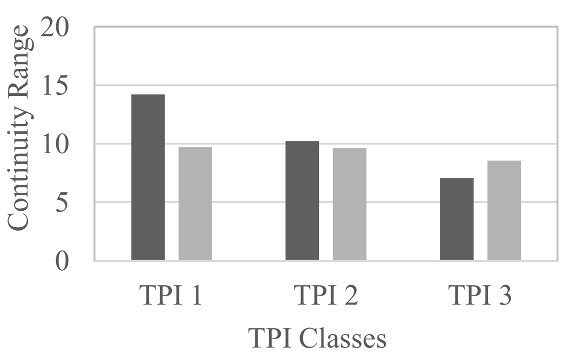

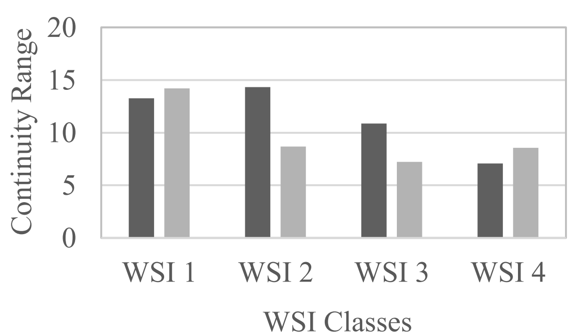

Analysis Period: December 2016

■ Spatial Range (km) ■ Temporal Range (hrs)

Topographic zones	**Weather severity zones**

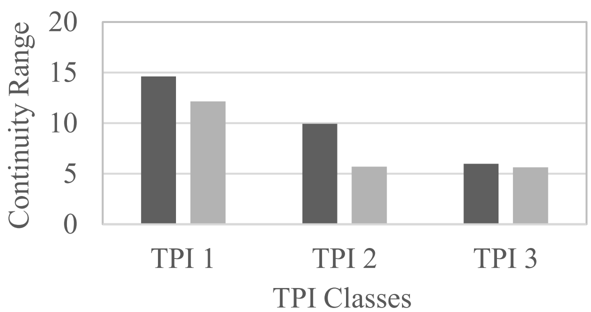

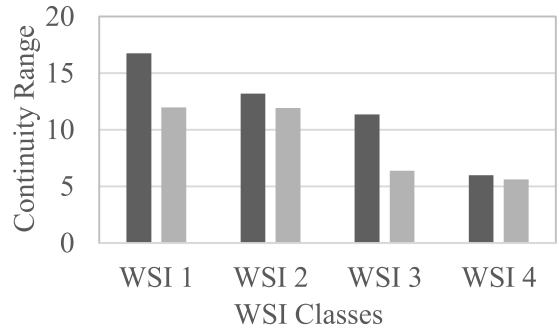

Analysis Period: January 2017

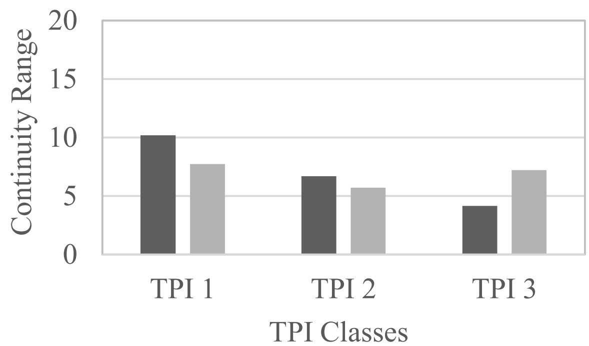

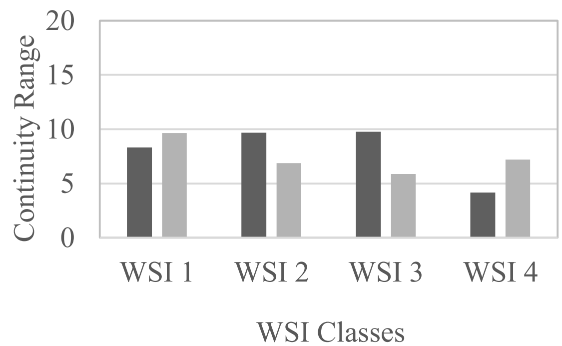

Analysis Period: February 2017

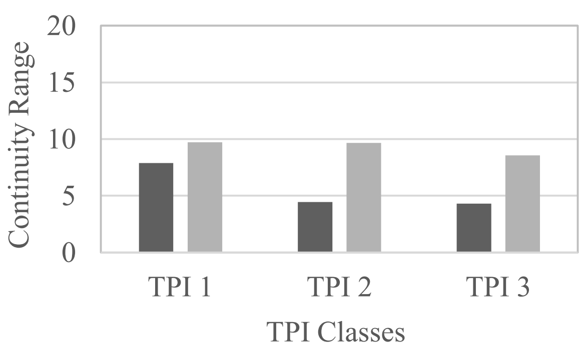

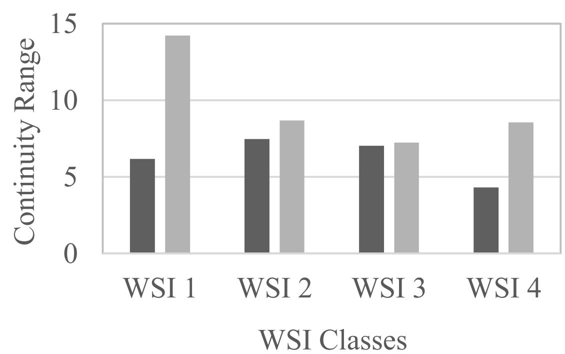

Analysis Period: March 2017

■ Spatial Range (km) ■ Temporal Range (hrs)

Appendix B

FIRST 8 LOCATION SOLUTION

(8 out of 18 Predetermined Locations)

ID	Name	Long	Lat
1	RWIS Proposal	-67.649623	44.966088
2	RWIS Proposal	-67.982601	46.141023
3	RWIS Proposal	-70.609883	44.921429
4	RWIS Proposal	-70.744961	43.468646
5	Mini-RWIS Proposal	-67.869165	46.709123
6	RWIS Location Proposal	-70.959525	44.020557
7	RWIS Proposal	-69.422884	44.10053
8	RWIS Proposal	-68.60773	45.353481

Appendix C

SENSITIVITY ANALYSIS RESULTS – I

(First 8 Optimal Locations)

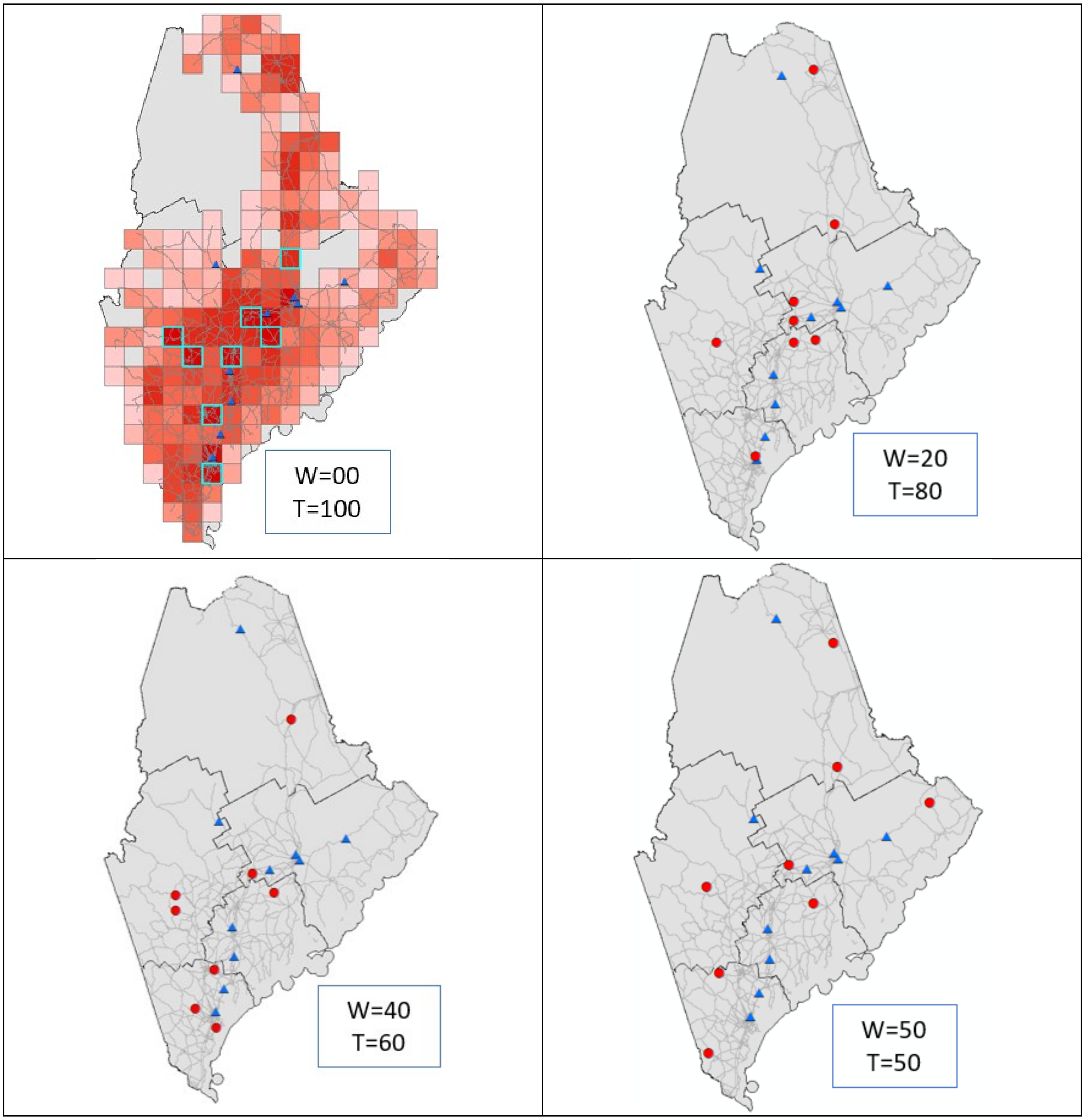

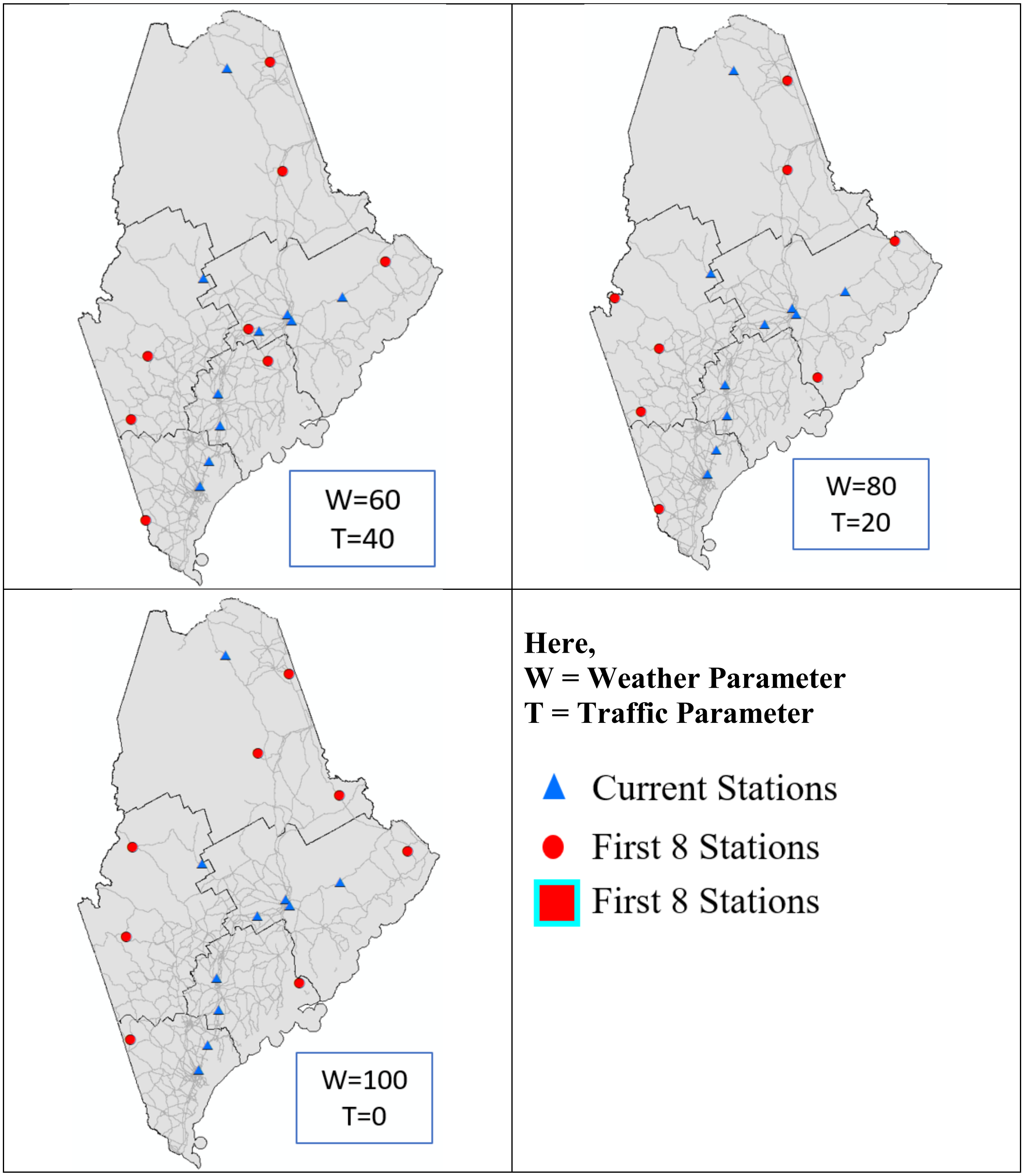
W=60
T=40
W=80
T=20
W=100
T=0
Here,
W = Weather Parameter
T = Traffic Parameter
Current Stations
First 8 Stations
First 8 Stations

Table B.1. Sensitivity analysis location solutions (First 8 locations)

Station #	W = 00, T = 100		W = 20, T = 80		W = 40, T = 60		W = 50, T = 50	
	Long.	Lat.	Long.	Lat.	Long.	Lat.	Long.	Lat.
1	-70.31	43.56	-70.26	43.73	-70.31	43.56	-70.85	43.50
2	-70.13	44.07	-70.33	44.81	-70.49	43.78	-70.47	44.14
3	-70.16	44.61	-69.40	44.62	-70.13	44.07	-69.15	44.48
4	-69.70	44.51	-69.13	44.58	-70.38	44.68	-70.32	44.88
5	-70.33	44.81	-69.32	44.80	-70.33	44.81	-69.29	44.86
6	-69.13	44.58	-69.25	44.95	-69.13	44.58	-67.45	45.00
7	-69.32	44.80	-68.46	45.51	-69.32	44.80	-68.37	45.54
8	-68.62	45.18	-68.10	46.87	-68.26	46.01	-67.94	46.56
Station #	**W = 60, T = 40**		**W = 80, T = 20**		**W = 100, T = 00**			
	Long.	**Lat.**	**Long.**	**Lat.**	**Long.**	**Lat.**		
1	-70.95	43.55	-70.91	43.53	-70.92	44.10		
2	-70.80	44.39	-70.80	44.37	-68.87	44.14		
3	-69.11	44.53	-68.68	44.22	-70.63	44.94		
4	-70.41	44.85	-70.40	44.84	-67.22	44.90		
5	-69.21	44.82	-70.73	45.37	-70.26	45.63		
6	-67.46	45.00	-67.32	45.11	-67.76	45.52		
7	-68.27	45.97	-68.27	45.97	-68.52	46.06		
8	-68.00	46.85	-67.92	46.68	-67.86	46.60		

Appendix D

SENSITIVITY ANALYSIS RESULTS – II

(Second 10 Optimal Locations)

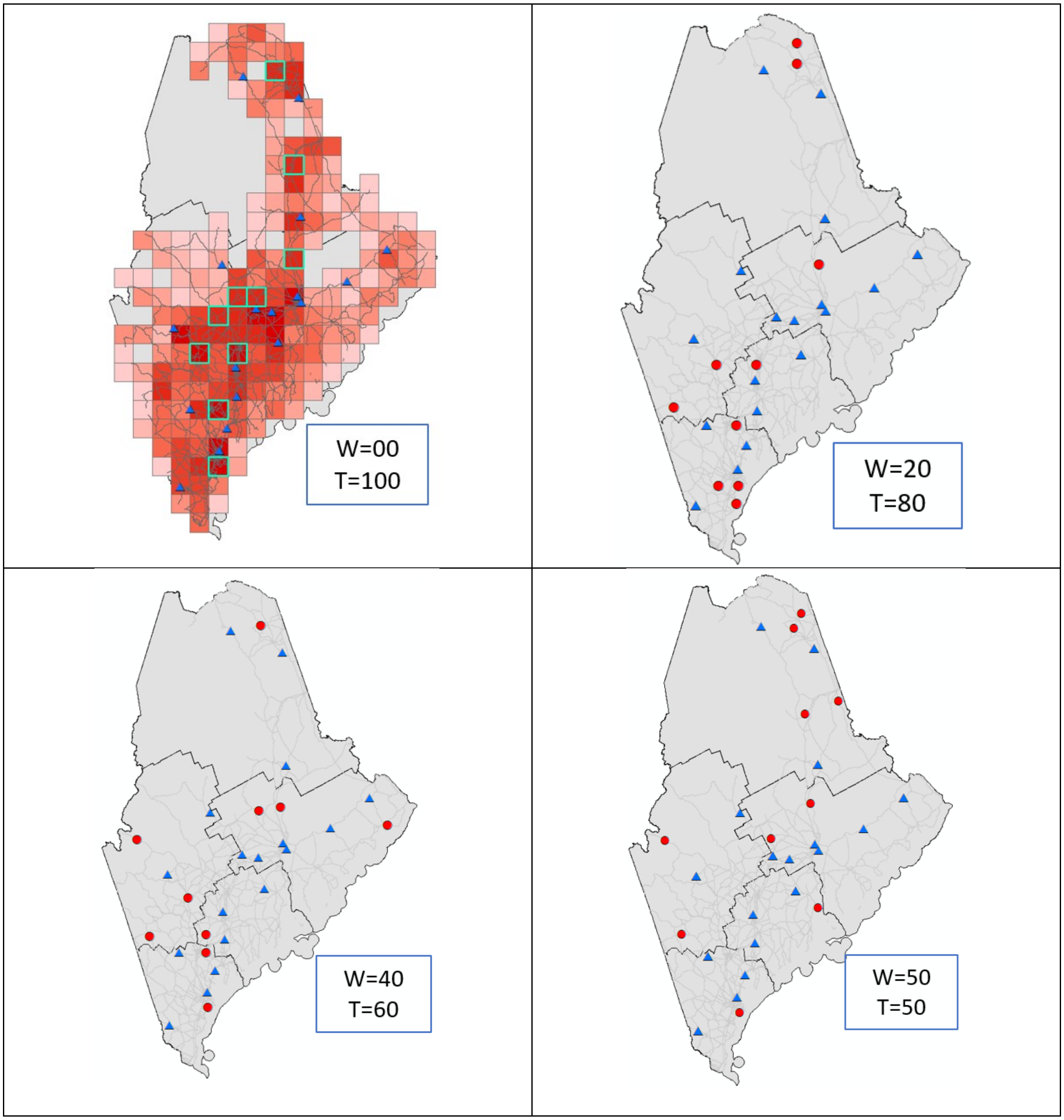

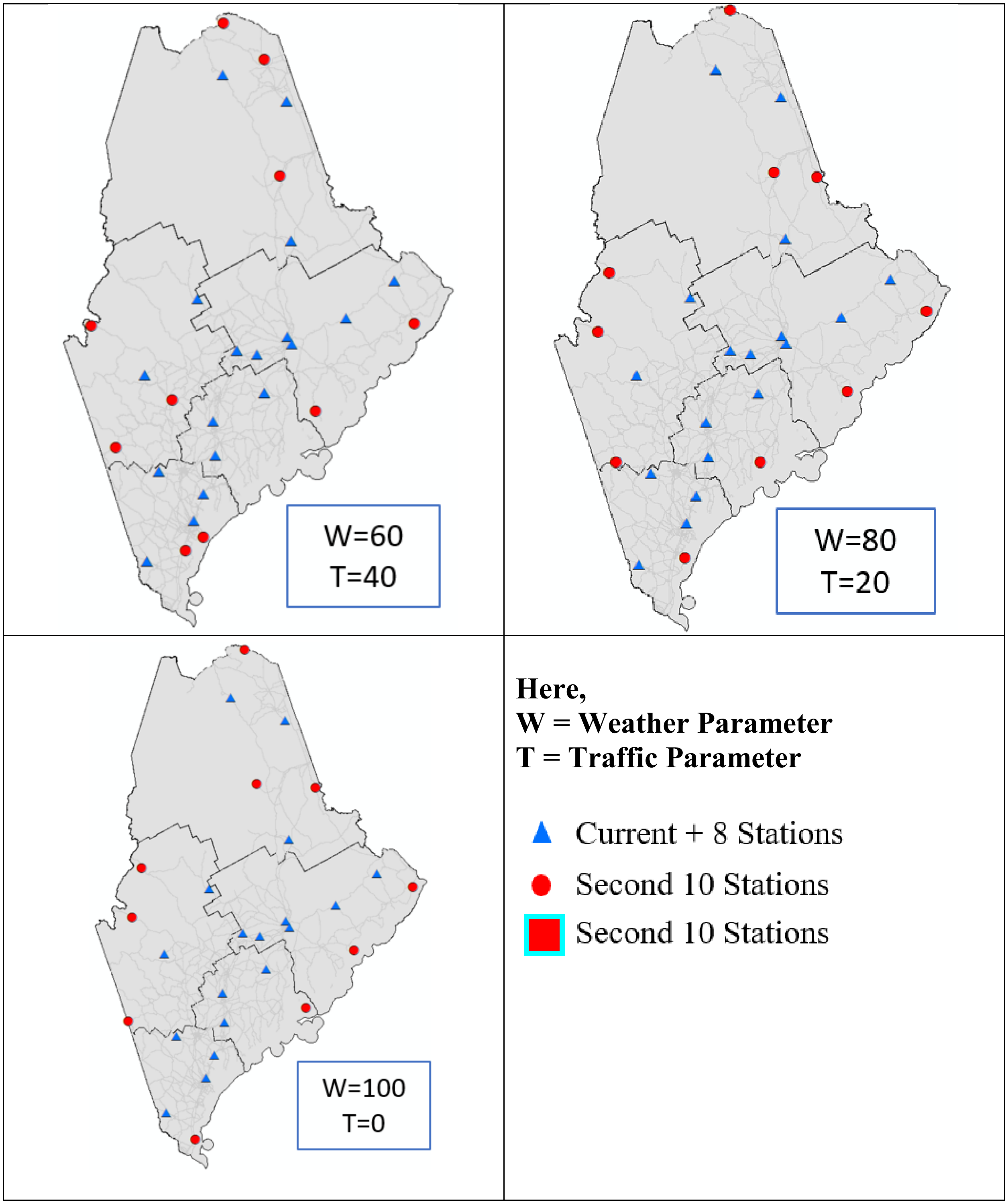
W=60
T=40
W=80
T=20
W=100
T=0
Here,
W = Weather Parameter
T = Traffic Parameter
Current + 8 Stations
Second 10 Stations
Second 10 Stations

Table C.1. Sensitivity analysis location solutions (Second 10 locations)

Station #	W = 00, T = 100		W = 20, T = 80		W = 40, T = 60		W = 50, T = 50	
	Long.	Lat.	Long.	Lat.	Long.	Lat.	Long.	Lat.
1	-70.31	43.56	-70.39	43.42	-70.31	43.56	-70.29	43.56
2	-70.13	44.07	-70.53	43.61	-70.13	44.07	-70.72	44.41
3	-70.16	44.61	-70.31	43.56	-70.79	44.36	-68.94	44.28
4	-69.70	44.51	-70.13	44.07	-70.07	44.24	-70.59	45.28
5	-69.78	44.89	-70.79	44.36	-70.16	44.61	-69.25	45.02
6	-69.48	45.01	-70.16	44.61	-70.59	45.28	-68.63	45.21
7	-69.25	44.95	-69.70	44.51	-67.34	44.70	-68.33	46.01
8	-68.62	45.18	-68.62	45.18	-68.91	45.21	-67.86	46.03
9	-68.26	46.01	-68.10	46.87	-68.62	45.18	-68.11	46.81
10	-68.10	46.87	-68.01	47.03	-68.10	46.87	-67.94	46.91

Station #	W = 60, T = 40		W = 80, T = 20		W = 100, T = 00	
	Long.	Lat.	Long.	Lat.	Long.	Lat.
1	-70.43	43.50	-70.38	43.45	-70.60	43.19
2	-70.21	43.56	-70.78	44.29	-71.00	44.39
3	-70.84	44.41	-69.34	43.99	-68.81	44.05
4	-68.68	44.24	-68.25	44.29	-68.03	44.41
5	-70.12	44.65	-70.59	45.28	-70.59	45.28
6	-70.73	45.37	-67.19	44.68	-67.07	44.78
7	-67.39	44.64	-70.29	45.69	-70.29	45.69
8	-68.26	46.04	-67.84	45.91	-67.84	45.91
9	-68.02	46.93	-68.26	46.04	-68.55	46.10
10	-68.32	47.29	-68.15	47.30	-68.13	47.29

Appendix E

SENSITIVITY ANALYSIS RESULTS – III

(Third 6 Optimal Locations)

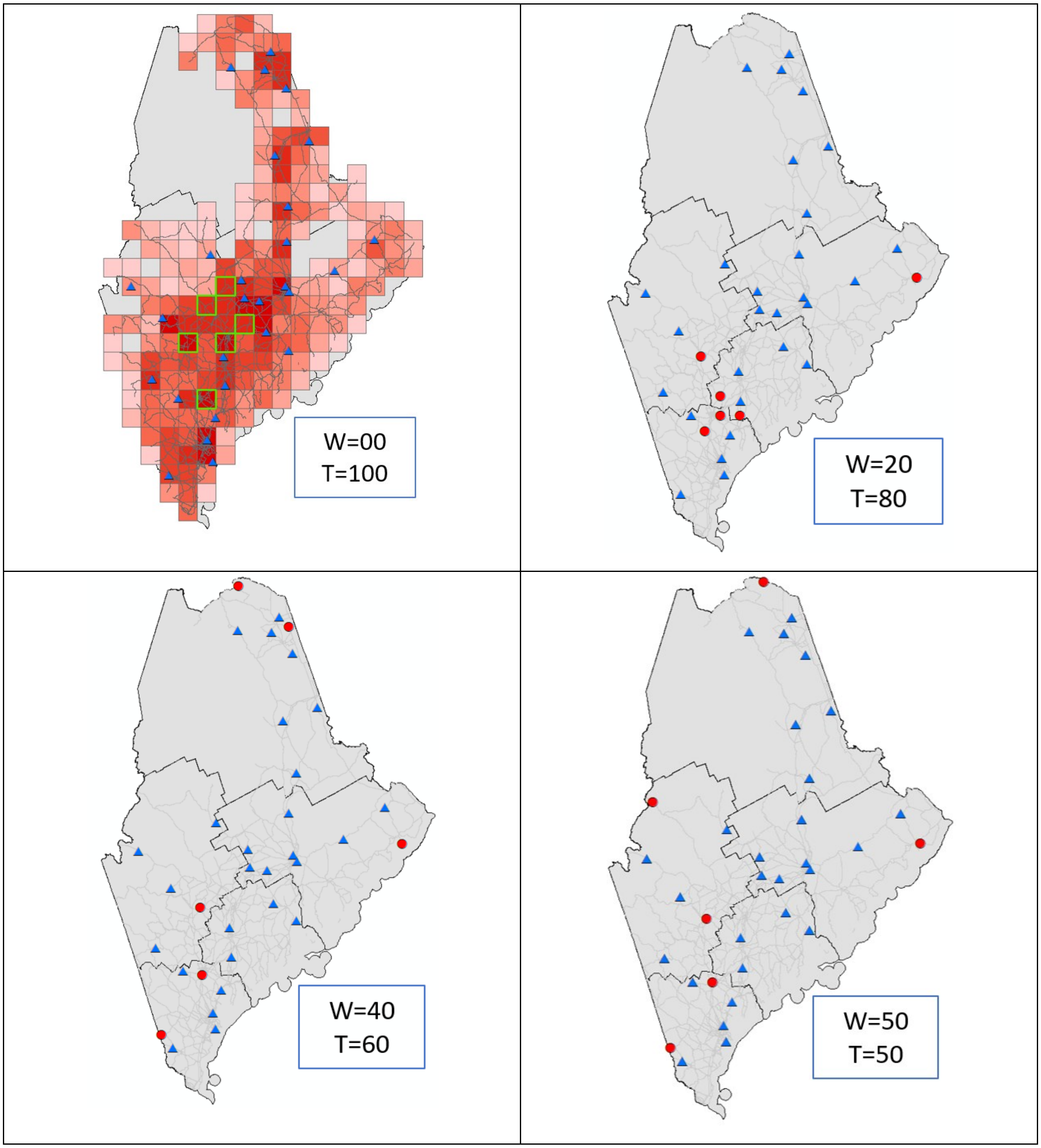

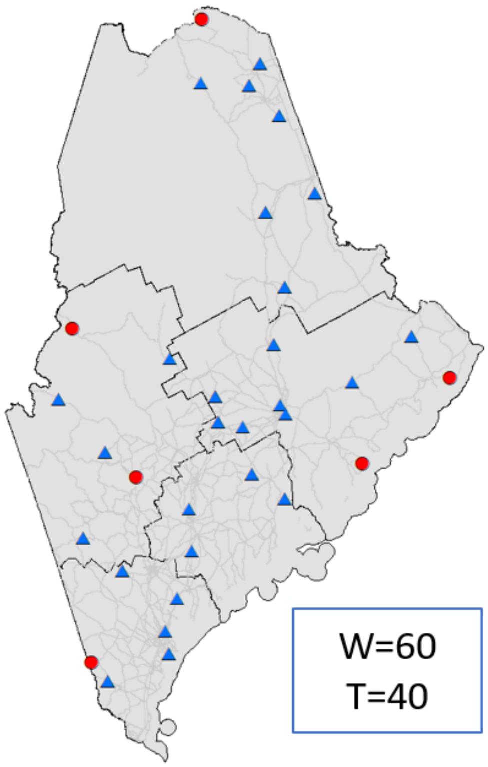

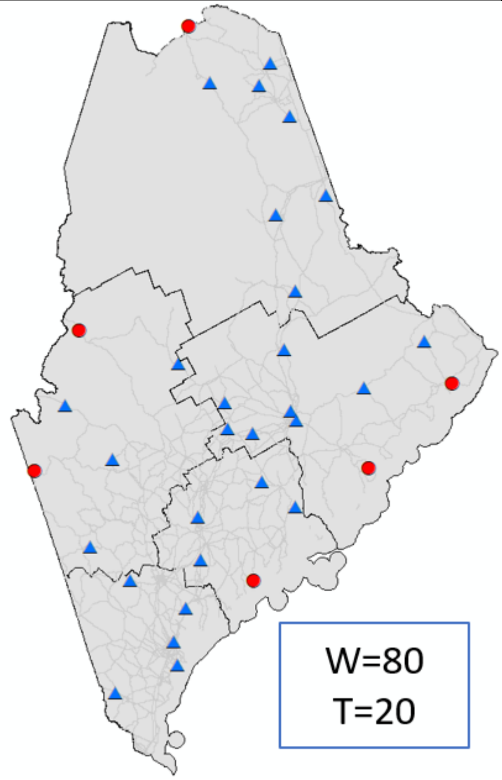

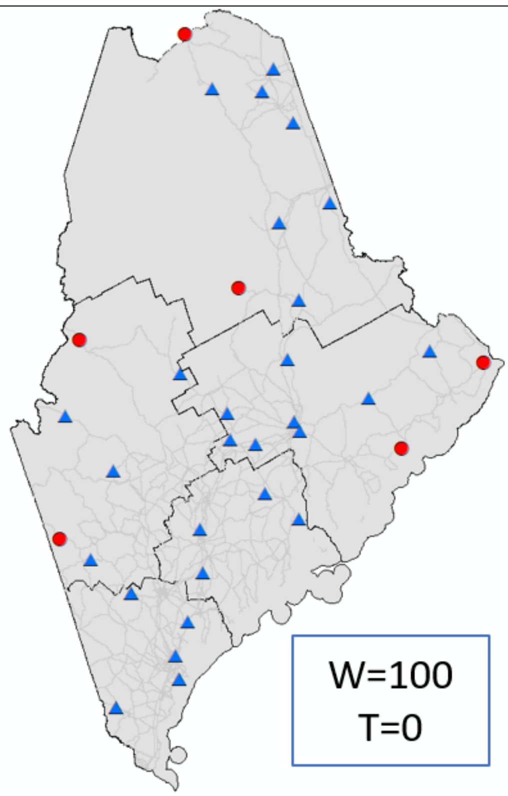

Here,
W = Weather Parameter
T = Traffic Parameter

Current + 18 Stations
Third 6 Stations
Third 6 Stations

Table D.1. Sensitivity analysis location solutions (Third 6 locations)

Station #	W = 00, T = 100		W = 20, T = 80		W = 40, T = 60		W = 50, T = 50	
	Long.	Lat.	Long.	Lat.	Long.	Lat.	Long.	Lat.
1	-70.13	44.07	-70.37	43.97	-70.95	43.64	-70.95	43.64
2	-70.16	44.61	-70.13	44.07	-70.26	44.06	-70.25	44.09
3	-69.70	44.51	-69.90	44.02	-70.04	44.64	-70.10	44.64
4	-69.40	44.62	-70.07	44.24	-67.39	44.64	-67.34	44.70
5	-69.78	44.89	-70.16	44.61	-67.87	46.80	-70.31	45.75
6	-69.48	45.01	-67.34	44.70	-68.32	47.29	-68.13	47.29
Station #	W = 60, T = 40		W = 80, T = 20		W = 100, T = 00			
	Long.	Lat.	Long.	Lat.	Long.	Lat.		
1	-70.95	43.64	-69.47	43.92	-70.93	44.58		
2	-70.13	44.68	-71.01	44.95	-67.93	44.51		
3	-68.20	44.34	-68.24	44.38	-67.04	44.83		
4	-67.25	44.67	-67.34	44.70	-70.29	45.70		
5	-70.29	45.69	-70.29	45.70	-68.83	45.72		
6	-68.32	47.29	-68.53	47.28	-68.59	47.28		

Appendix F

R-RWIS & M-RWIS COMBINATIONS

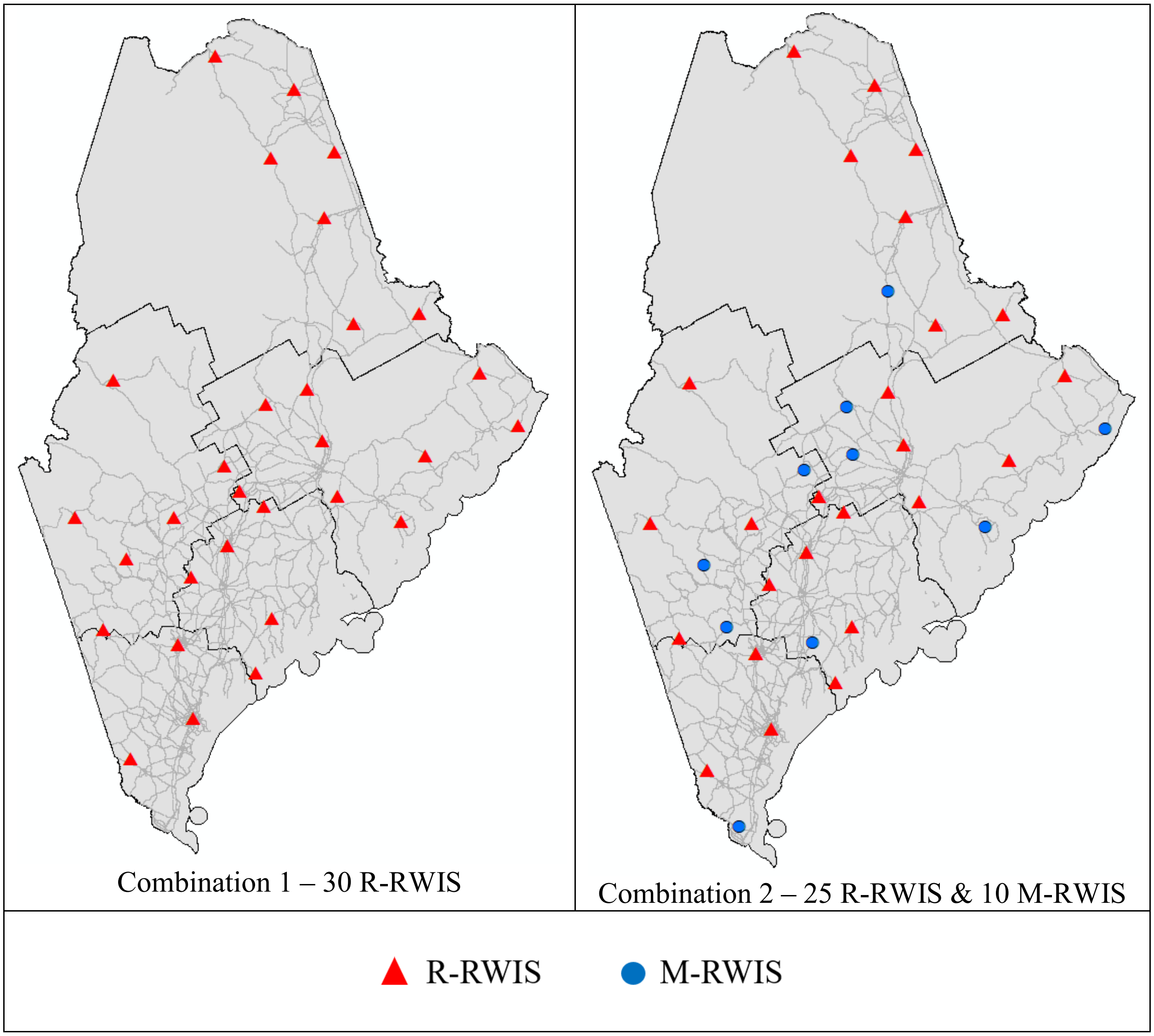

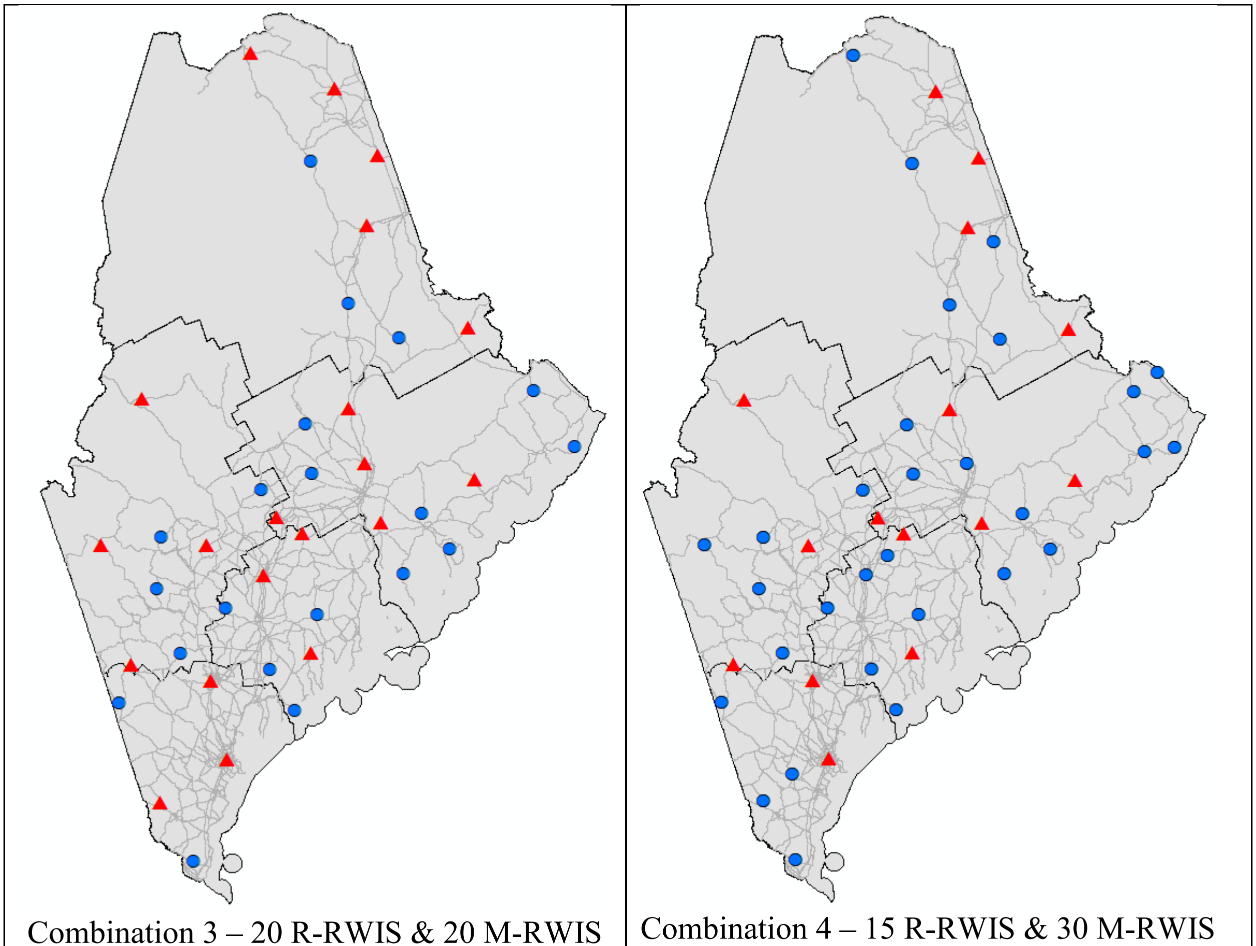

Combination 3 – 20 R-RWIS & 20 M-RWIS

Combination 4 – 15 R-RWIS & 30 M-RWIS

▲ R-RWIS ● M-RWIS

Table E.1. Optimized locations for combination 1 – 30 Regular RWIS (R)

Station #	Long.	Lat.	Station #	Long.	Lat.
R-1	-70.29	43.66	R-16	-70.85	43.54
R-2	-70.25	44.08	R-17	-70.75	44.94
R-3	-70.78	44.28	R-18	-69.65	44.54
R-4	-69.48	44.07	R-19	-68.69	44.95
R-5	-69.99	44.78	R-20	-68.54	47.20
R-6	-69.28	44.69	R-21	-68.37	46.55
R-7	-68.71	44.62	R-22	-68.16	45.52
R-8	-67.95	44.69	R-23	-67.33	45.03
R-9	-68.68	45.25	R-24	-70.00	44.43
R-10	-67.64	45.46	R-25	-69.72	43.80
R-11	-67.87	46.47	R-26	-67.18	44.68
R-12	-68.01	46.88	R-27	-69.03	45.24
R-13	-69.44	44.81	R-28	-69.49	44.98
R-14	-70.14	45.62	R-29	-68.29	44.38
R-15	-68.12	46.14	R-30	-70.45	44.63

Table E.2. Optimized locations for combination 2 – 25 Regular RWIS (R) and 10 Mini- RWIS (M)

Station #	Long.	Lat.	Station #	Long.	Lat.
R-1	-70.29	43.66	R-21	-68.37	46.55
R-2	-70.25	44.08	R-22	-68.16	45.52
R-3	-70.78	44.28	R-23	-67.33	45.03
R-4	-69.48	44.07	R-24	-70.00	44.43
R-5	-69.99	44.78	R-25	-69.72	43.80
R-6	-69.28	44.69	M-1	-67.18	44.68
R-7	-68.71	44.62	M-2	-69.03	45.24
R-8	-67.95	44.69	M-3	-69.49	44.98
R-9	-68.68	45.25	M-4	-68.29	44.38
R-10	-67.64	45.46	M-5	-70.45	44.63
R-11	-67.87	46.47	M-6	-68.44	45.78
R-12	-68.01	46.88	M-7	-69.09	44.98
R-13	-69.44	44.81	M-8	-70.42	44.27
R-14	-70.14	45.62	M-9	-69.82	44.05
R-15	-68.12	46.14	M-10	-70.74	43.18
R-16	-70.85	43.54			
R-17	-70.75	44.94			
R-18	-69.65	44.54			
R-19	-68.69	44.95			
R-20	-68.54	47.20			

Table E.3. Optimized locations for combination 3 – 20 Regular RWIS (R) and 20 Mini-RWIS (M)

Station #	Long.	Lat.	Station #	Long.	Lat.
R-1	-70.29	43.66	M-1	-67.18	44.68
R-2	-70.25	44.08	M-2	-69.03	45.24
R-3	-70.78	44.28	M-3	-69.49	44.98
R-4	-69.48	44.07	M-4	-68.29	44.38
R-5	-69.99	44.78	M-5	-70.45	44.63
R-6	-69.28	44.69	M-6	-68.44	45.78
R-7	-68.71	44.62	M-7	-69.09	44.98
R-8	-67.95	44.69	M-8	-70.42	44.27
R-9	-68.68	45.25	M-9	-69.82	44.05
R-10	-67.64	45.46	M-10	-70.74	43.18
R-11	-67.87	46.47	M-11	-68.37	46.55
R-12	-68.01	46.88	M-12	-68.16	45.52
R-13	-69.44	44.81	M-13	-67.33	45.03
R-14	-70.14	45.62	M-14	-70.00	44.43
R-15	-68.12	46.14	M-15	-69.72	43.80
R-16	-70.85	43.54	M-16	-70.95	44.10
R-17	-70.75	44.94	M-17	-68.40	44.60
R-18	-69.65	44.54	M-18	-68.67	44.33
R-19	-68.69	44.95	M-19	-69.37	44.26
R-20	-68.54	47.20	M-20	-70.31	44.89

Table E.4. Optimized locations for combination 4 – 15 Regular RWIS (R) and 30 Mini-RWIS (M)

Station #	Long.	Lat.	Station #	Long.	Lat.
R-1	-70.29	43.66	M-11	-68.37	46.55
R-2	-70.25	44.08	M-12	-68.16	45.52
R-3	-70.78	44.28	M-13	-67.33	45.03
R-4	-69.48	44.07	M-14	-70.00	44.43
R-5	-69.99	44.78	M-15	-69.72	43.80
R-6	-69.28	44.69	M-16	-70.95	44.10
R-7	-68.71	44.62	M-17	-68.40	44.60
R-8	-67.95	44.69	M-18	-68.67	44.33
R-9	-68.68	45.25	M-19	-69.37	44.26
R-10	-67.64	45.46	M-20	-70.31	44.89
R-11	-67.87	46.47	M-21	-70.85	43.54
R-12	-68.01	46.88	M-22	-70.75	44.94
R-13	-69.44	44.81	M-23	-69.65	44.54
R-14	-70.14	45.62	M-24	-68.69	44.95
R-15	-68.12	46.14	M-25	-68.54	47.20
M-1	-67.18	44.68	M-26	-67.97	46.02
M-2	-69.03	45.24	M-27	-67.12	45.09
M-3	-69.49	44.98	M-28	-67.40	44.71
M-4	-68.29	44.38	M-29	-69.46	44.60
M-5	-70.45	44.63	M-30	-70.60	43.63
M-6	-68.44	45.78			
M-7	-69.09	44.98			
M-8	-70.42	44.27			
M-9	-69.82	44.05			
M-10	-70.74	43.18			